

## **Supporting Information**

### ***Kinetic studies on strand displacement in de novo designed parallel heterodimeric coiled coils***

Mike C. Groth,<sup>a</sup> W. Mathis Rink,<sup>a</sup> Nils F. Meyer,<sup>a</sup> and Franziska Thomas<sup>\*a, b</sup>

<sup>a</sup>Institute of Organic and Biomolecular Chemistry, Georg-August-Universität Göttingen, Tammannstr. 2, 37077 Göttingen, Germany

<sup>b</sup>Center for Biostructural Imaging of Neurodegeneration, von-Siebold-Straße 3a, 37075 Göttingen, Germany

\*To correspondence should be addressed: [ftomas@gwdg.de](mailto:ftomas@gwdg.de)

### **Table of Content**

1. Peptide sequences.....	S2
2. Determination of unfolding constants .....	S4
3. CD-titration experiments.....	S10
4. FRET-based strand-displacement assay .....	S22
5. MALDI-TOF mass spectrometry and HPLC .....	S52
6. CD spectroscopy and thermal denaturation of C-truncated heterodimeric coiled coils .....	S59
7. References.....	S64

## 1. Peptide sequences

**Table S1.** Sequences of the *N*-terminally truncated set of *de novo* designed heterodimeric coiled coils. K<sup>+</sup>-Dansyl-labelled lysine residue.

	<b>N-A<sub>x</sub>B<sub>y</sub></b>	<b>Sequence and heptad register<sup>b</sup></b>			
		<i>gabcdef gabcdef gabcdef gabcdef</i>			
<b>1</b>	N-A <sub>3</sub>	G	EIAALEK	ENAALEW	EIAALEQ GG
<b>2</b>	N-A <sub>3.5</sub>	G	LEQ EIAALEK	ENAALEW	EIAALEQ GG
<b>3</b>	A <sub>4</sub>	G	EIAALEQ EIAALEK	ENAALEW	EIAALEQ GG
<b>4</b>	N-B <sub>3</sub>	G	KIAALKY	KNAALKK	KIAALKQ GG
<b>5</b>	N-B <sub>3.5</sub>	G	LKQ KIAALKY	KNAALKK	KIAALKQ GG
<b>6</b>	B <sub>4</sub>	G	KIAALKQ KIAALKY	KNAALKK	KIAALKQ GG
<b>7</b>	N-A <sub>3</sub> <sup>*</sup>	G	EIAALEW	ENAALEK	EIAALEQ GG
<b>8</b>	N-A <sub>3.5</sub> <sup>*</sup>	G	LEQ EIAALEW	ENAALEK	EIAALEQ GG
<b>9</b>	A <sub>4</sub> <sup>*</sup>	G	EIAALEQ EIAALEW	ENAALEK	EIAALEQ GG
<b>10</b>	N-B <sub>3</sub> <sup>*</sup>	G	KIAALKK <sup>*</sup>	KNAALKK	KIAALKQ GG
<b>11</b>	N-B <sub>3.5</sub> <sup>*</sup>	G	LKQ KIAALKK <sup>*</sup>	KNAALKK	KIAALKQ GG
<b>12</b>	B <sub>4</sub> <sup>*</sup>	G	KIAALKQ KIAALKK <sup>*</sup>	KNAALKK	KIAALKQ GG
<b>13</b>	N-A <sub>3</sub> _W15K (N-A <sub>3</sub> comp)	G	EIAALEK	ENAALEK	EIAALEQ GG
<b>14</b>	N-A <sub>3.5</sub> _W18K (N-A <sub>3.5</sub> comp)	G	LEQ EIAALEK	ENAALEK	EIAALEQ GG
<b>15</b>	A <sub>4</sub> _W22K (A <sub>4</sub> comp)	G	EIAALEQ EIAALEK	ENAALEK	EIAALEQ GG

**Table S2.** Sequences of the C-terminally truncated set of *de novo* designed heterodimeric coiled coils. K<sup>\*</sup>-Dansyl-labelled lysine residue.

	<b>C-A<sub>x</sub>B<sub>y</sub></b>	<b>Sequence and heptad register<sup>b</sup></b>			
		<i>gabcdef</i>	<i>gabcdef</i>	<i>gabcdef</i>	<i>gabcdef</i>
<b>1</b>	C-A <sub>3</sub>	G EIAALEQ	EIAALEK	ENAALEW	GG
<b>2</b>	C-A <sub>3.5</sub>	G EIAALEQ	EIAALEK	ENAALEW EIAA	GG
<b>3</b>	A <sub>4</sub>	G EIAALEQ	EIAALEK	ENAALEW EIAALEQ	GG
<b>4</b>	C-B <sub>3</sub>	G KIAALKQ	KIAALKY	KNAALKK	GG
<b>5</b>	C-B <sub>3.5</sub>	G KIAALKQ	KIAALKY	KNAALKK KIAA	GG
<b>6</b>	B <sub>4</sub>	G KIAALKQ	KIAALKY	KNAALKK KIAALKQ	GG
<b>7</b>	C-A <sub>3</sub> <sup>*</sup>	G EIAALEQ	EIAALEW	ENAALEK	GG
<b>8</b>	C-A <sub>3.5</sub> <sup>*</sup>	G EIAALEQ	EIAALEW	ENAALEK EIAA	GG
<b>9</b>	A <sub>4</sub> <sup>*</sup>	G EIAALEQ	EIAALEW	ENAALEK EIAALEQ	GG
<b>10</b>	C-B <sub>3</sub> <sup>*</sup>	G KIAALKQ	KIAALKK <sup>*</sup>	KNAALKK	GG
<b>11</b>	C-B <sub>3.5</sub> <sup>*</sup>	G KIAALKQ	KIAALKK <sup>*</sup>	KNAALKK KIAA	GG
<b>12</b>	B <sub>4</sub> <sup>*</sup>	G KIAALKQ	KIAALKK <sup>*</sup>	KNAALKK KIAALKQ	GG
<b>13</b>	C-A <sub>3</sub> _W22K (C-A <sub>3</sub> comp)	G EIAALEQ	EIAALEK	ENAALEK	GG
<b>14</b>	C-A <sub>3.5</sub> _W22K (C-A <sub>3.5</sub> comp)	G EIAALEQ	EIAALEK	ENAALEK EIAA	GG
<b>15</b>	A <sub>4</sub> _W22K (A <sub>4</sub> comp)	G EIAALEQ	EIAALEK	ENAALEK EIAALEQ	GG

A<sub>4</sub> and B<sub>4</sub> are the same in both sets of heterodimeric coiled coils.

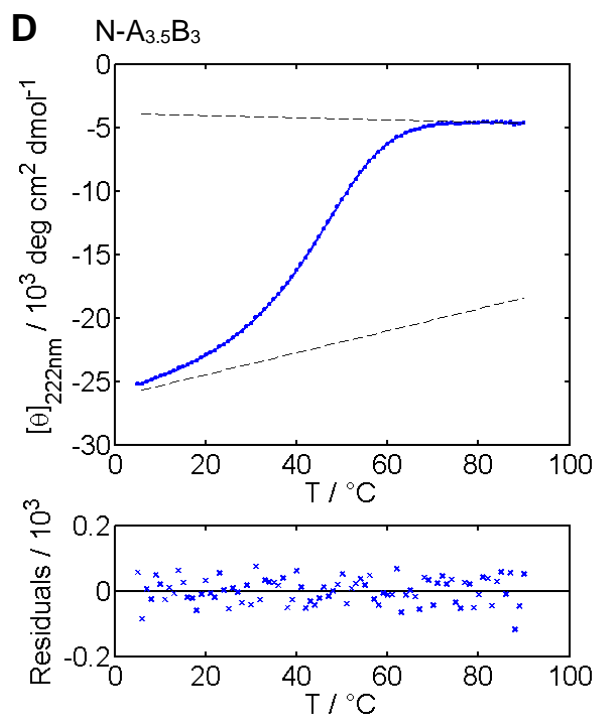
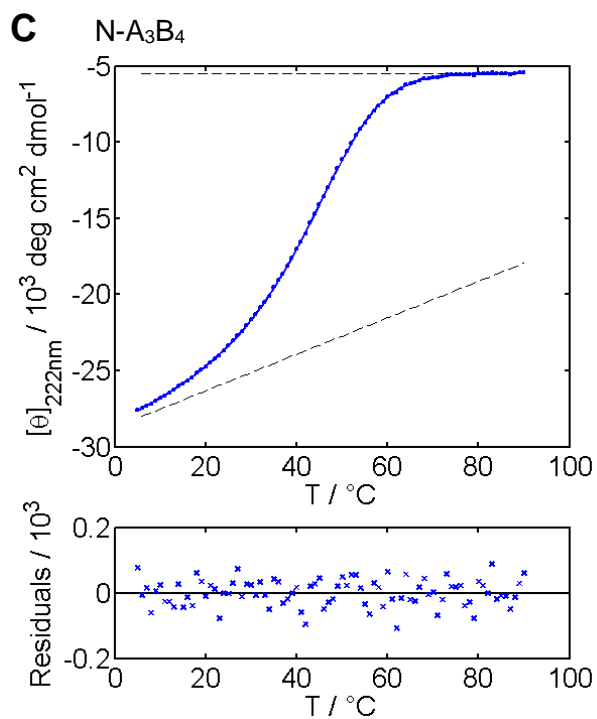
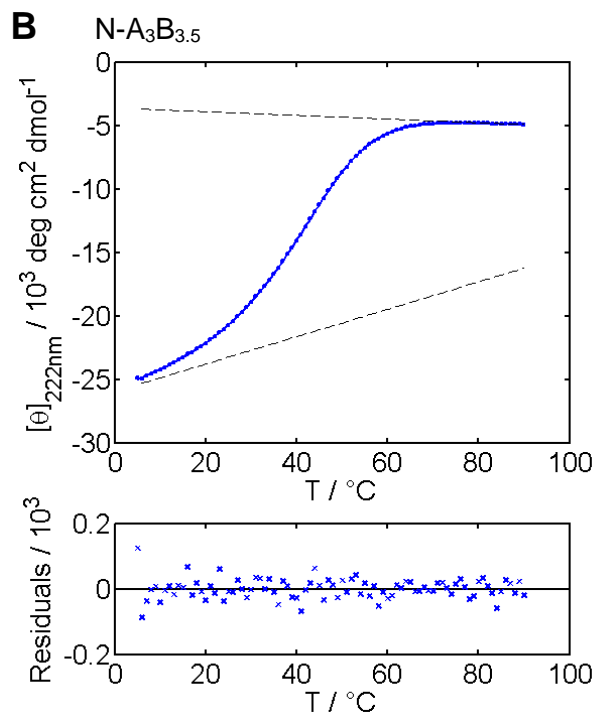
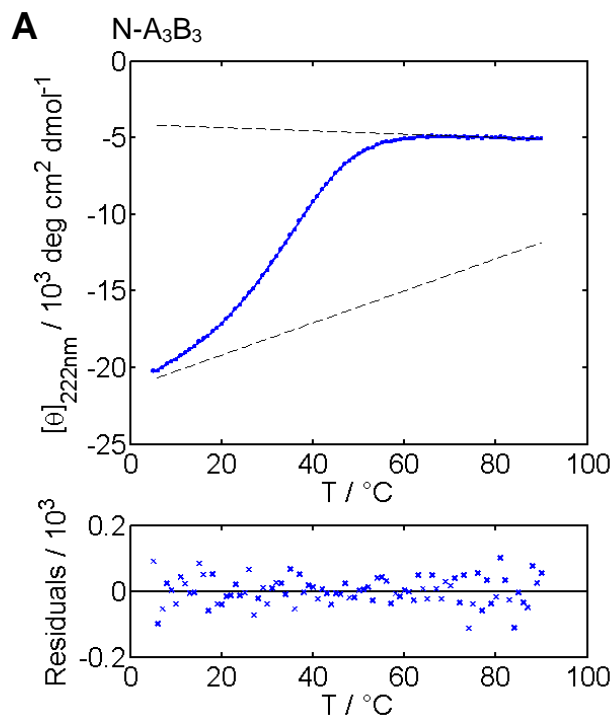
## 2. Determination of unfolding constants

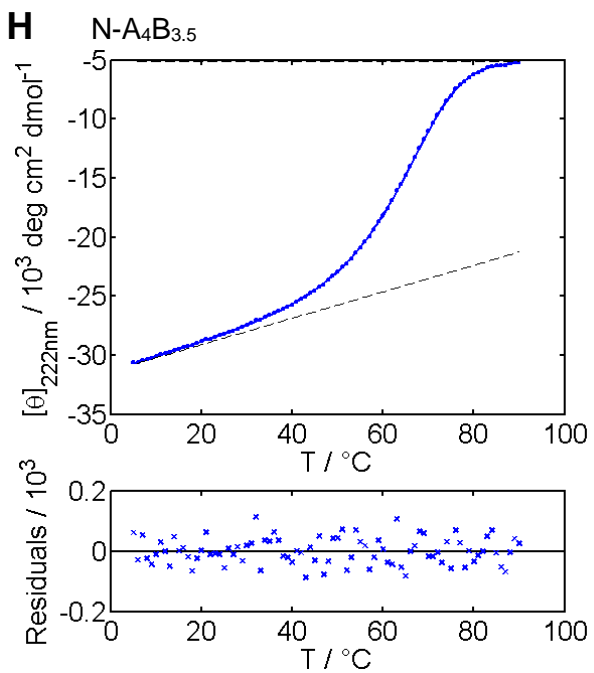
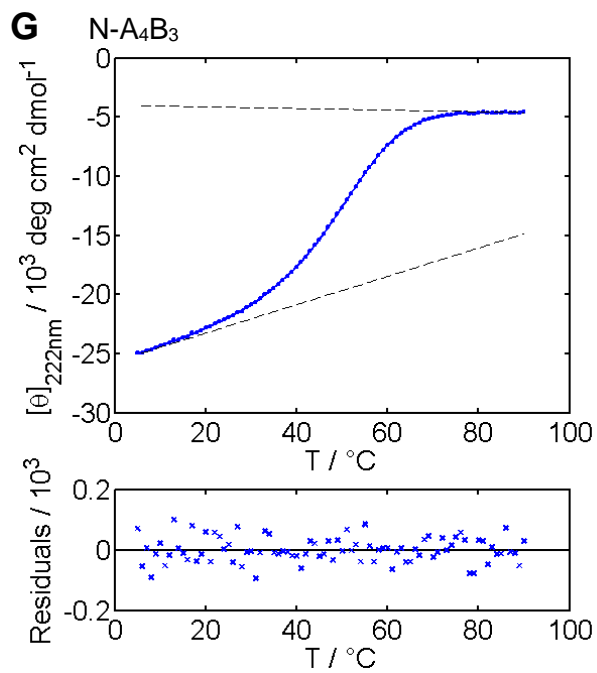
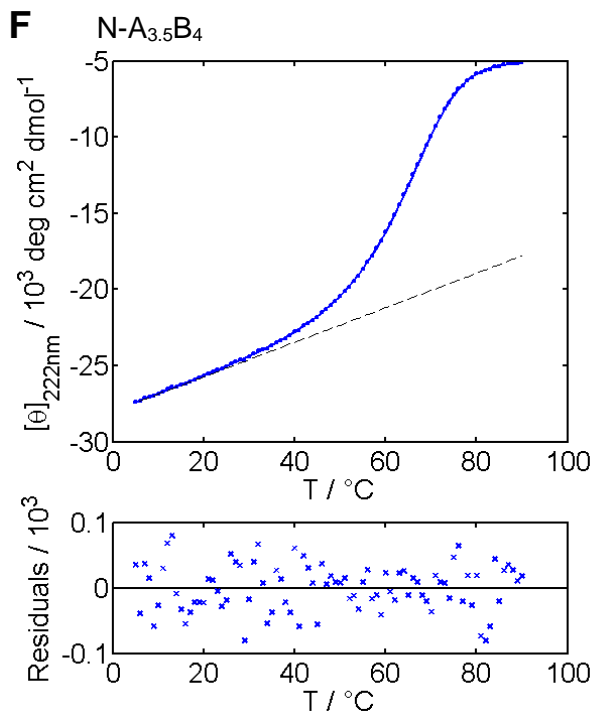
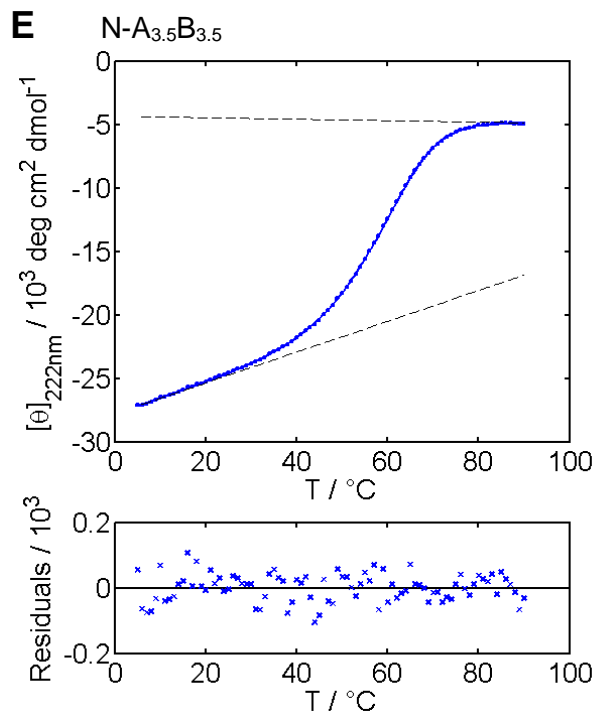
**Table S3.** Equilibrium constants of dissociation  $K_D$  of the N- $A_xB_y$  peptides obtained from the thermal denaturation curves at 50  $\mu$ M coiled-coil concentration (N- $A_3B_3$  – N- $A_4B_{3.5}$ ) and 25  $\mu$ M ( $A_4B_4$ ) using FitDis! analysis software.<sup>1</sup>

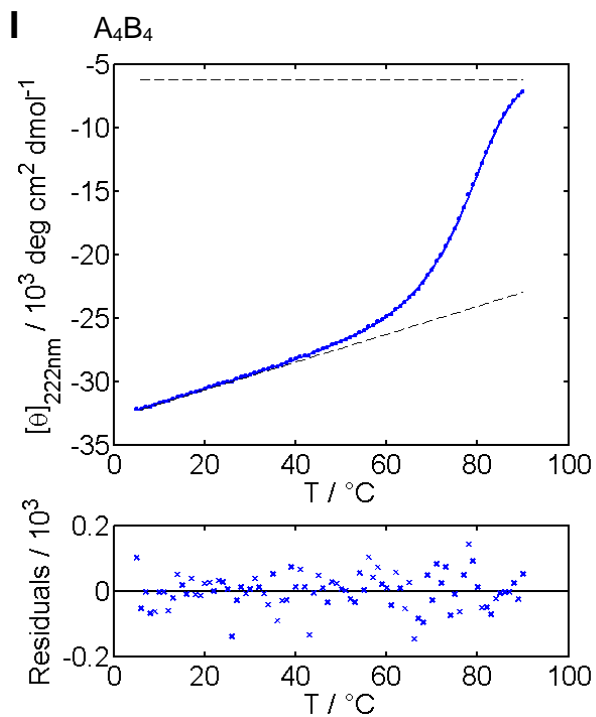
$K_D$ (M)	N- $A_3$	N- $A_{3.5}$	$A_4$
N- $B_3$	$(4.5 \pm 2.2) \cdot 10^{-6}$	$(8.0 \pm 7.2) \cdot 10^{-7}$	$(2.5 \pm 1.9) \cdot 10^{-7}$
N- $B_{3.5}$	$(1.9 \pm 1.1) \cdot 10^{-6}$	$(6.4 \pm 3.7) \cdot 10^{-9}$	$(9.2 \pm 5.9) \cdot 10^{-10}$
$B_4$	$(8.8 \pm 3.5) \cdot 10^{-7}$	$(1.0 \pm 1.1) \cdot 10^{-9}$	$(5.7 \pm 1.1) \cdot 10^{-10}$

**Table S4.** Equilibrium constants of dissociation  $K_D$  of the C- $A_xB_y$  peptides obtained from the thermal denaturation curves at 50  $\mu$ M coiled-coil concentration (C- $A_3B_3$  – C- $A_4B_{3.5}$ ) and 25  $\mu$ M ( $A_4B_4$ ) using FitDis! analysis software.<sup>1</sup>

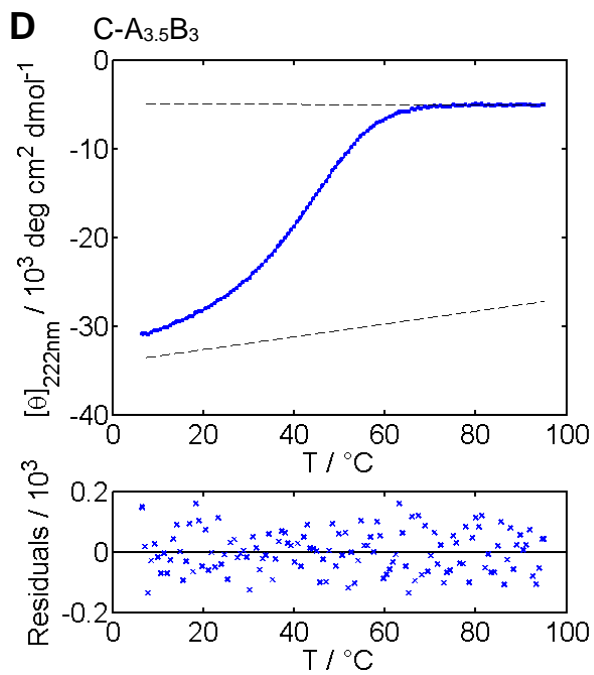
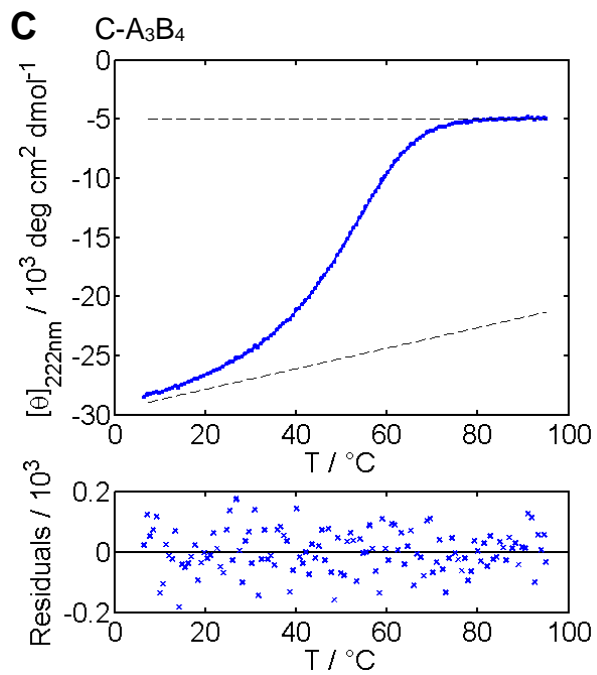
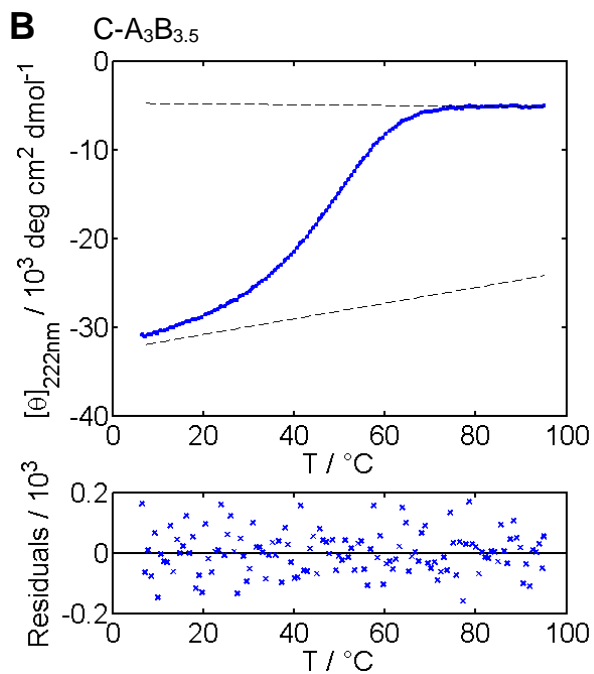
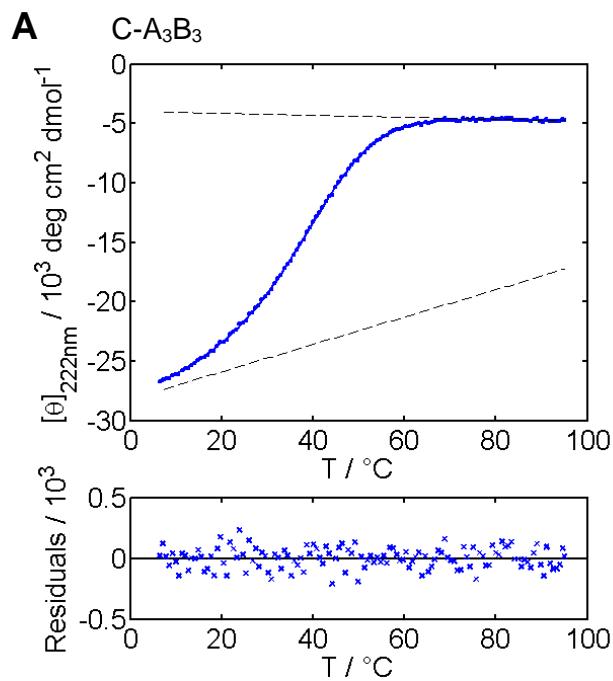
$K_D$ (M)	C- $A_3$	C- $A_{3.5}$	$A_4$
C- $B_3$	$(4.9 \pm 3.5) \cdot 10^{-6}$	$(2.8 \pm 0.5) \cdot 10^{-6}$	$(3.1 \pm 1.5) \cdot 10^{-6}$
C- $B_{3.5}$	$(1.5 \pm 3.0) \cdot 10^{-6}$	$(8.9 \pm 5.8) \cdot 10^{-8}$	$(5.5 \pm 2.4) \cdot 10^{-8}$
$B_4$	$(8.6 \pm 2.1) \cdot 10^{-7}$	$(7.3 \pm 1.1) \cdot 10^{-9}$	$(5.7 \pm 1.06) \cdot 10^{-10}$







**Figure S1.** CD-thermal denaturation curves of the  $N-A_xB_y$  peptides fit to a two-state unfolding model (top) and residuals depicting the quality of the fit (bottom). A)  $N-A_3B_3$ , B)  $N-A_3B_{3.5}$ , C)  $N-A_3B_4$ , D)  $N-A_{3.5}B_3$ , E)  $N-A_{3.5}B_{3.5}$ , F)  $N-A_{3.5}B_4$ , G)  $N-A_4B_3$ , H)  $N-A_4B_{3.5}$ , I)  $A_4B_4$ . Thermal denaturation curves were recorded at  $50 \mu\text{M}$  coiled-coil concentration ( $A_4B_4$ :  $25 \mu\text{M}$  coiled-coil concentration) in PBS buffer. Data were processed using the FitDis! analysis software.<sup>1</sup>





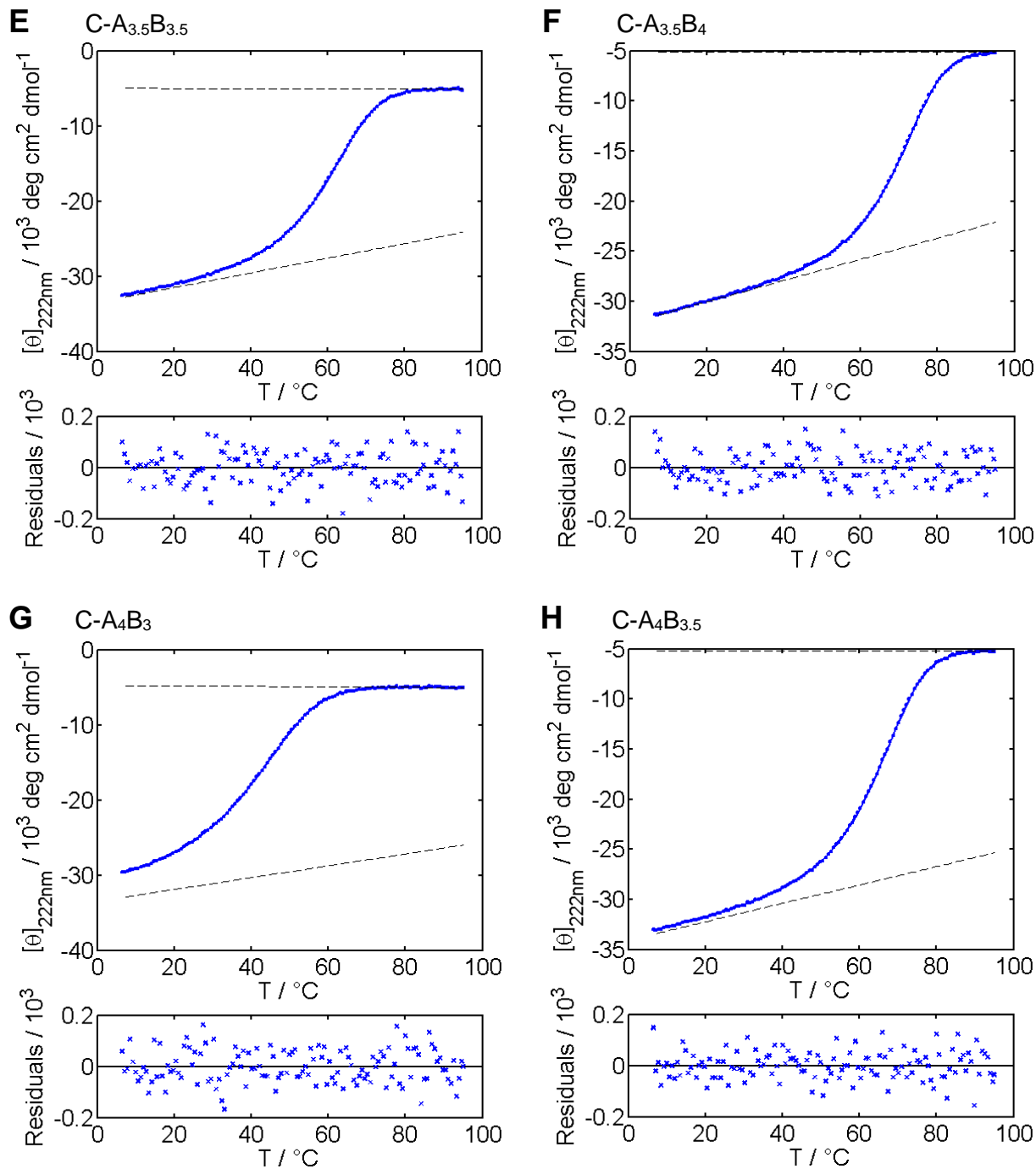
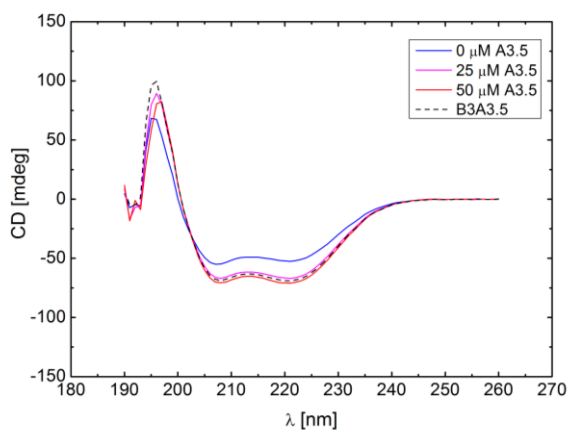


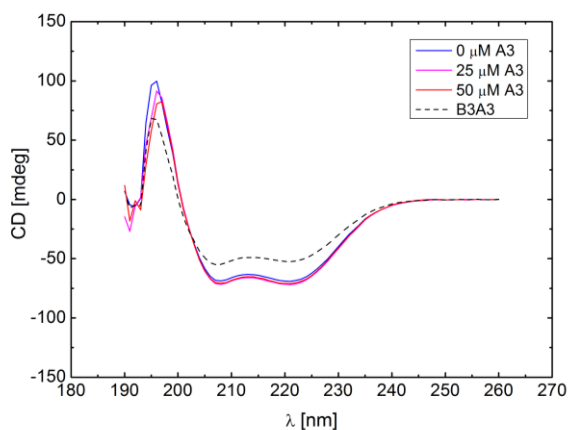
**Figure S2.** CD-thermal denaturation curves of the C-A<sub>x</sub>B<sub>y</sub> peptides fit to a two-state unfolding model (top) and residuals depicting the quality of the fit (bottom). A) C-A<sub>3</sub>B<sub>3</sub>, B) C-A<sub>3</sub>B<sub>3.5</sub>, C) C-A<sub>3</sub>B<sub>4</sub>, D) C-A<sub>3.5</sub>B<sub>3</sub>, E) C-A<sub>3.5</sub>B<sub>3.5</sub>, F) C-A<sub>3.5</sub>B<sub>4</sub>, G) C-A<sub>4</sub>B<sub>3</sub>, H) C-A<sub>4</sub>B<sub>3.5</sub>. Thermal denaturation curves were recorded at 50 μM coiled-coil concentration (A<sub>4</sub>B<sub>4</sub>: 25 μM coiled-coil concentration) in PBS buffer. Data were processed using the FitDis! analysis software.<sup>1</sup>

### 3. CD-titration experiments

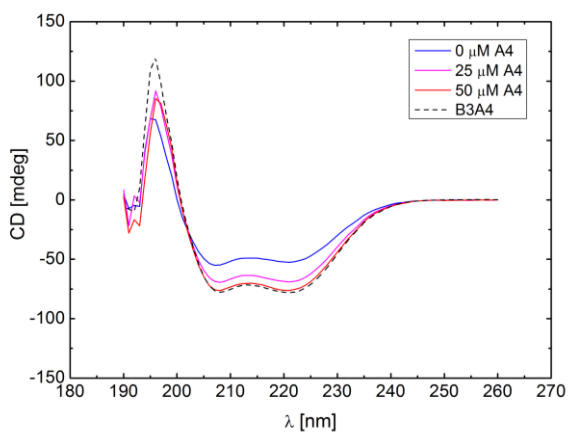
**A** N-A<sub>3</sub>B<sub>3</sub>  $\uparrow\downarrow$  A<sub>3.5</sub>



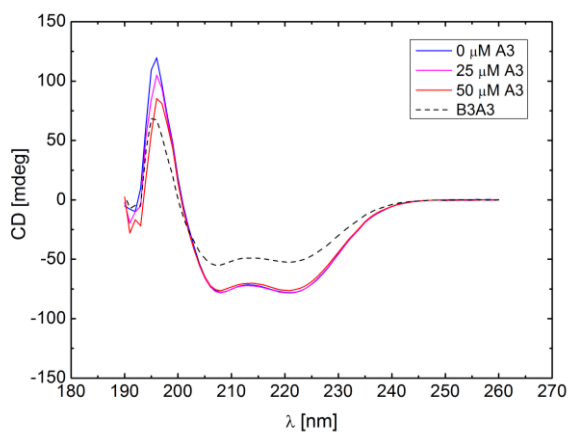
**B** N-A<sub>3.5</sub>B<sub>3</sub>  $\uparrow\downarrow$  A<sub>3</sub>



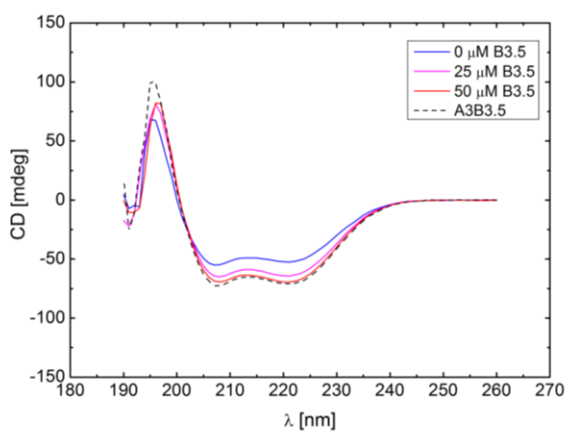
**C** N-A<sub>3</sub>B<sub>3</sub>  $\uparrow\downarrow$  A<sub>4</sub>



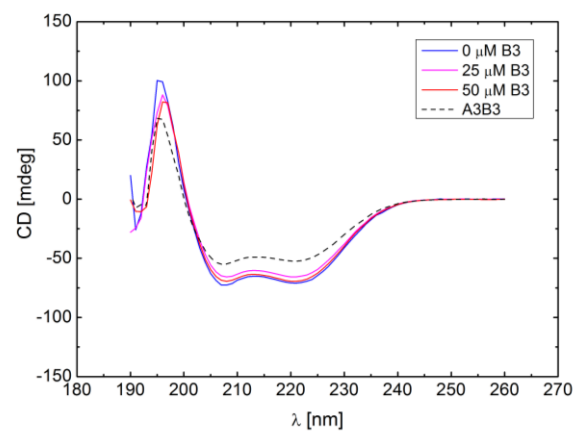
**D** N-A<sub>4</sub>B<sub>3</sub>  $\uparrow\downarrow$  A<sub>3</sub>

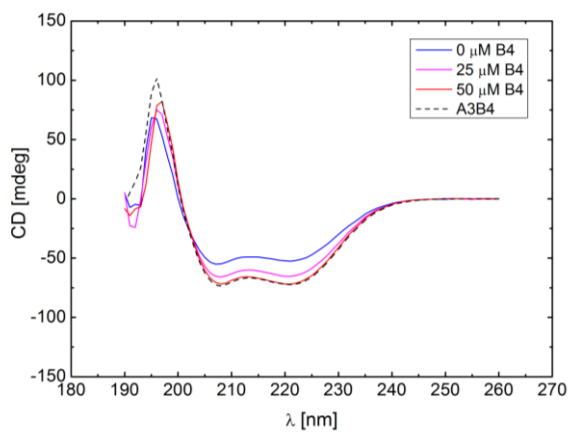
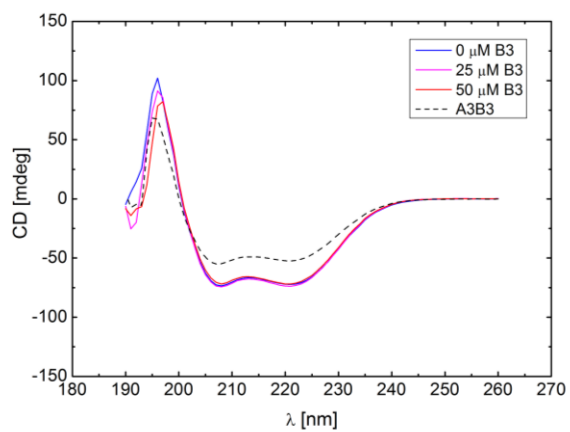
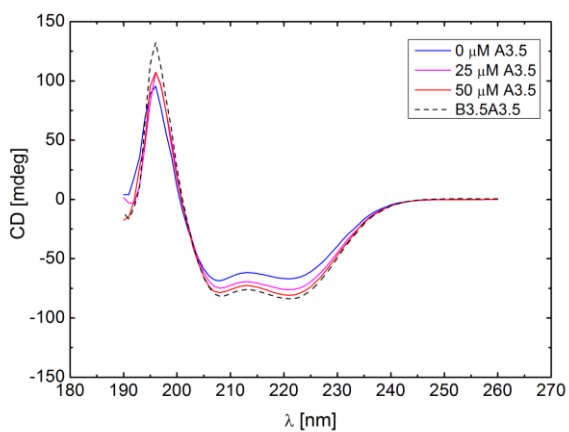
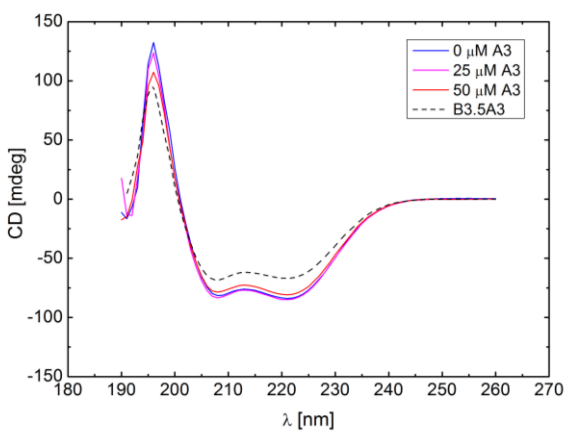
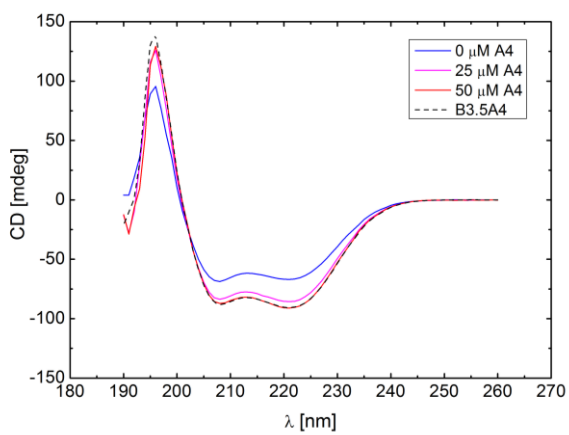
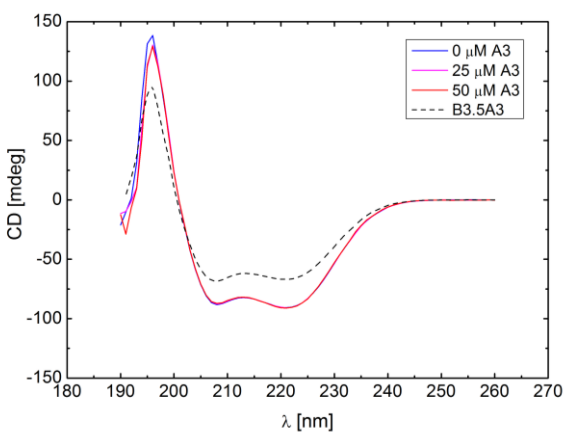


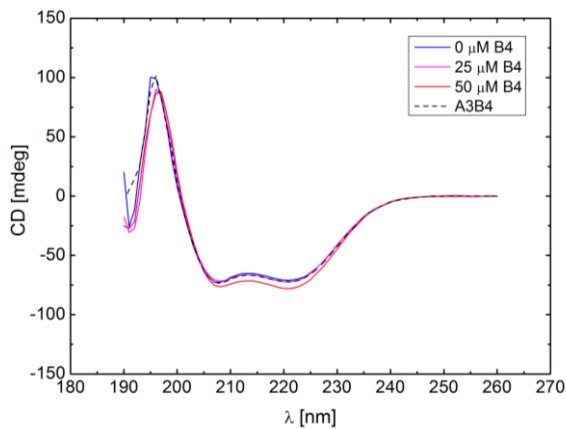
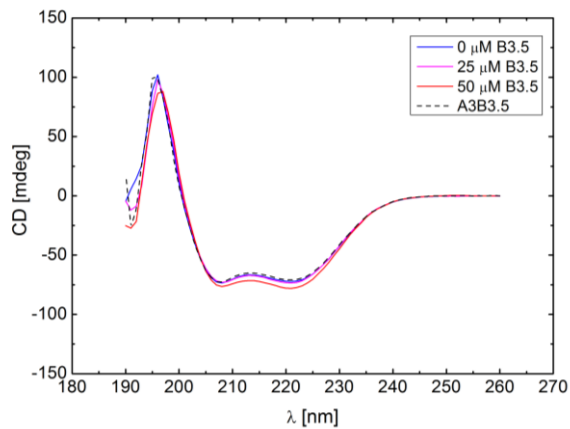
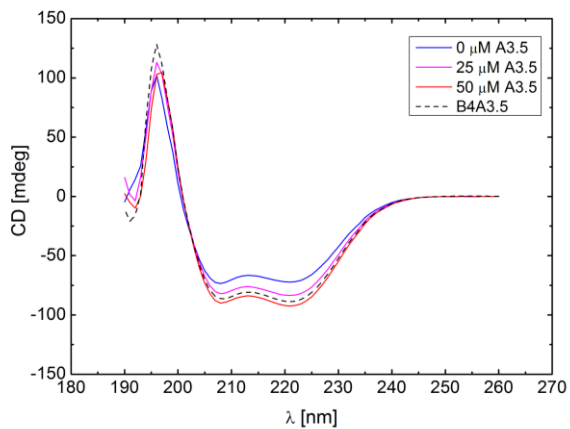
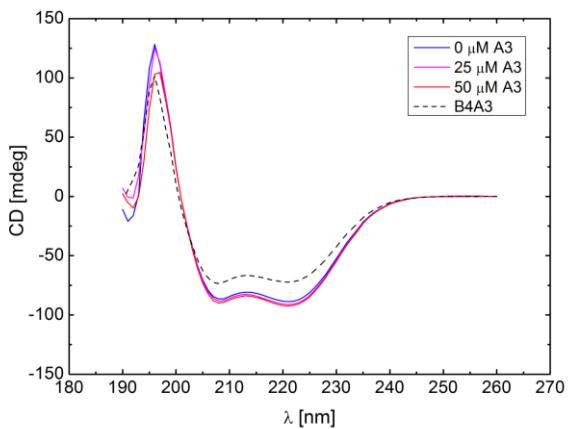
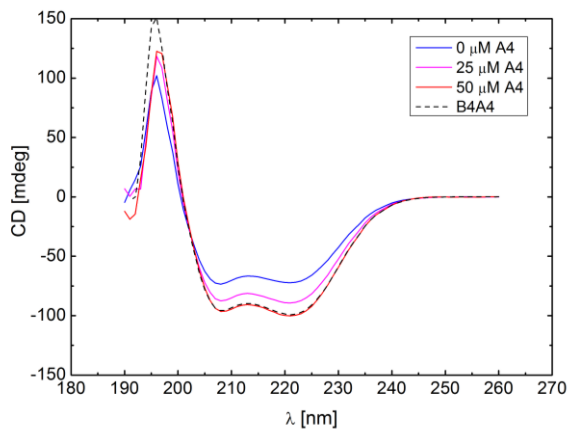
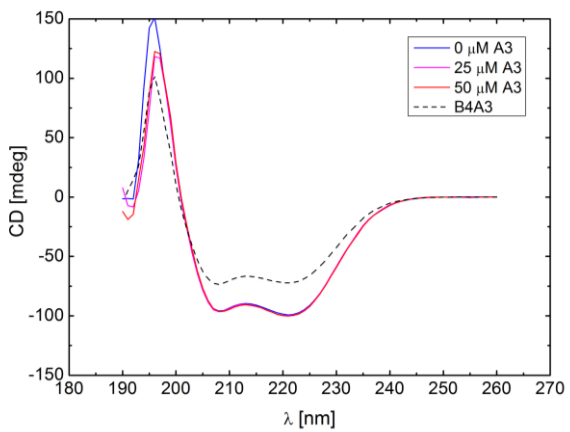
**E** N-A<sub>3</sub>B<sub>3</sub>  $\uparrow\downarrow$  B<sub>3.5</sub>

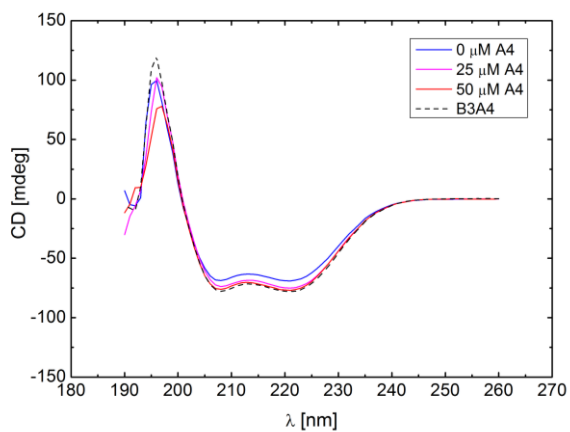
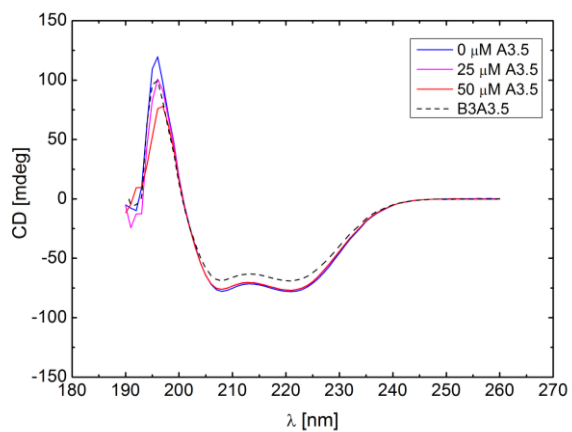
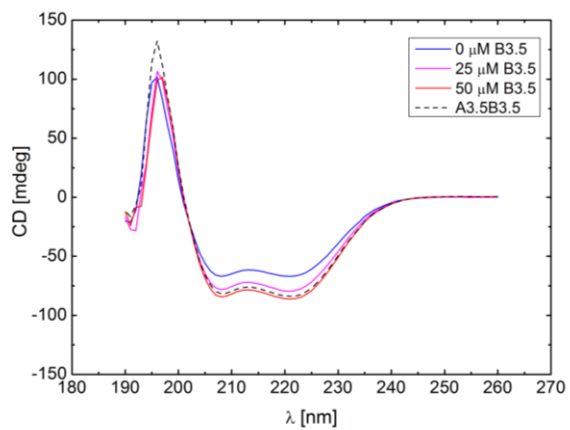
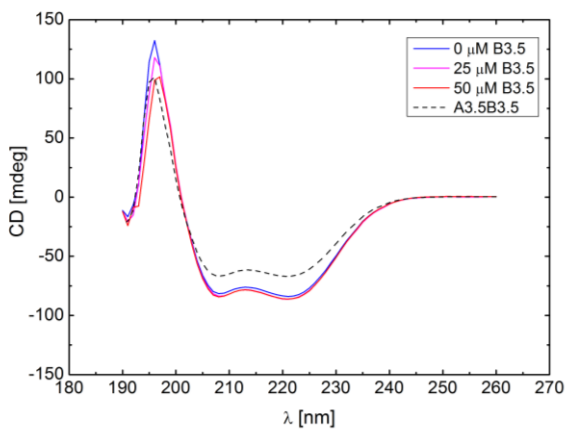
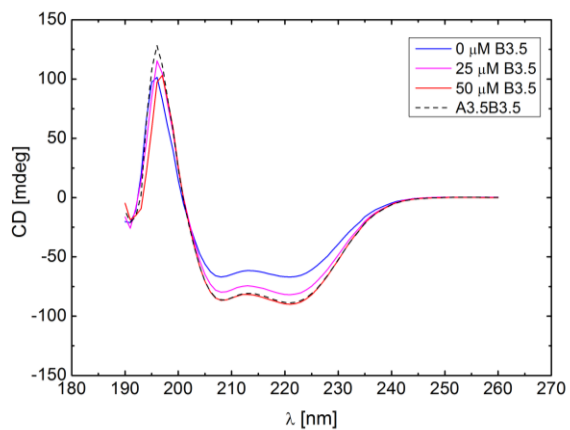
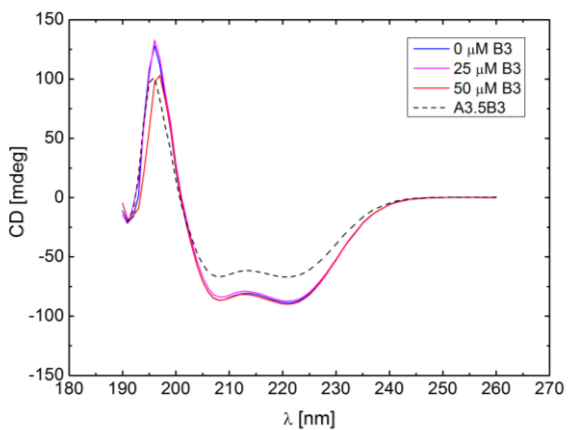


**F** N-A<sub>3</sub>B<sub>3.5</sub>  $\uparrow\downarrow$  B<sub>3</sub>

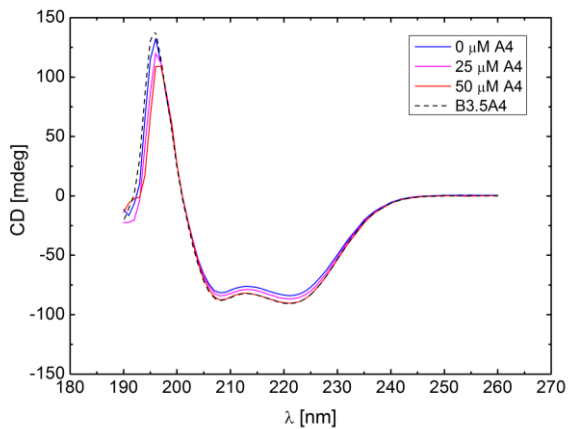


**G** N-A<sub>3</sub>B<sub>3</sub> ⇌ B<sub>4</sub>**H** N-A<sub>3</sub>B<sub>4</sub> ⇌ B<sub>3</sub>**I** N-A<sub>3</sub>B<sub>3.5</sub> ⇌ A<sub>3.5</sub>**J** N-A<sub>3.5</sub> B<sub>3.5</sub> ⇌ A<sub>3</sub>**K** N-A<sub>3</sub>B<sub>3.5</sub> ⇌ A<sub>4</sub>**L** N-A<sub>4</sub>B<sub>3.5</sub> ⇌ A<sub>3</sub>

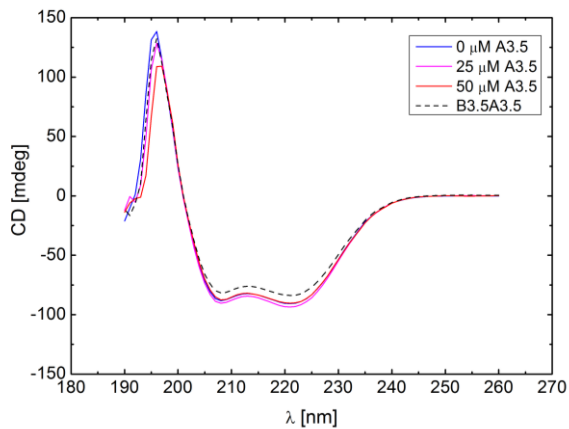
**M** N-A<sub>3</sub>B<sub>3.5</sub>  $\uparrow\downarrow$  B<sub>4</sub>**N** N-A<sub>3</sub>B<sub>4</sub>  $\uparrow\downarrow$  B<sub>3.5</sub>**O** N-A<sub>3</sub>B<sub>4</sub>  $\uparrow\downarrow$  A<sub>3.5</sub>**P** N-A<sub>3.5</sub>B<sub>4</sub>  $\uparrow\downarrow$  A<sub>3</sub>**Q** N-A<sub>3</sub>B<sub>4</sub>  $\uparrow\downarrow$  A<sub>4</sub>**R** N-A<sub>4</sub>B<sub>4</sub>  $\uparrow\downarrow$  A<sub>3</sub>

**S** N-A<sub>3.5</sub>B<sub>3</sub> ↑↓ A<sub>4</sub>**T** N-A<sub>4</sub>B<sub>3</sub> ↑↓ A<sub>3.5</sub>**U** N-A<sub>3.5</sub>B<sub>3</sub> ↑↓ B<sub>3.5</sub>**V** N-A<sub>3.5</sub>B<sub>3.5</sub> ↑↓ B<sub>3</sub>**W** N-A<sub>3.5</sub>B<sub>3</sub> ↑↓ B<sub>4</sub>**X** N-A<sub>3.5</sub>B<sub>4</sub> ↑↓ B<sub>3</sub>

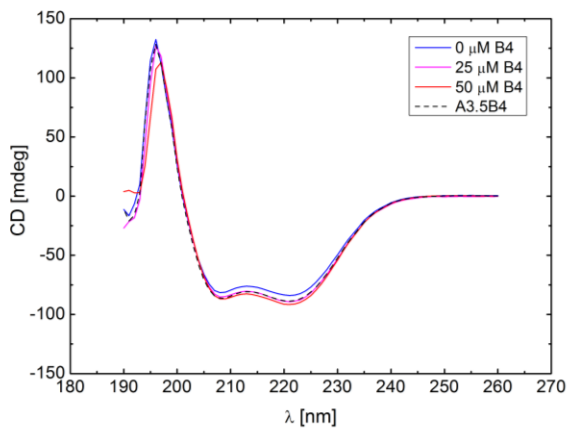
**Y** N-A<sub>3.5</sub>B<sub>3.5</sub>  $\uparrow\downarrow$  A<sub>4</sub>



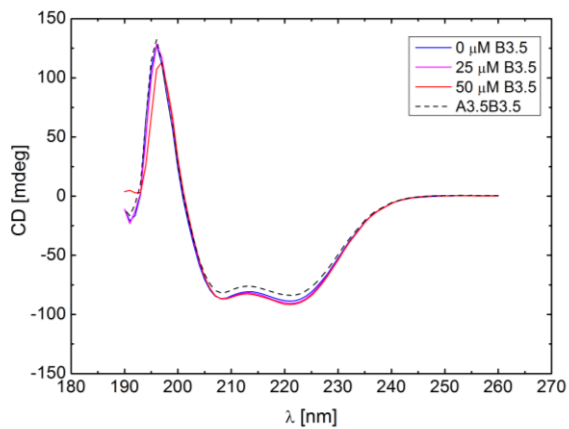
**Z** N-A<sub>4</sub>B<sub>3.5</sub>  $\uparrow\downarrow$  A<sub>3.5</sub>



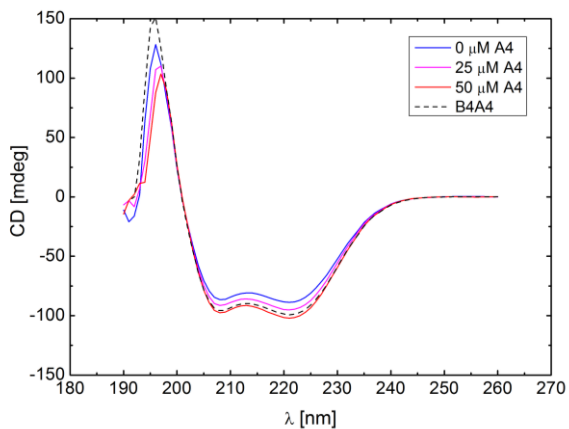
**Aa** N-A<sub>3.5</sub>B<sub>3.5</sub>  $\uparrow\downarrow$  B<sub>4</sub>



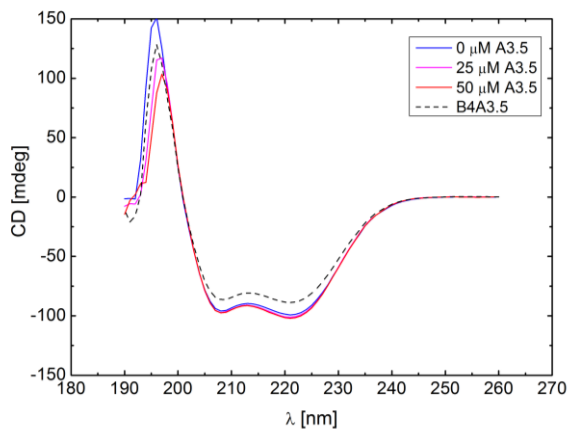
**Bb** N-A<sub>3.5</sub>B<sub>4</sub>  $\uparrow\downarrow$  B<sub>3.5</sub>

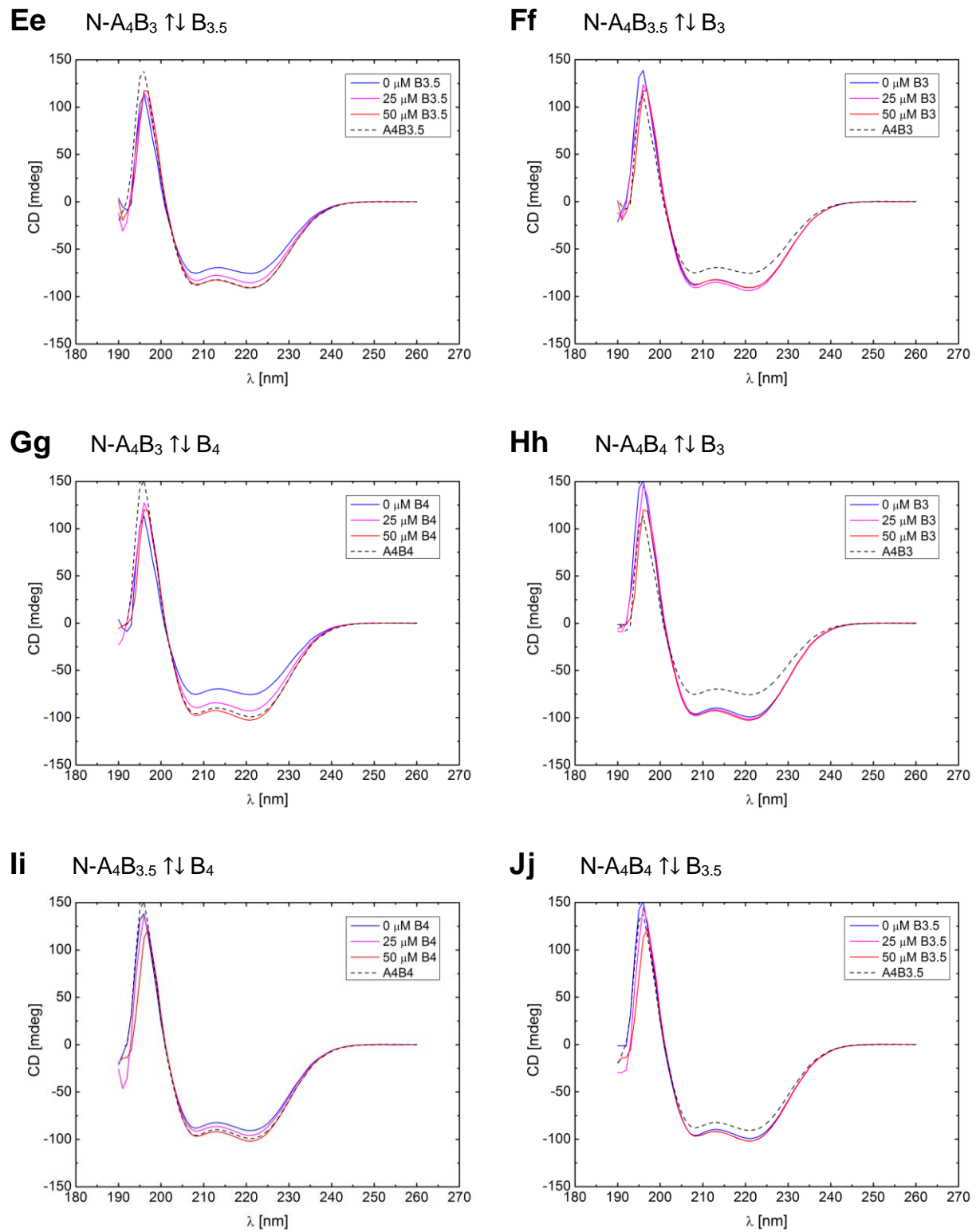


**Cc** N-A<sub>3.5</sub>B<sub>4</sub>  $\uparrow\downarrow$  A<sub>4</sub>

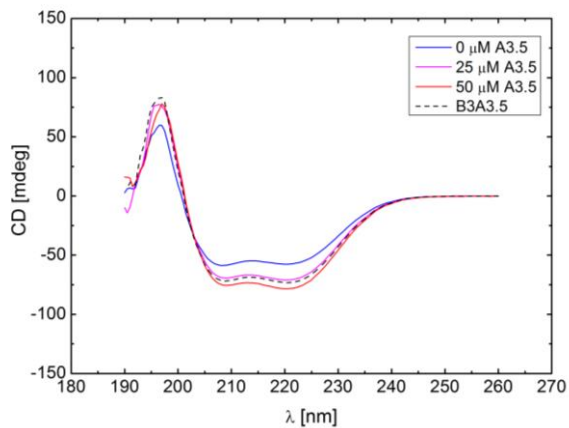
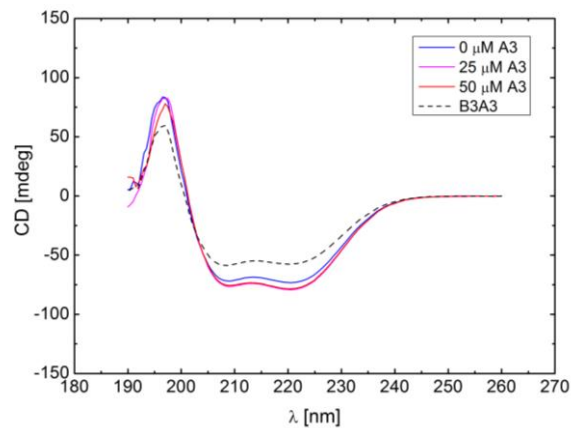
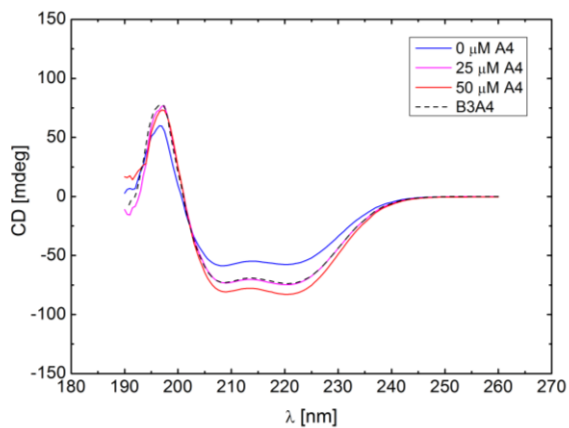
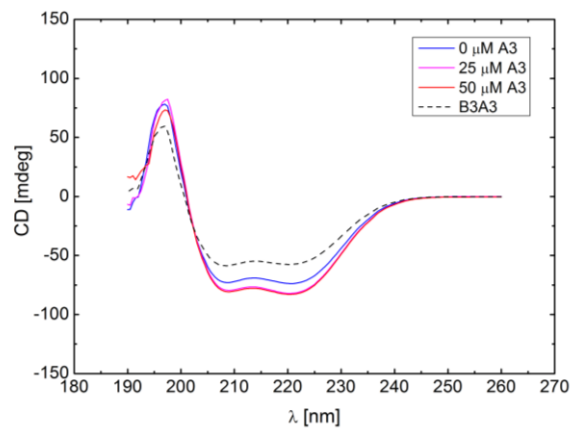
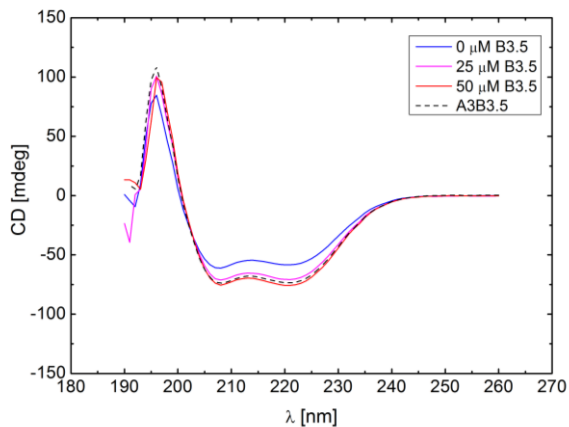
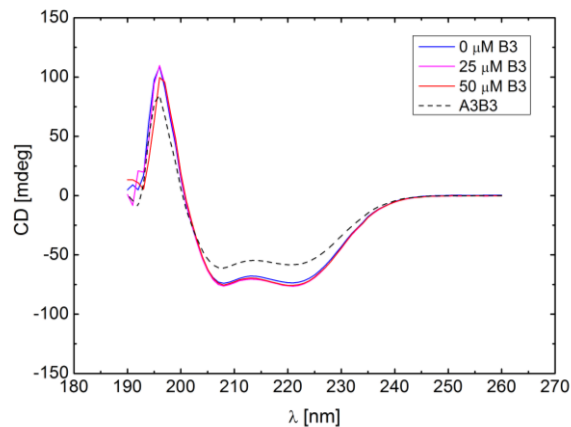


**Dd** N-A<sub>4</sub>B<sub>4</sub>  $\uparrow\downarrow$  A<sub>3.5</sub>

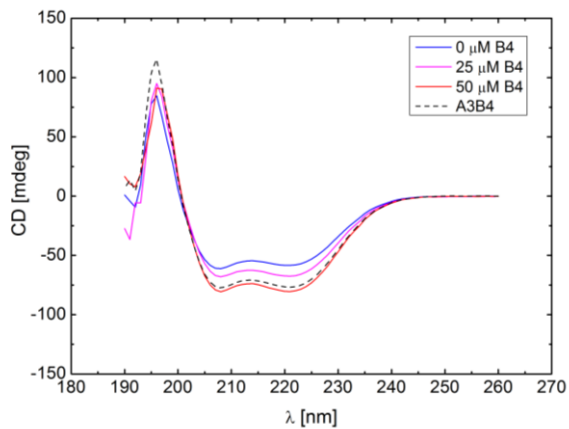
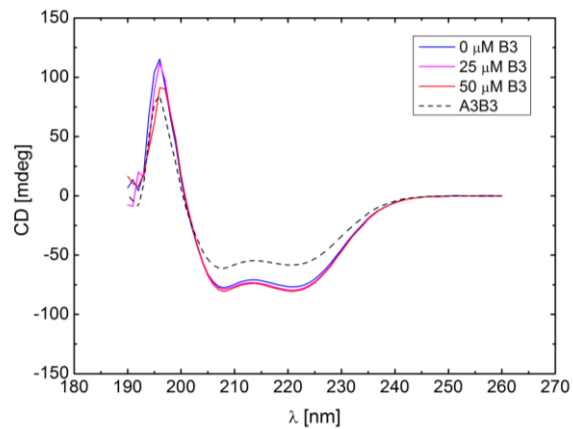
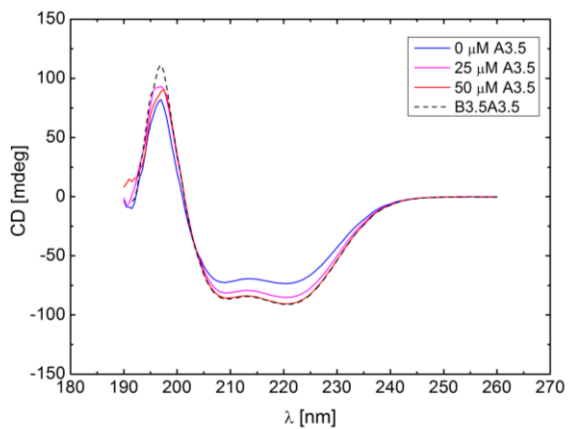
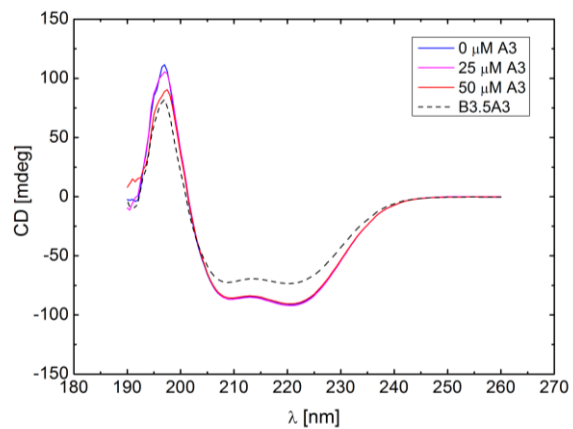
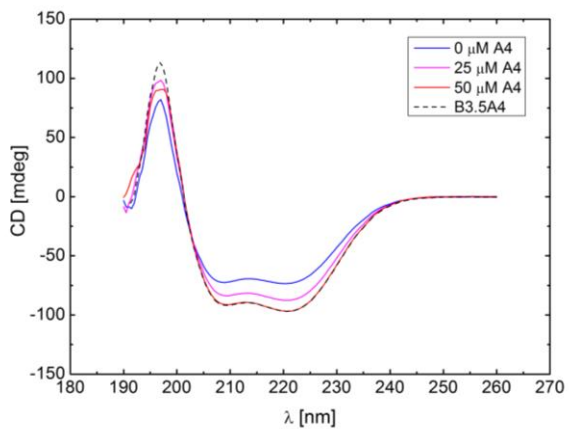
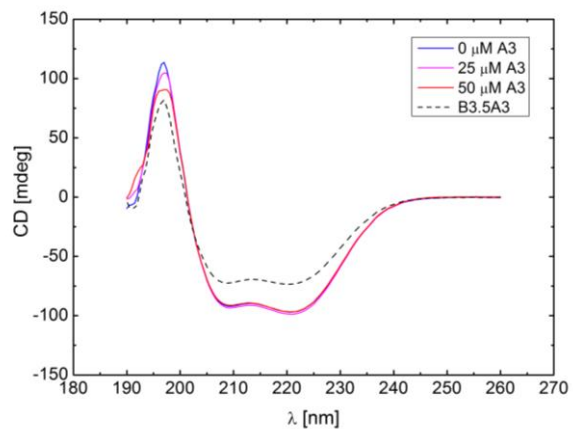


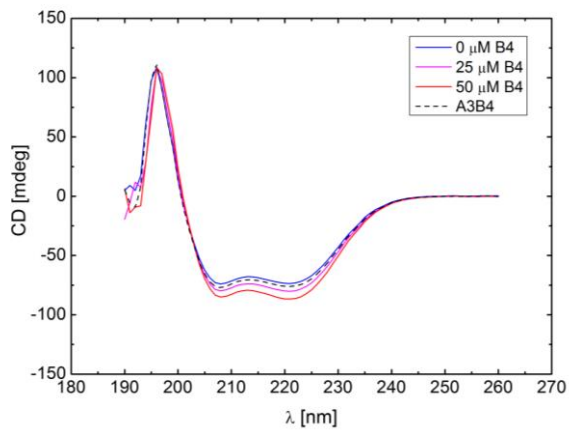
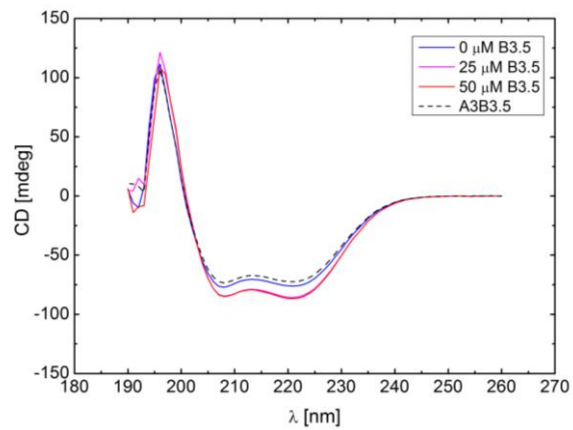
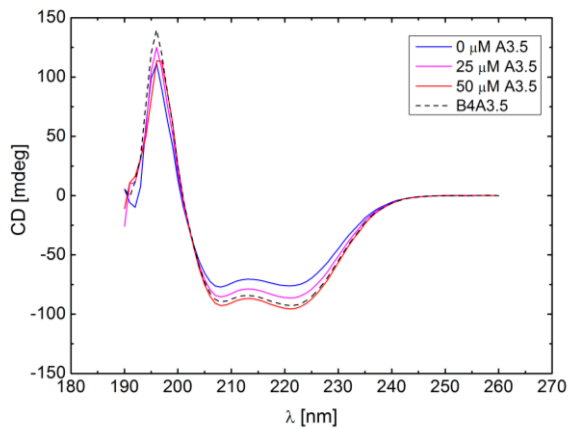
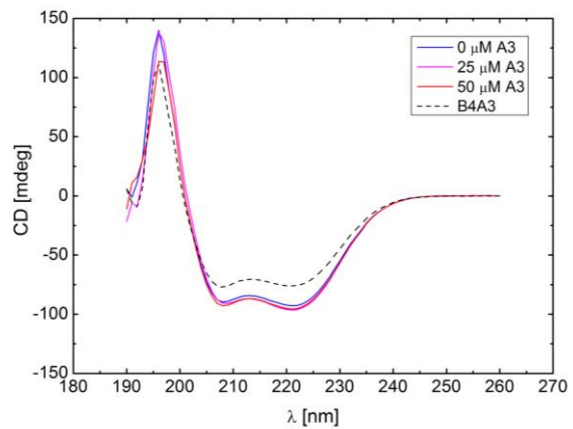
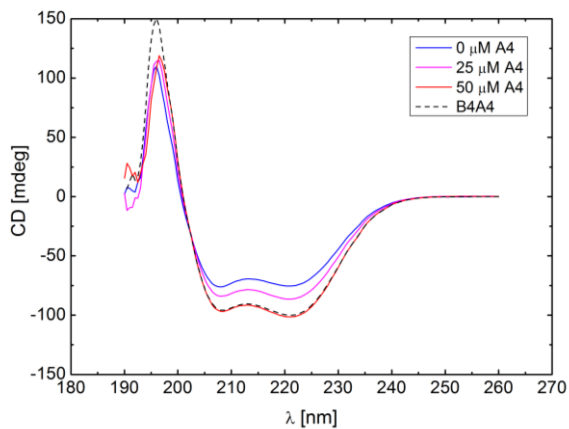
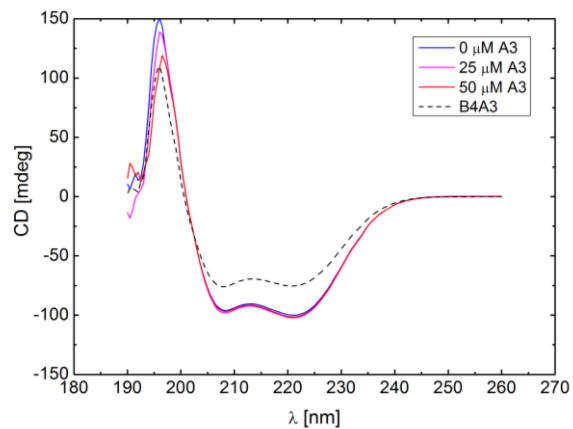


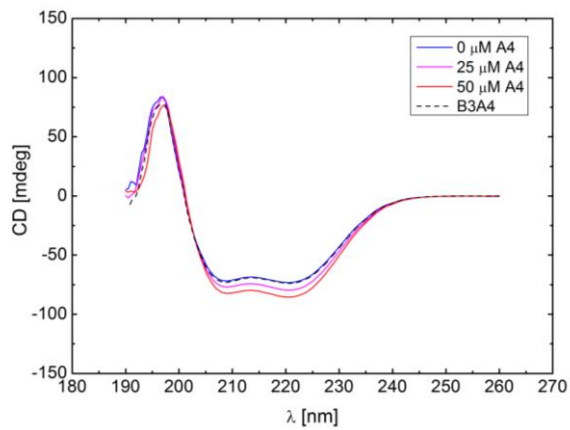
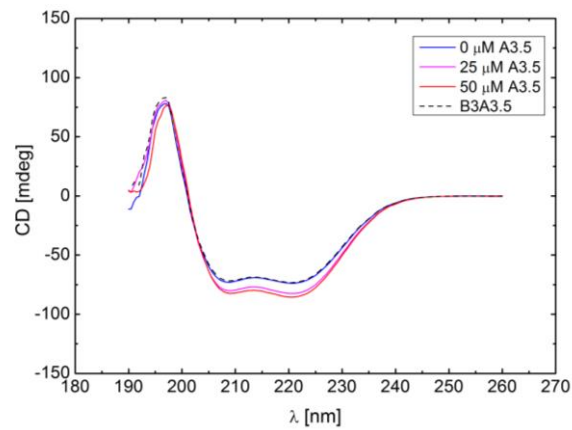
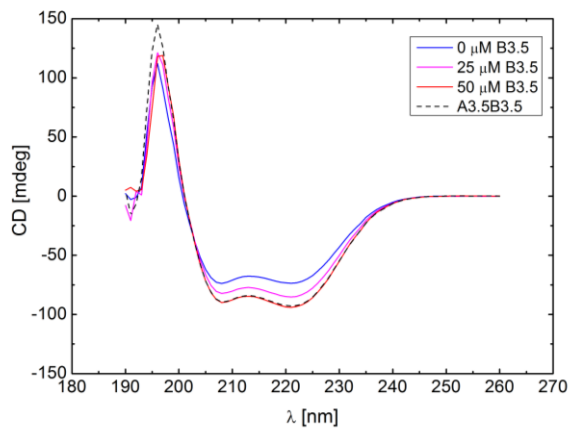
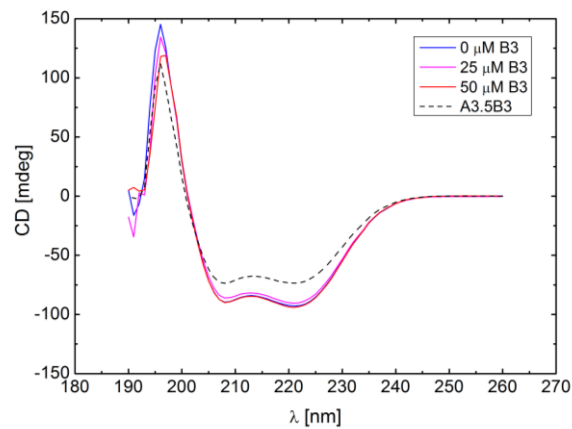
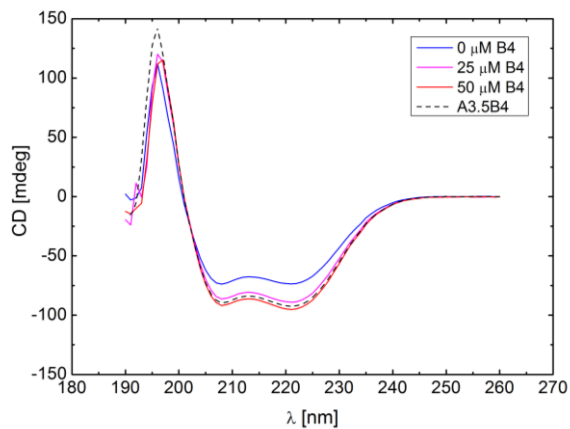
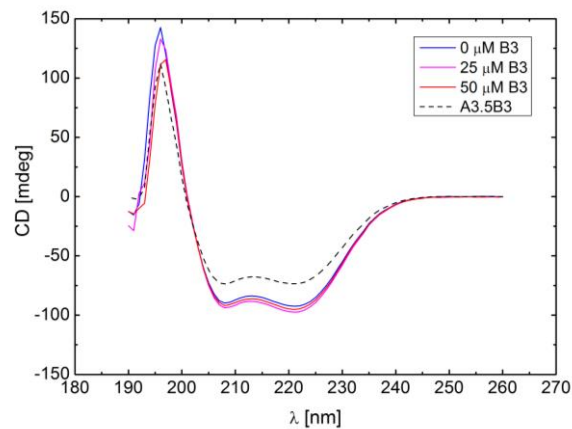
**Figure S3.** CD spectra of CD-titration experiments using the *N*-terminal truncated set of heterodimeric coiled coils. The most stable heterodimeric coiled coil is predominantly formed in solution.

**A** C-A<sub>3</sub>B<sub>3</sub>  $\uparrow\downarrow$  A<sub>3.5</sub>**B** C-A<sub>3.5</sub>B<sub>3</sub>  $\uparrow\downarrow$  A<sub>3</sub>**C** C-A<sub>3</sub>B<sub>3</sub>  $\uparrow\downarrow$  A<sub>4</sub>**D** C-A<sub>4</sub>B<sub>3</sub>  $\uparrow\downarrow$  A<sub>3</sub>**E** C-A<sub>3</sub>B<sub>3</sub>  $\uparrow\downarrow$  B<sub>3.5</sub>**F** C-A<sub>3</sub>B<sub>3.5</sub>  $\uparrow\downarrow$  B<sub>3</sub>

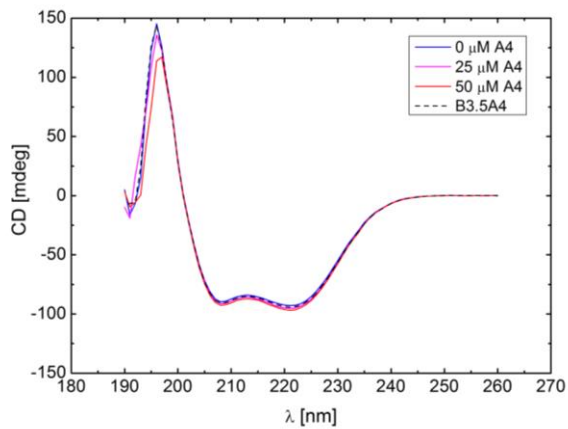


**G** C-A<sub>3</sub>B<sub>3</sub>  $\uparrow\downarrow$  B<sub>4</sub>**H** C-A<sub>3</sub>B<sub>4</sub>  $\uparrow\downarrow$  B<sub>3</sub>**I** C-A<sub>3</sub>B<sub>3.5</sub>  $\uparrow\downarrow$  A<sub>3.5</sub>**J** C-A<sub>3.5</sub>B<sub>3.5</sub>  $\uparrow\downarrow$  A<sub>3</sub>**K** C-A<sub>3</sub>B<sub>3.5</sub>  $\uparrow\downarrow$  A<sub>4</sub>**L** C-A<sub>4</sub>B<sub>3.5</sub>  $\uparrow\downarrow$  A<sub>3</sub>

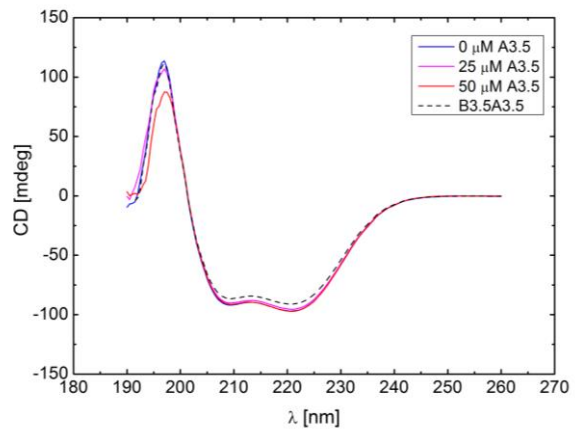
**M** C-A<sub>3</sub>B<sub>3.5</sub>  $\uparrow\downarrow$  B<sub>4</sub>**N** C-A<sub>3</sub>B<sub>4</sub>  $\uparrow\downarrow$  B<sub>3.5</sub>**O** C-A<sub>3</sub>B<sub>4</sub>  $\uparrow\downarrow$  A<sub>3.5</sub>**P** C-A<sub>3.5</sub>B<sub>4</sub>  $\uparrow\downarrow$  A<sub>3</sub>**Q** C-A<sub>3</sub>B<sub>4</sub>  $\uparrow\downarrow$  A<sub>4</sub>**R** C-A<sub>4</sub>B<sub>4</sub>  $\uparrow\downarrow$  A<sub>3</sub>

**S** C-A<sub>3.5</sub>B<sub>3</sub> ↑↓ A<sub>4</sub>**T** C-A<sub>4</sub>B<sub>3</sub> ↑↓ A<sub>3.5</sub>**U** C-A<sub>3.5</sub>B<sub>3</sub> ↑↓ B<sub>3.5</sub>**V** C-A<sub>3.5</sub>B<sub>3.5</sub> ↑↓ B<sub>3</sub>**W** C-A<sub>3.5</sub>B<sub>3</sub> ↑↓ B<sub>4</sub>**X** C-A<sub>3.5</sub>B<sub>4</sub> ↑↓ B<sub>3</sub>

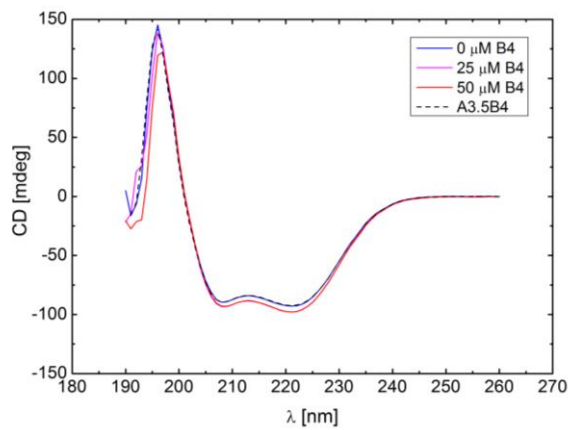
**Y** C-A<sub>3.5</sub>B<sub>3.5</sub>  $\uparrow\downarrow$  A<sub>4</sub>



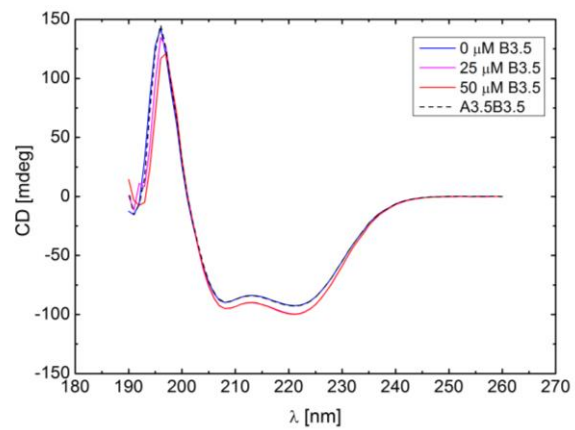
**Z** C-B<sub>3.5</sub>A<sub>4</sub>  $\uparrow\downarrow$  A<sub>3.5</sub>



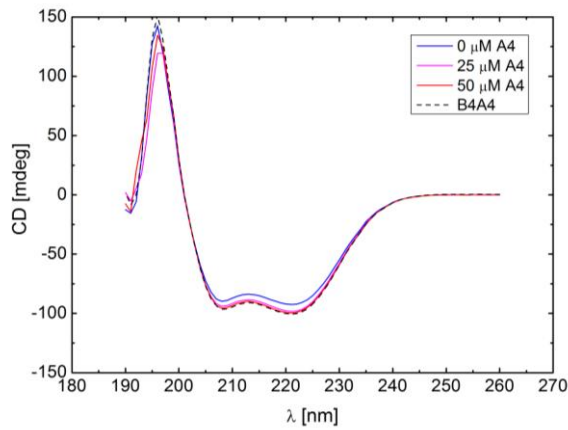
**Aa** C-A<sub>3.5</sub>B<sub>3.5</sub>  $\uparrow\downarrow$  B<sub>4</sub>



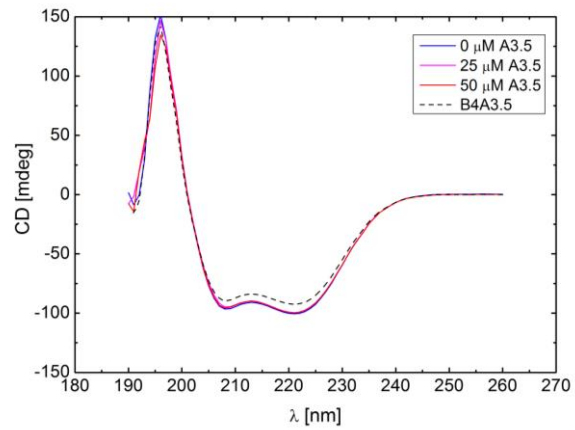
**Bb** C-A<sub>3.5</sub>B<sub>4</sub>  $\uparrow\downarrow$  B<sub>3.5</sub>



**Cc** C-A<sub>3.5</sub>B<sub>4</sub>  $\uparrow\downarrow$  A<sub>4</sub>



**Dd** C-A<sub>4</sub>B<sub>4</sub>  $\uparrow\downarrow$  A<sub>3.5</sub>



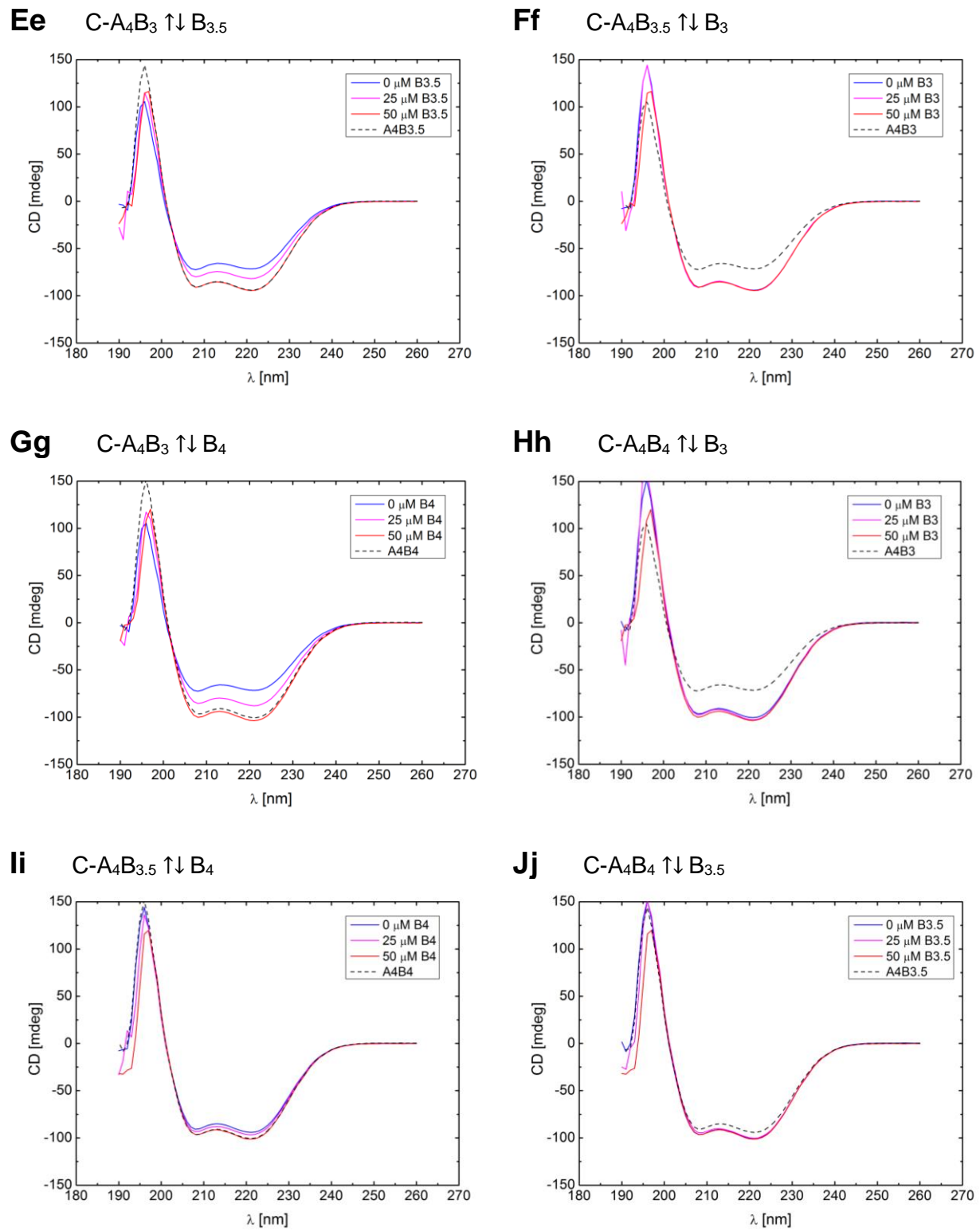


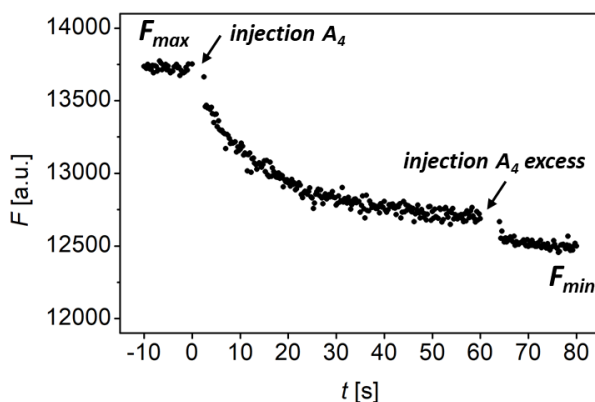
**Figure S4.** CD spectra of CD-titration experiments experiments using the C-terminal truncated set of heterodimeric coiled coils. The most stable heterodimeric coiled coil is predominantly formed in solution.

## 4. FRET-based strand-displacement assay

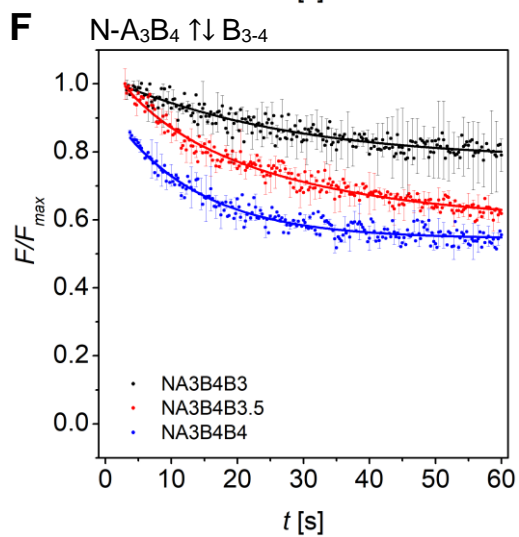
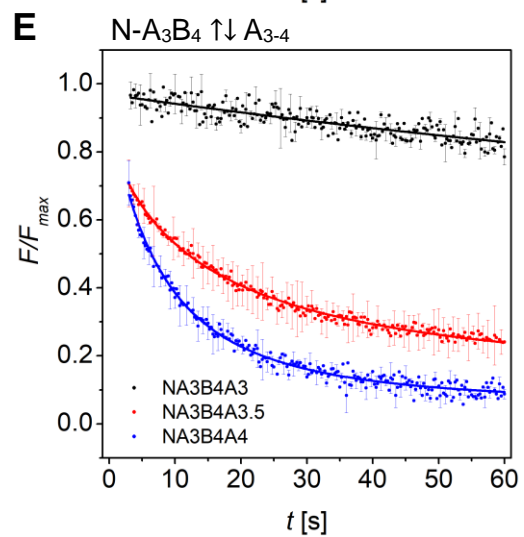
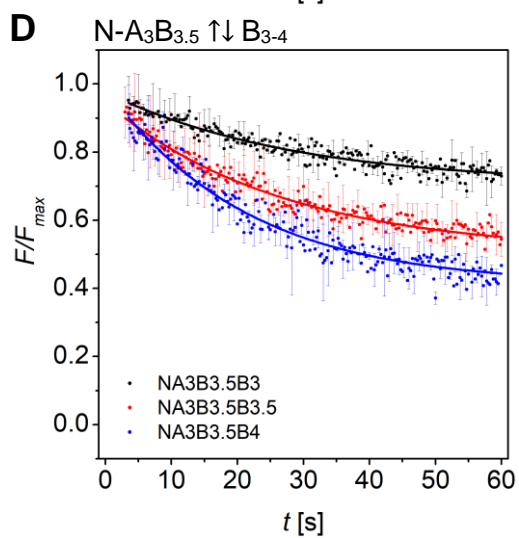
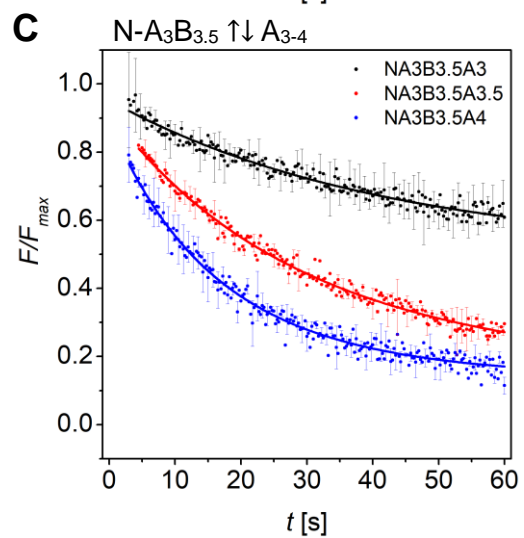
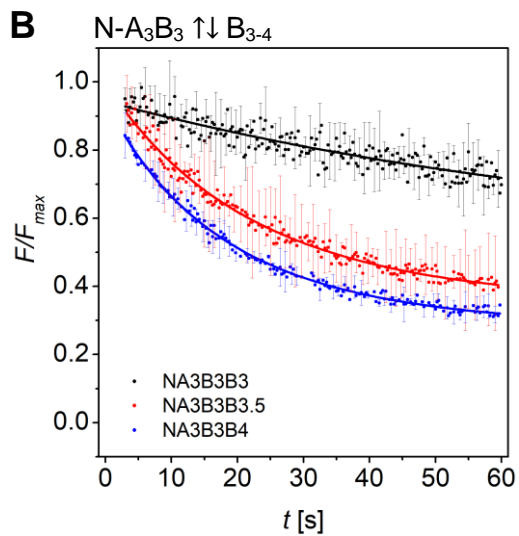
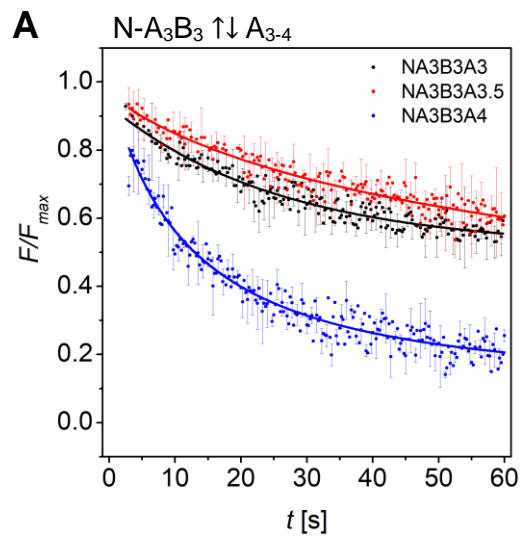
### *Time-resolved measurement of strand displacement monitored by FRET*

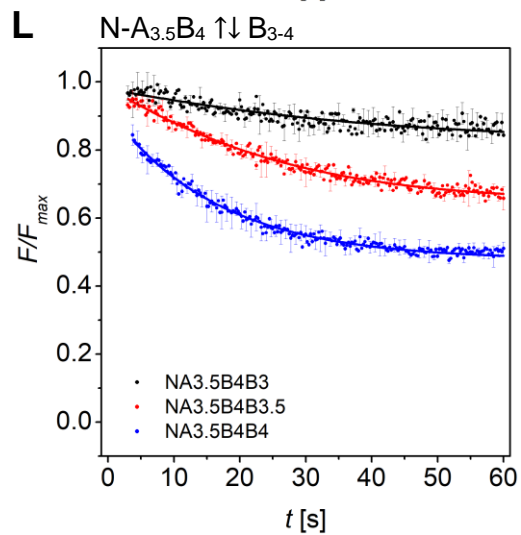
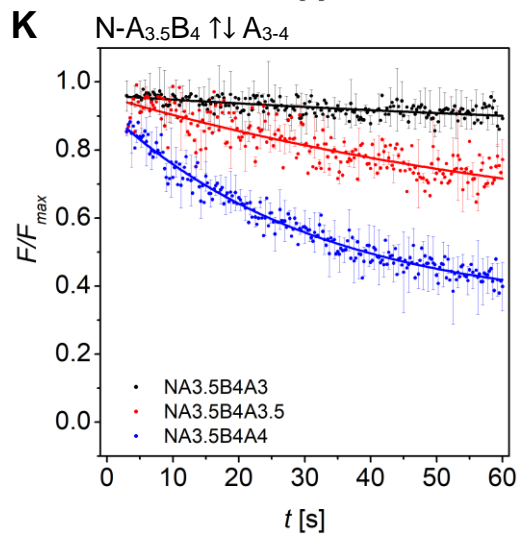
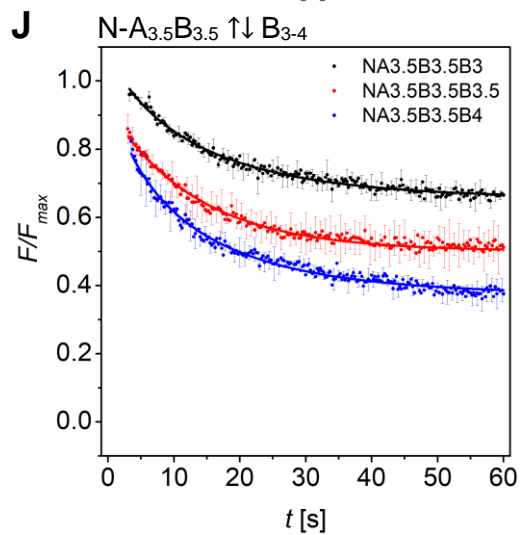
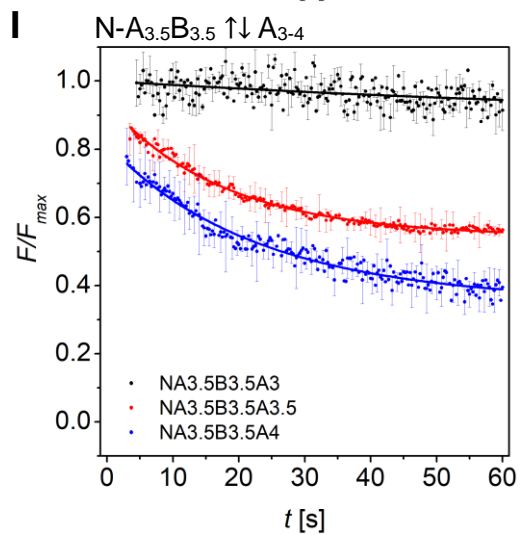
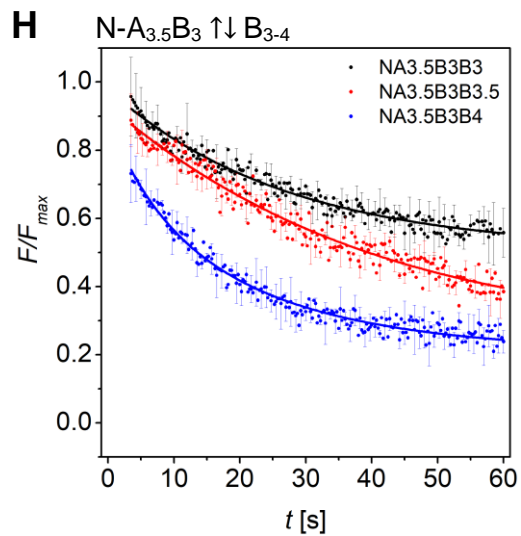
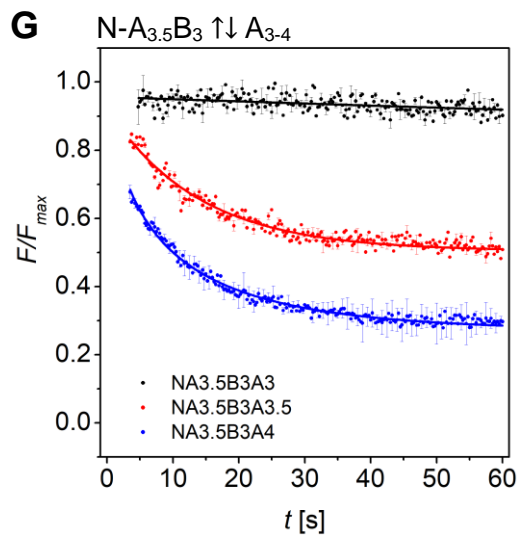
To measure strand-displacement kinetics, A strands with intrinsically fluorescent Trp and Dansyl-labelled B-strands were used as FRET-donor-acceptor pairs ( $\lambda_{\text{ex}} = 270 \text{ nm}$ ,  $\lambda_{\text{em}} = 540 \text{ nm}$ , Table S1). Labelled AB pairs were equilibrated at  $15 \mu\text{M}$  concentration in PBS at  $20 \text{ }^\circ\text{C}$  for 1 h and then at  $4 \text{ }^\circ\text{C}$  for another 15 h in *Microfluor 1* 96 well plates, which were treated with  $300 \mu\text{L}$  per well *Roche*<sup>®</sup> *Blocking reagent* ( $1 \text{ mg/mL}$ ) for 1 h and then washed with PBS ( $3 \times 100 \mu\text{L}$ ) prior to use. We used a *Clariostar* platereader from *BMG Labtech* equipped with a 1 mL dispenser to record decrease of the FRET signal as a result of strand exchange. Strand displacement was performed by injecting equimolar amounts of non-labeled A and B strands (competitor peptide  $P_{\text{comp}}$ ), respectively. First, maximum fluorescence ( $F_{\text{max}}$ ) over 50 s was measured. Then,  $1.5 \mu\text{L}$  of  $1 \text{ mM } P_{\text{comp}}$  were added and strand displacement was followed over 60 s at 540 nm. To obtain minimum fluorescence ( $F_{\text{min}}$ ), another  $5 \mu\text{L}$  of  $P_{\text{comp}}$  were added. Exemplarily, in Figure S5 time-resolved decrease of FRET signal in N-A<sub>3</sub>B<sub>4</sub> upon the addition of non-labelled A<sub>4</sub> is shown. The obtained data was baseline-corrected by  $F_{\text{min}}$ , normalized to  $F_{\text{max}}$  and fitted to a single exponential decay (equation 1, Figures S6-S7).

$$F = F_{\text{eq}} + F_0 e^{-k_{\text{obs}}/t} \quad (1)$$

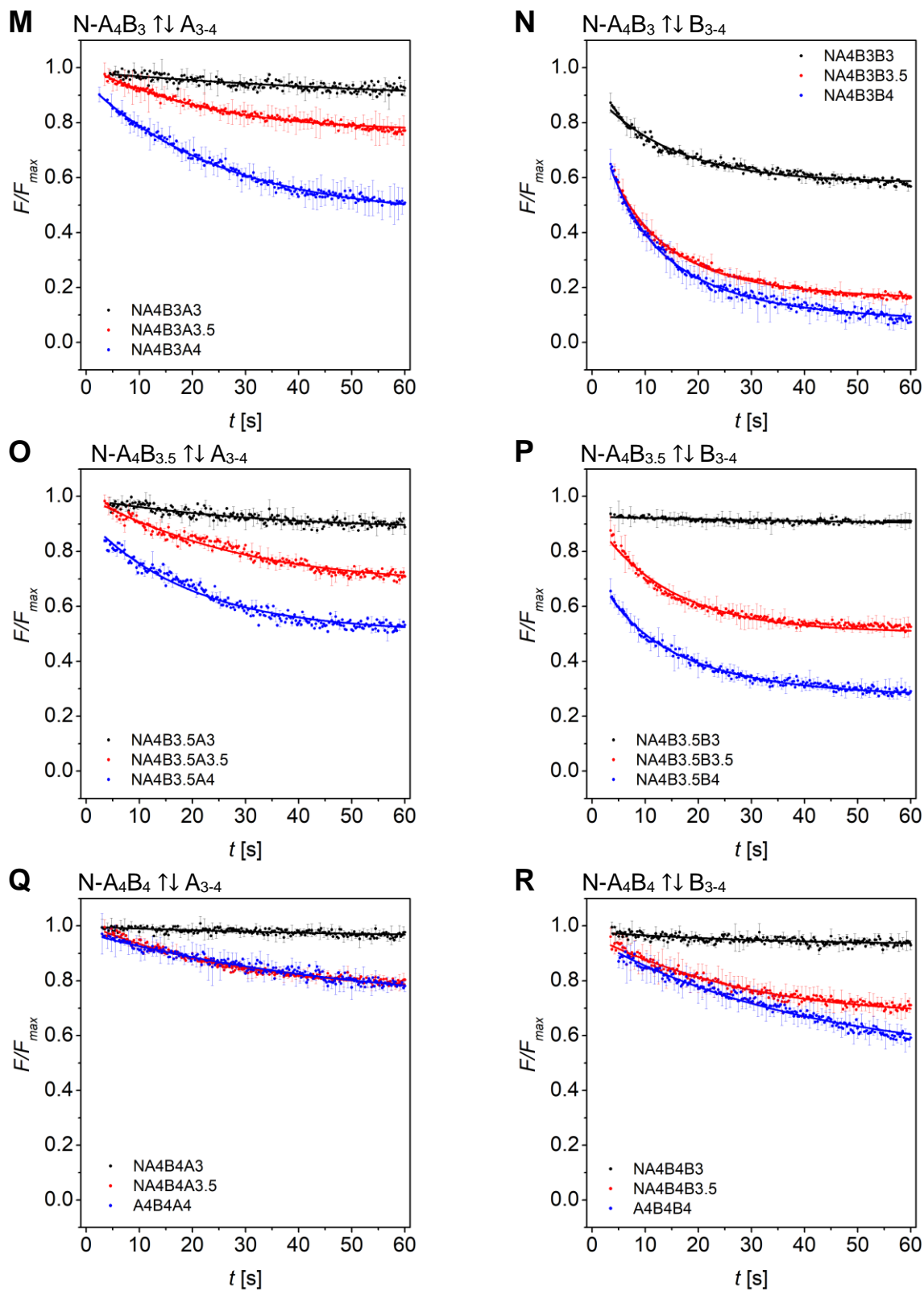


**Figure S5.** Strand displacement in N-A<sub>3</sub>B<sub>4</sub> by A<sub>4</sub>. Labelled N-A<sub>3</sub> and B<sub>4</sub> were equilibrated at  $15 \mu\text{M}$  peptide concentration in PBS. Change in Dansyl fluorescence was recorded at 540 nm. After 50 s equimolar amounts of non-labelled A<sub>4</sub> were added and fluorescence decrease was monitored for 60 s. To determine  $F_{\text{min}}$ , another  $5 \mu\text{L}$  non-labelled A<sub>4</sub> were added.

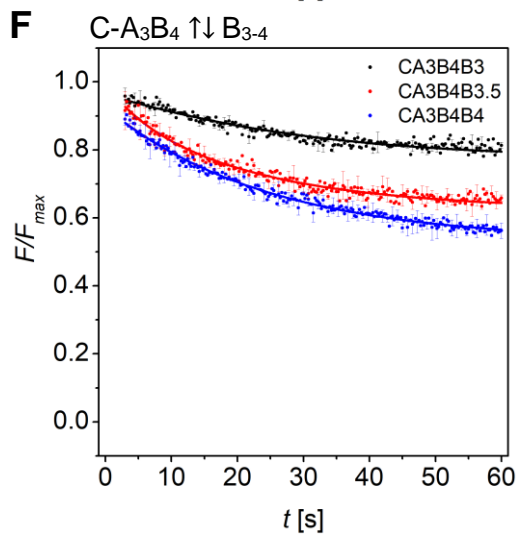
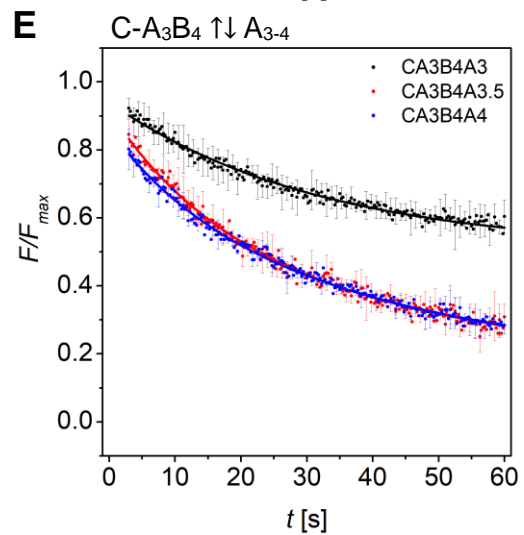
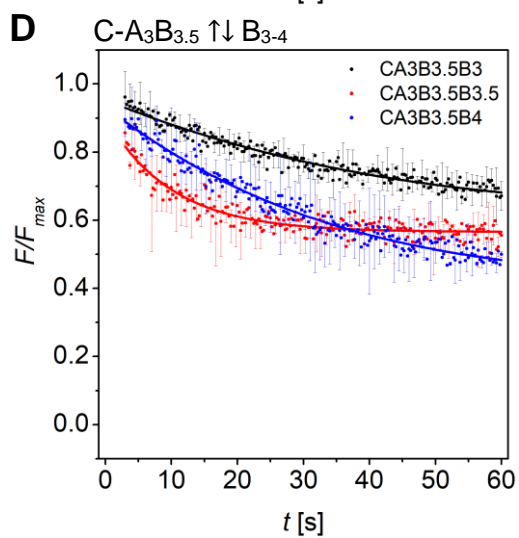
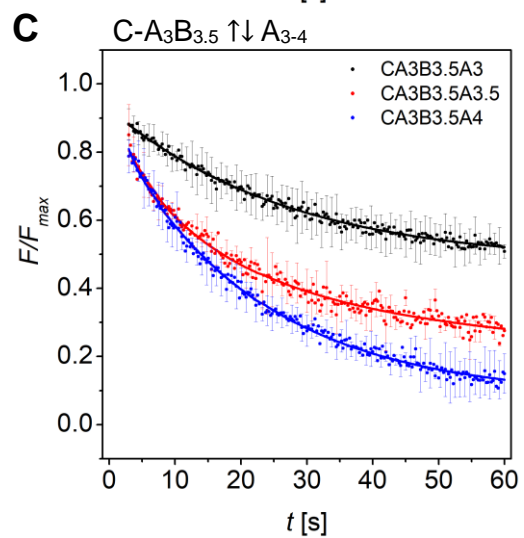
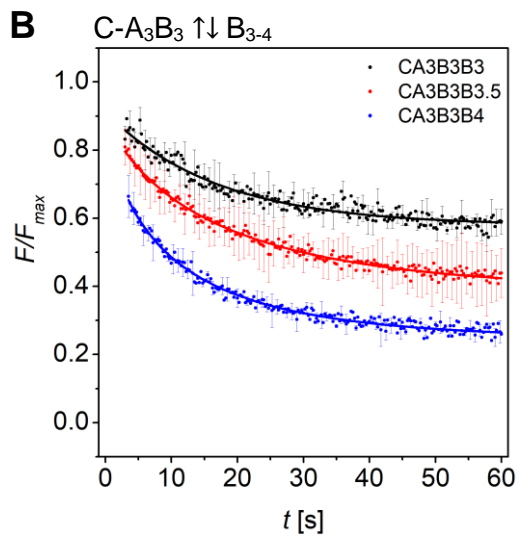
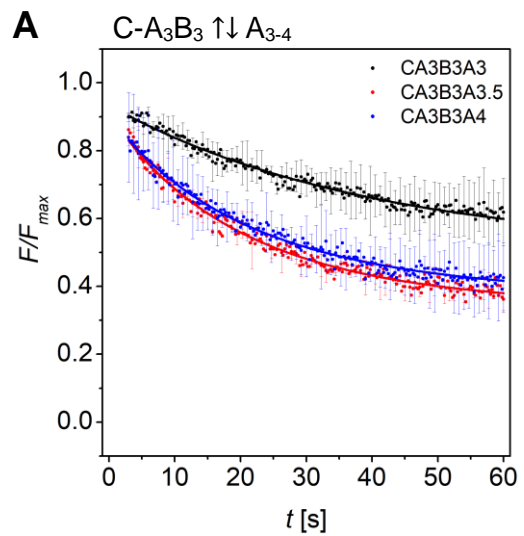


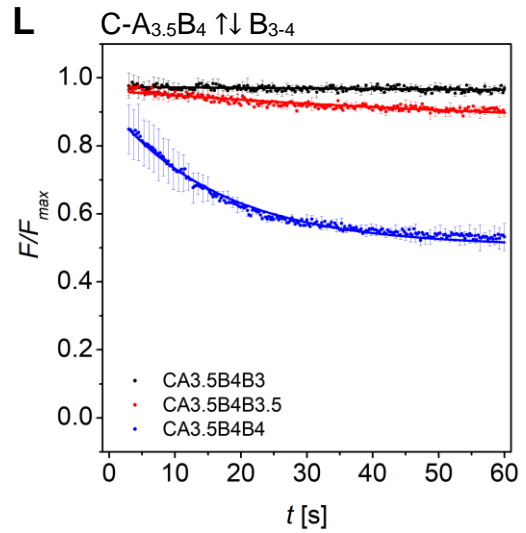
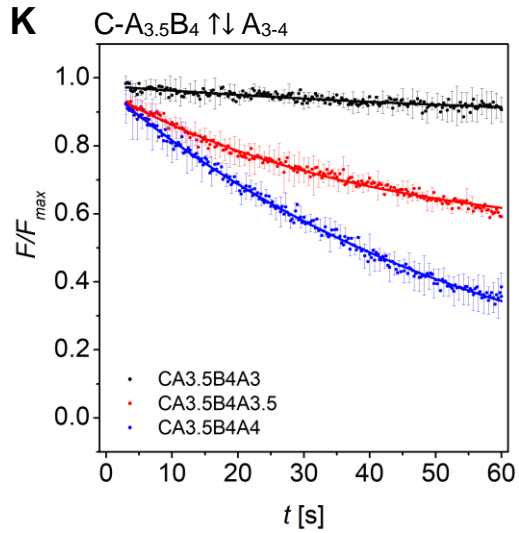
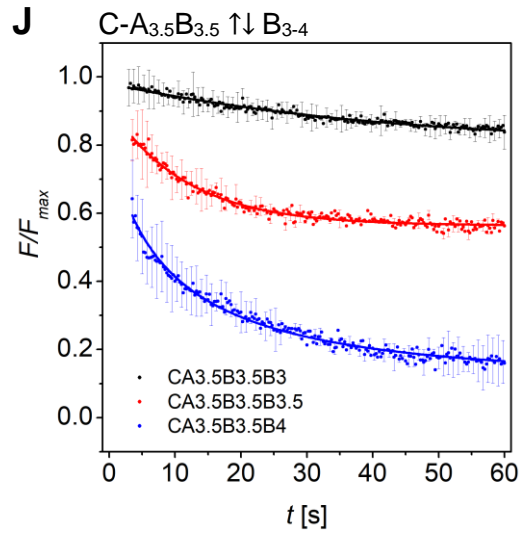
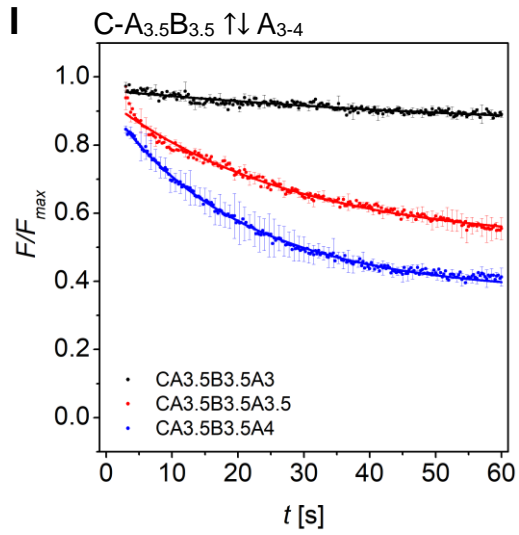
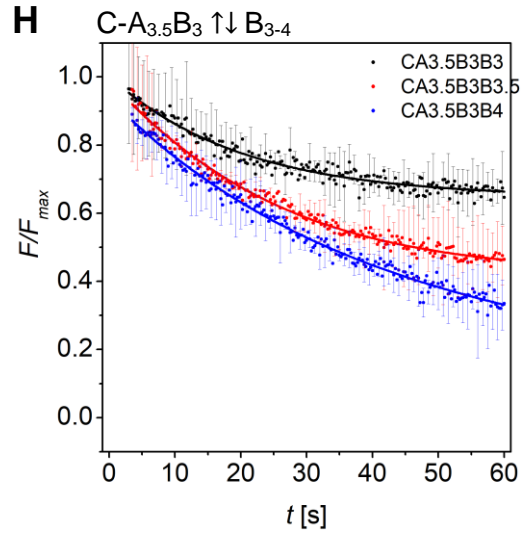
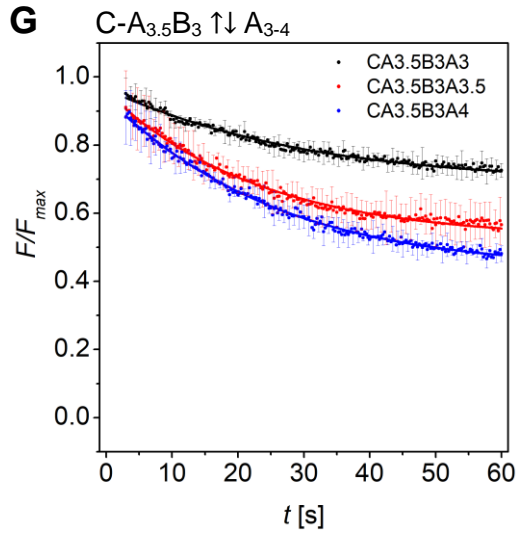






**Figure S6.** Normalized time-resolved fluorescence decrease upon strand displacement in N-A<sub>x</sub>B<sub>y</sub> peptides. Fluorescence data was recorded at Dansyl fluorescence at 540 nm ( $\lambda_{\text{ex}} = 270 \text{ nm}$ ). Data were baseline-corrected by  $F_{\text{min}}$  and normalized to  $F_{\text{max}}$ , respectively, and is the average of three measurements.





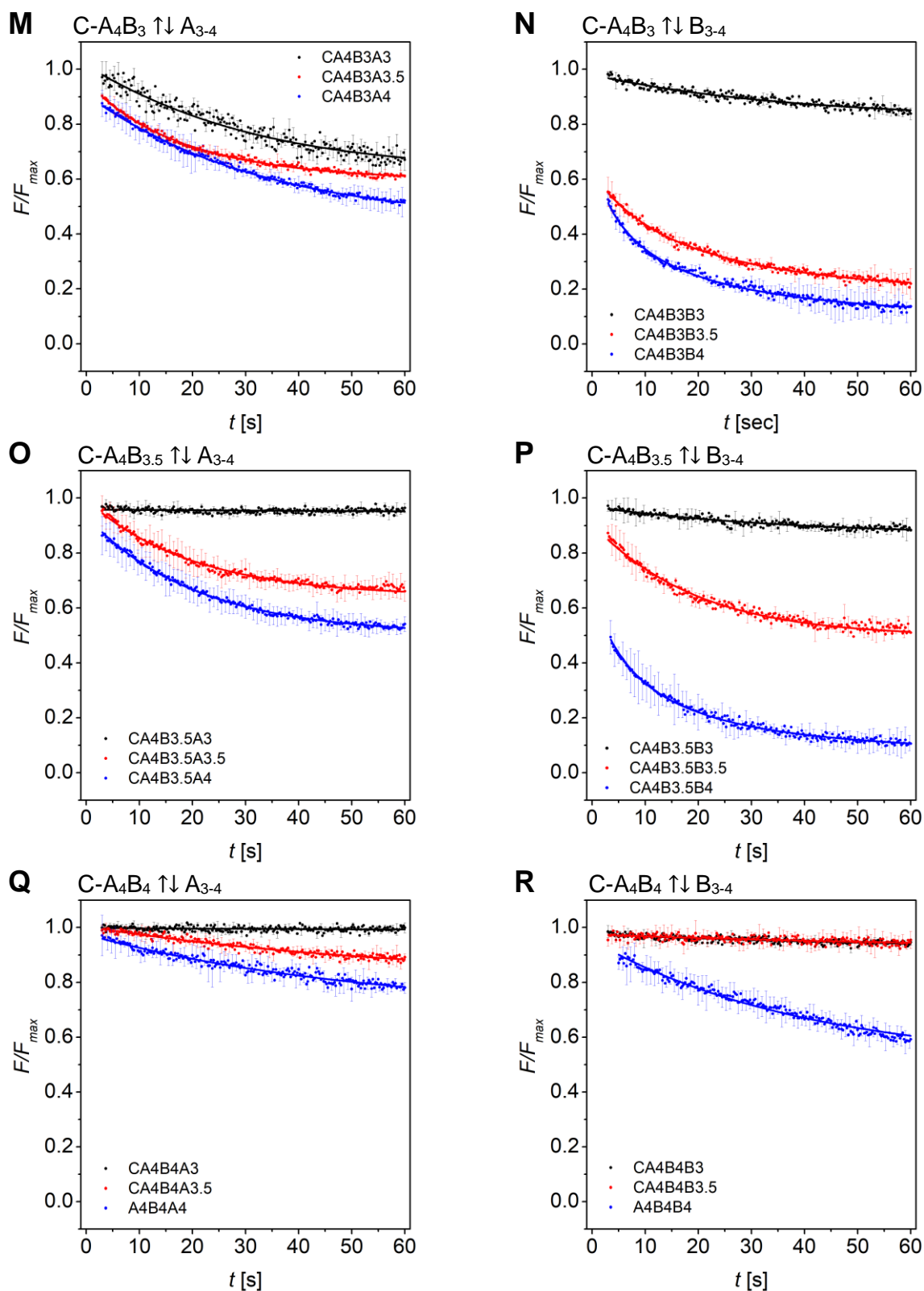


**Figure S7.** Normalized time-resolved fluorescence decrease upon strand displacement in C-A<sub>x</sub>B<sub>y</sub> peptides. Fluorescence data was recorded at Dansyl fluorescence at 540 nm ( $\lambda_{\text{ex}} = 270$  nm). Data were baseline-corrected by  $F_{\text{min}}$  and normalized to  $F_{\text{max}}$ , respectively, and is the average of three measurements.

**Table S5.** Best-fit values of observed rate constants ( $k_{obs}$ ) and half-lives ( $t_{1/2}$ ) of strand displacement in N-A<sub>x</sub>B<sub>y</sub> peptides. Values were obtained from a FRET-based kinetic assay and data fitting by a single exponential decay model ( $k_{obs}$ ,  $t_{1/2}$ ), and by a competitive binding model using DynaFit.<sup>2,3</sup> Overall affinities ( $k_1k_4/k_2k_3$ ) match well with the ratios of the  $K_D$  values determined from CD thermal denaturation curves.

N-A <sub>x</sub> B <sub>y</sub> peptide		P <sub>comp</sub>	$k_{obs}$ [s <sup>-1</sup> ]	$t_{1/2}$ [s]
N-A <sub>3</sub>	B <sub>3</sub>	A <sub>3</sub>	0.037 ± 0.003	17.3 ± 1.4
		A <sub>3.5</sub>	0.025 ± 0.003	27.7 ± 3.3
		A <sub>4</sub>	0.063 ± 0.003	11.0 ± 0.5
		B <sub>3</sub>	0.010 ± 0.004	69.3 ± 27.7
		B <sub>3.5</sub>	0.046 ± 0.002	15.1 ± 0.7
		B <sub>4</sub>	0.055 ± 0.001	12.6 ± 0.2
	B <sub>3.5</sub>	A <sub>3</sub>	0.025 ± 0.002	27.7 ± 2.2
		A <sub>3.5</sub>	0.032 ± 0.001	21.7 ± 0.5
		A <sub>4</sub>	0.058 ± 0.002	12.0 ± 0.4
		B <sub>3</sub>	0.033 ± 0.003	21.0 ± 1.9
		B <sub>3.5</sub>	0.045 ± 0.002	15.4 ± 0.7
		B <sub>4</sub>	0.042 ± 0.002	16.5 ± 0.8
	B <sub>4</sub>	A <sub>3</sub>	n.a. <sup>a</sup>	n.a. <sup>a</sup>
		A <sub>3.5</sub>	0.057 ± 0.001	12.2 ± 0.2
		A <sub>4</sub>	0.085 ± 0.002	8.2 ± 0.2
		B <sub>3</sub>	0.040 ± 0.004	17.3 ± 1.7
		B <sub>3.5</sub>	0.048 ± 0.002	14.4 ± 0.6
		B <sub>4</sub>	0.076 ± 0.004	9.1 ± 0.5
N-A <sub>3.5</sub>	B <sub>3</sub>	A <sub>3</sub>	n.a. <sup>a</sup>	n.a. <sup>a</sup>
		A <sub>3.5</sub>	0.082 ± 0.003	8.5 ± 0.3
		A <sub>4</sub>	0.087 ± 0.002	8.0 ± 0.2
		B <sub>3</sub>	0.037 ± 0.002	18.7 ± 1.0
		B <sub>3.5</sub>	0.029 ± 0.003	23.9 ± 2.5
		B <sub>4</sub>	0.064 ± 0.002	10.8 ± 0.3
	B <sub>3.5</sub>	A <sub>3</sub>	n.a. <sup>a</sup>	n.a. <sup>a</sup>
		A <sub>3.5</sub>	0.056 ± 0.001	12.4 ± 0.2
		A <sub>4</sub>	0.045 ± 0.002	15.4 ± 0.7
		B <sub>3</sub>	0.068 ± 0.002	10.2 ± 0.3
		B <sub>3.5</sub>	0.085 ± 0.002	8.2 ± 0.2
		B <sub>4</sub>	0.071 ± 0.002	9.8 ± 0.3
	B <sub>4</sub>	A <sub>3</sub>	n.a. <sup>a</sup>	n.a. <sup>a</sup>
		A <sub>3.5</sub>	0.024 ± 0.005	28.9 ± 6.0
		A <sub>4</sub>	0.033 ± 0.001	21.0 ± 0.6
		B <sub>3</sub>	0.048 ± 0.005	14.4 ± 1.5
		B <sub>3.5</sub>	0.040 ± 0.002	17.3 ± 0.9
		B <sub>4</sub>	0.065 ± 0.001	10.7 ± 0.2
N-A <sub>4</sub>	B <sub>3</sub>	A <sub>3</sub>	0.032 ± 0.008	21.7 ± 5.4
		A <sub>3.5</sub>	0.033 ± 0.001	21.0 ± 0.6
		A <sub>4</sub>	0.039 ± 0.001	17.8 ± 0.5
		B <sub>3</sub>	0.068 ± 0.002	10.2 ± 0.3
		B <sub>3.5</sub>	0.079 ± 0.001	8.8 ± 0.1
		B <sub>4</sub>	0.080 ± 0.001	8.7 ± 0.1
	B <sub>3.5</sub>	A <sub>3</sub>	0.034 ± 0.006	20.4 ± 3.6
		A <sub>3.5</sub>	0.027 ± 0.002	25.7 ± 1.9
		A <sub>4</sub>	0.043 ± 0.002	16.1 ± 0.7
		B <sub>3</sub>	n.a. <sup>a</sup>	n.a. <sup>a</sup>
		B <sub>3.5</sub>	0.092 ± 0.001	7.5 ± 0.1
		B <sub>4</sub>	0.072 ± 0.001	9.6 ± 0.1
	B <sub>4</sub>	A <sub>3</sub>	n.a. <sup>a</sup>	n.a. <sup>a</sup>
		A <sub>3.5</sub>	0.042 ± 0.002	16.5 ± 0.8
		A <sub>4</sub>	0.019 ± 0.002	36.5 ± 3.8
		B <sub>3</sub>	n.a. <sup>a</sup>	n.a. <sup>a</sup>
		B <sub>3.5</sub>	0.042 ± 0.002	16.5 ± 0.8
		B <sub>4</sub>	0.012 ± 0.001	57.8 ± 4.8

<sup>a</sup>Data did not fit the single exponential model.

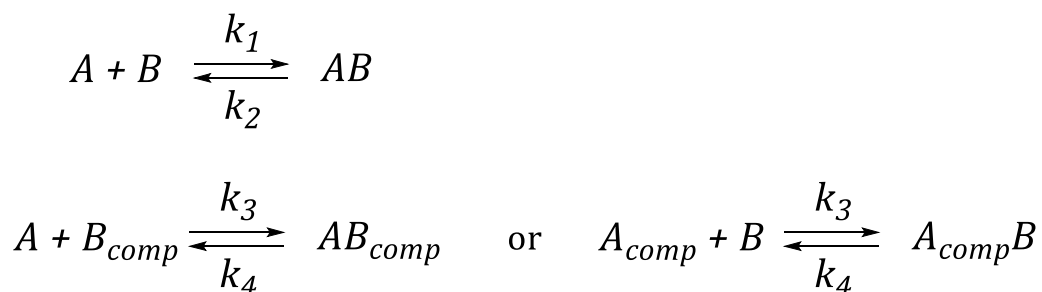
**Table S6.** Best-fit values of observed rate constants ( $k_{obs}$ ) and half-lives ( $t_{1/2}$ ) of strand displacement in C-A<sub>x</sub>B<sub>y</sub> peptides. Values were obtained from a FRET-based kinetic assay and data fitting by a single exponential decay model ( $k_{obs}$ ,  $t_{1/2}$ ), and by a competitive binding model using DynaFit.<sup>2,3</sup> Overall affinities ( $k_1k_4/k_2k_3$ ) match well with the ratios of the  $K_D$  values determined from CD thermal denaturation curves.

C-A <sub>x</sub> B <sub>y</sub> peptide		P <sub>comp</sub>	$k_{obs}$ [s <sup>-1</sup> ]	$t_{1/2}$ [s]
C-A <sub>3</sub>	B <sub>3</sub>	A <sub>3</sub>	0.034 ± 0.002	20.4 ± 1.2
		A <sub>3.5</sub>	0.050 ± 0.002	13.9 ± 0.6
		A <sub>4</sub>	0.044 ± 0.001	15.8 ± 0.4
		B <sub>3</sub>	0.059 ± 0.003	11.7 ± 0.6
		B <sub>3.5</sub>	0.057 ± 0.002	12.2 ± 0.4
		B <sub>4</sub>	0.078 ± 0.002	8.9 ± 0.2
	B <sub>3.5</sub>	A <sub>3</sub>	0.037 ± 0.001	18.7 ± 0.5
		A <sub>3.5</sub>	0.055 ± 0.002	12.6 ± 0.5
		A <sub>4</sub>	0.048 ± 0.001	14.4 ± 0.3
		B <sub>3</sub>	0.033 ± 0.002	21.0 ± 1.3
		B <sub>3.5</sub>	0.102 ± 0.006	6.8 ± 0.4
		B <sub>4</sub>	0.031 ± 0.002	22.4 ± 1.4
	B <sub>4</sub>	A <sub>3</sub>	0.039 ± 0.001	17.8 ± 0.5
		A <sub>3.5</sub>	0.039 ± 0.001	17.8 ± 0.5
		A <sub>4</sub>	0.036 ± 0.001	19.3 ± 0.5
		B <sub>3</sub>	0.050 ± 0.003	13.9 ± 0.8
		B <sub>3.5</sub>	0.060 ± 0.002	11.6 ± 0.4
		B <sub>4</sub>	0.041 ± 0.001	16.9 ± 0.4
C-A <sub>3.5</sub>	B <sub>3</sub>	A <sub>3</sub>	0.041 ± 0.001	16.9 ± 0.4
		A <sub>3.5</sub>	0.050 ± 0.001	13.9 ± 0.3
		A <sub>4</sub>	0.040 ± 0.001	17.3 ± 0.4
		B <sub>3</sub>	0.050 ± 0.002	13.9 ± 0.6
		B <sub>3.5</sub>	0.040 ± 0.001	17.3 ± 0.4
		B <sub>4</sub>	0.024 ± 0.001	28.9 ± 1.2
	B <sub>3.5</sub>	A <sub>3</sub>	0.030 ± 0.004	23.1 ± 3.1
		A <sub>3.5</sub>	0.036 ± 0.001	19.3 ± 0.5
		A <sub>4</sub>	0.053 ± 0.001	13.1 ± 0.3
		B <sub>3</sub>	0.032 ± 0.002	21.7 ± 1.4
		B <sub>3.5</sub>	0.088 ± 0.003	7.9 ± 0.3
		B <sub>4</sub>	0.060 ± 0.002	11.6 ± 0.4
	B <sub>4</sub>	A <sub>3</sub>	n.a. <sup>a</sup>	n.a. <sup>a</sup>
		A <sub>3.5</sub>	0.022 ± 0.001	31.5 ± 1.4
		A <sub>4</sub>	0.017 ± 0.001	40.8 ± 2.4
		B <sub>3</sub>	n.a. <sup>a</sup>	n.a. <sup>a</sup>
		B <sub>3.5</sub>	0.046 ± 0.004	15.1 ± 1.3
		B <sub>4</sub>	0.074 ± 0.001	9.4 ± 0.1
C-A <sub>4</sub>	B <sub>3</sub>	A <sub>3</sub>	0.025 ± 0.003	27.7 ± 3.3
		A <sub>3.5</sub>	0.054 ± 0.001	12.8 ± 0.2
		A <sub>4</sub>	0.030 ± 0.001	23.1 ± 0.8
		B <sub>3</sub>	0.026 ± 0.003	26.7 ± 3.1
		B <sub>3.5</sub>	0.054 ± 0.001	12.8 ± 0.2
		B <sub>4</sub>	0.063 ± 0.002	11.0 ± 0.3
	B <sub>3.5</sub>	A <sub>3</sub>	n.a. <sup>a</sup>	n.a. <sup>a</sup>
		A <sub>3.5</sub>	0.059 ± 0.001	11.7 ± 0.2
		A <sub>4</sub>	0.049 ± 0.001	14.1 ± 0.3
		B <sub>3</sub>	0.034 ± 0.004	20.4 ± 2.4
		B <sub>3.5</sub>	0.061 ± 0.002	11.4 ± 0.4
		B <sub>4</sub>	0.067 ± 0.001	10.3 ± 0.2
	B <sub>4</sub>	A <sub>3</sub>	n.a. <sup>a</sup>	n.a. <sup>a</sup>
		A <sub>3.5</sub>	0.018 ± 0.002	38.5 ± 4.3
		A <sub>4</sub>	0.019 ± 0.002	36.5 ± 3.8
		B <sub>3</sub>	n.a. <sup>a</sup>	n.a. <sup>a</sup>
		B <sub>3.5</sub>	n.a. <sup>a</sup>	n.a. <sup>a</sup>
		B <sub>4</sub>	0.012 ± 0.001	57.8 ± 4.8

<sup>a</sup>Data did not fit the single exponential model.

### *Kinetic analysis of the time-resolved displacement using DynaFit*

Fluorescence data of time-resolved strand displacement were fit to a competitive binding model using the fitting software DynaFit.<sup>2,3</sup> DynaFit uses a general numerical method for the determination of rate constants that characterize simultaneous and competitive binding of a ligand to two receptors R<sub>1</sub> and R<sub>2</sub> presuming a dissociative pathway for receptor displacement. In the context of heterodimeric coiled coils of the type AB R<sub>1</sub> and R<sub>2</sub> can be regarded as A and A<sub>comp</sub> or as B and B<sub>comp</sub>, respectively. A dissociative pathway for coil-strand displacement can be presumed as the underlying coiled-coil design results in non-promiscuous coiled-coil interaction.



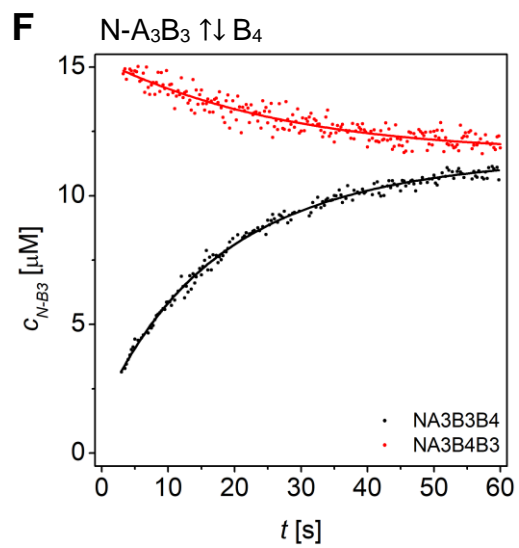
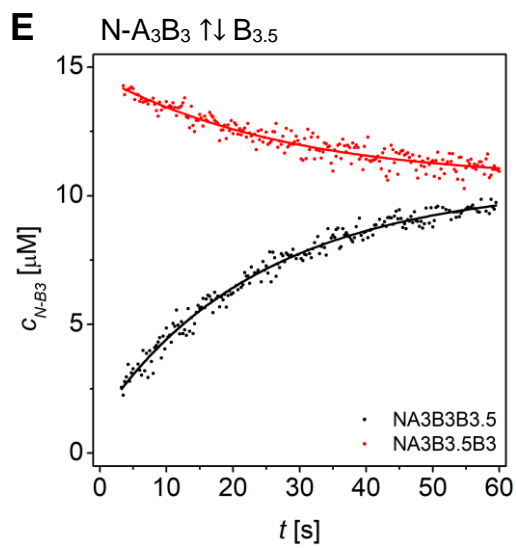
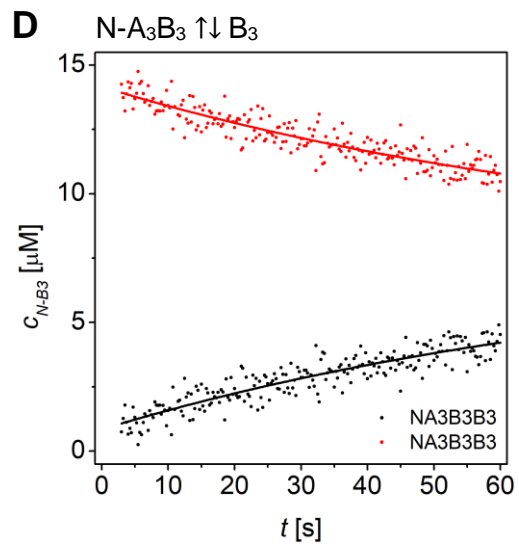
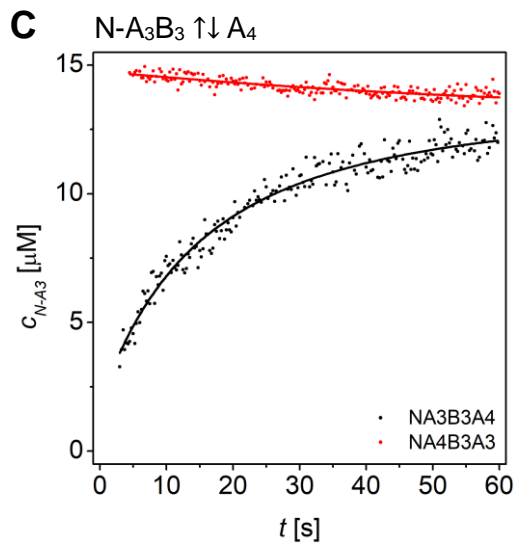
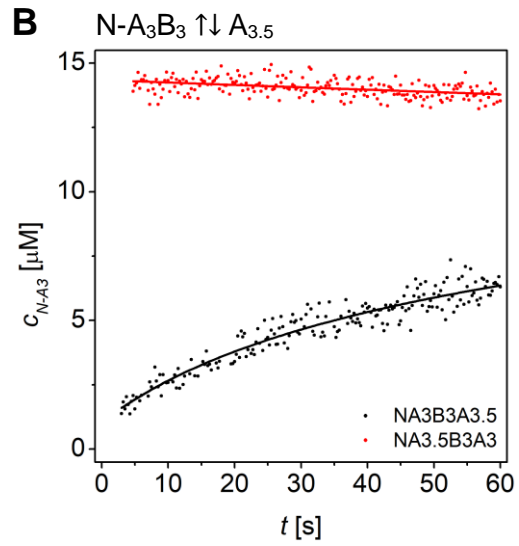
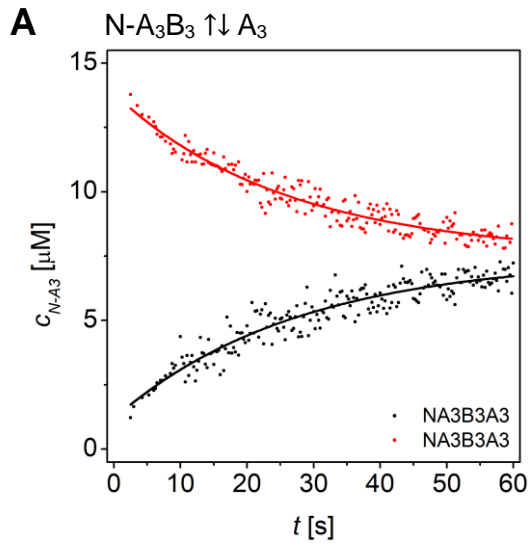
**Scheme S1.** Presumed dissociative mechanism of strand-displacement in AB heterodimeric coiled coils.

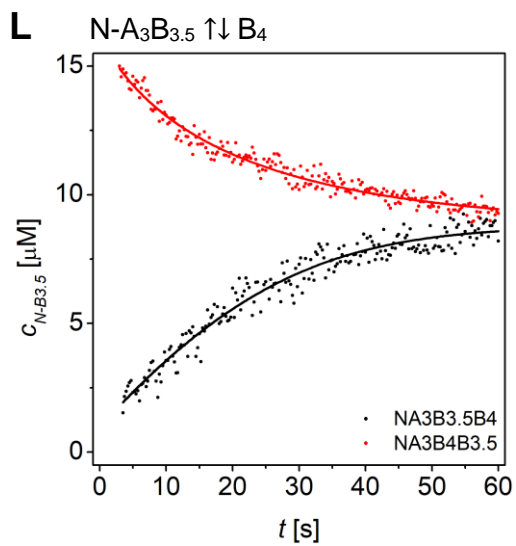
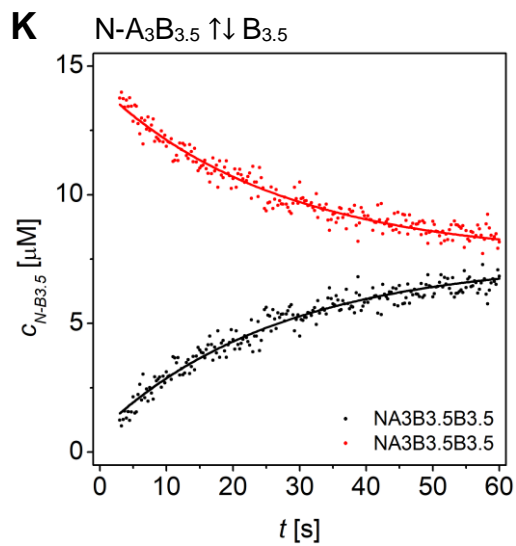
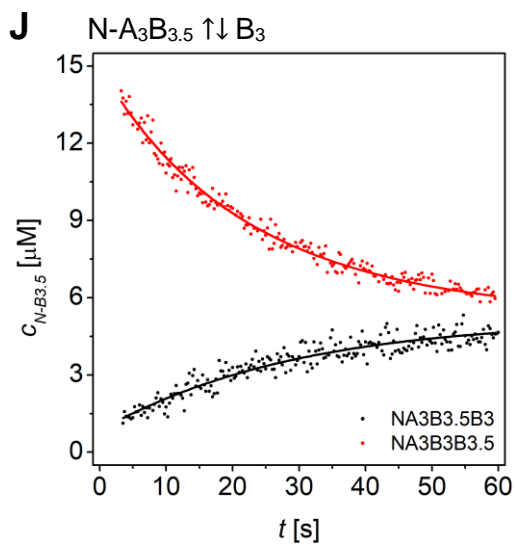
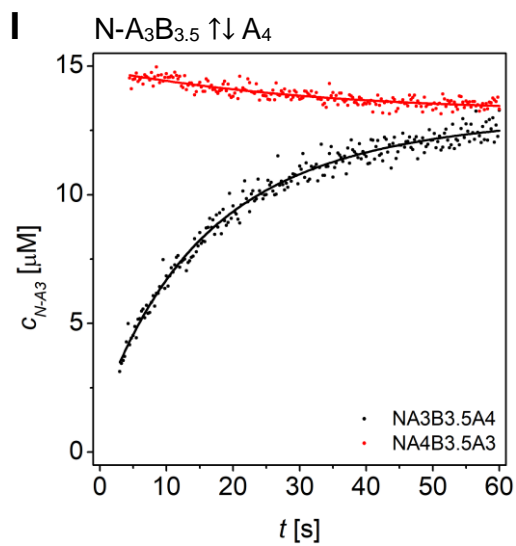
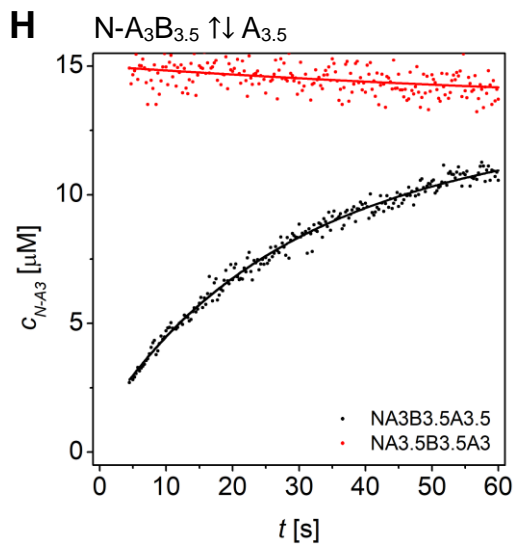
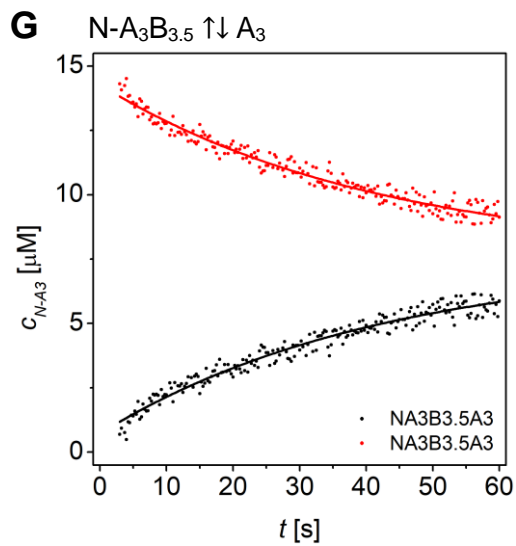
The time-resolved fluorescence data was converted into concentration of free A or B in the time course of displacement by A<sub>comp</sub> or B<sub>comp</sub> and competitive reformation of the AB coiled coil. Therefore,  $F_{max}$  was assigned to zero conversion of the initial AB coiled-coil complex (15 μM AB and 15 μM P<sub>comp</sub>) and  $F_{min}$  was assigned to full strand displacement in AB (15 μM AB<sub>comp</sub> or A<sub>comp</sub>B and 15 μM A or B) to AP<sub>comp</sub> or P<sub>comp</sub>B, respectively. We presumed that strand-displacement kinetics are the same in coiled coils of the same lengths of the individual strands whether or not labelled or unlabelled. Fitting of both events, displacement of A or B from the initial AB complex and re-association, gives relative rate constants  $k_1$  to  $k_4$  from which the overall affinities ( $k_1k_4/k_2k_3$ ) can be calculated. The results are summarized in tables S5 and S6. The curve fitting is shown in figures S8-S13.

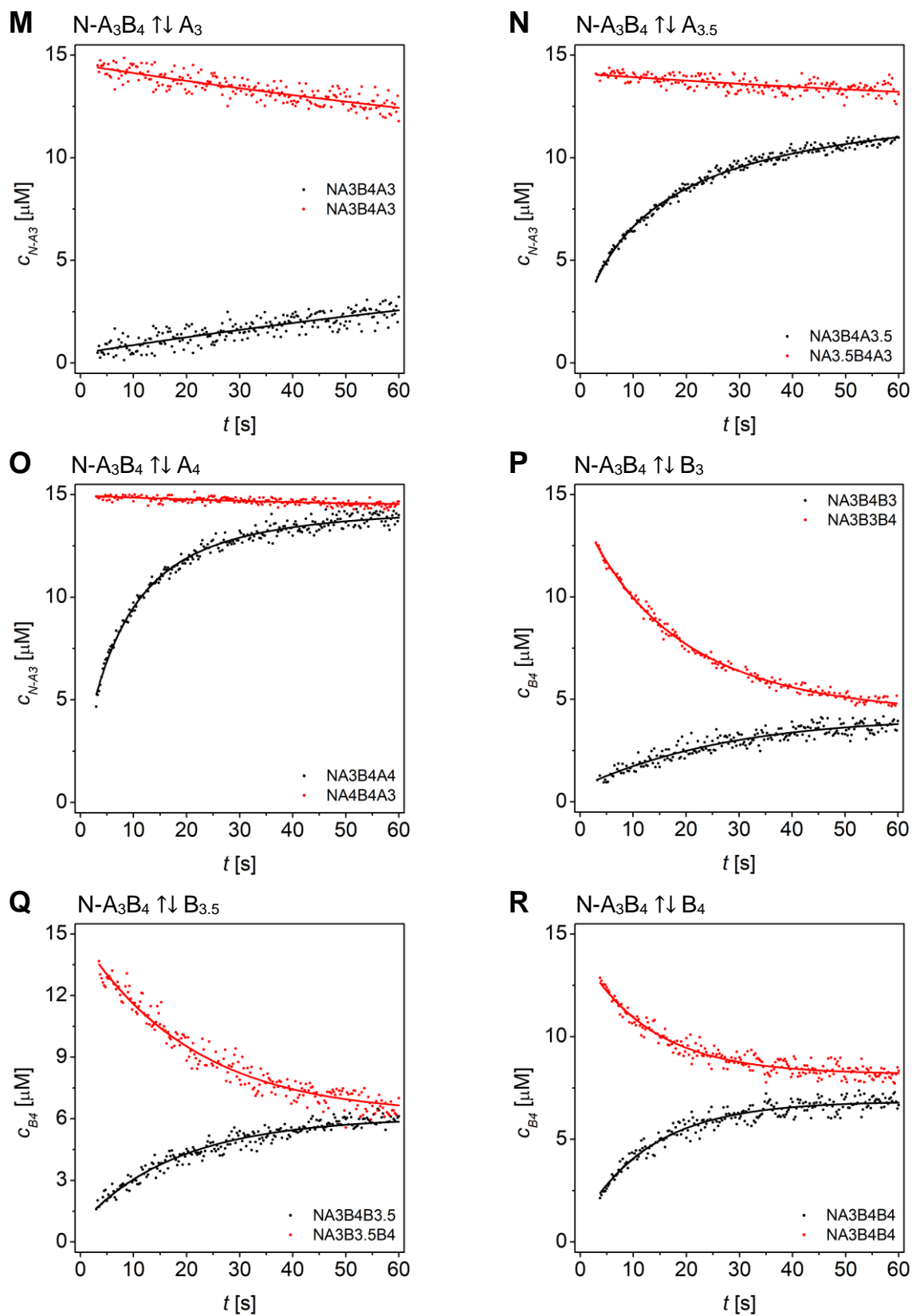
**Table S 7.** Best-fit values of rate constants of competitive strand displacement in N-A<sub>x</sub>B<sub>y</sub> peptides obtained from DynaFit analysis. Ratio of overall affinities ( $k_1k_4/k_2k_3$ ) matches well with the ratio of the  $K_D$  values determined from CD thermal denaturation curves.  $P_{comp}$  is the general term for peptide competitor (A<sub>comp</sub> or B<sub>comp</sub>).

AB peptide	$P_{comp}$	$k_1 [\mu M^{-1}s^{-1}]$	$k_2 [s^{-1}]$	$k_3 [\mu M^{-1}s^{-1}]$	$k_4 [s^{-1}]$	$k_1k_4/k_2k_3$	$K_D(comp)/K_D$	
N-A <sub>3</sub>	B <sub>3</sub>	A <sub>3</sub>	0.14 ± 0.05	0.02 ± 0.002	0.15 ± 0.04	0.02 ± 0.002	0.93	1.0
		A <sub>3.5</sub>	0.16 ± 0.08	0.019 ± 0.004	0.05 ± 0.01	$(7.0 \pm 1.2) \cdot 10^{-4}$	0.12	0.18
		A <sub>4</sub>	0.19 ± 0.07	0.064 ± 0.004	0.28 ± 0.08	$(1.7 \pm 0.2) \cdot 10^{-3}$	0.02	0.06
		B <sub>3</sub>	0.10 ± 0.03	$(6.0 \pm 0.8) \cdot 10^{-3}$	0.10 ± 0.04	$(6.0 \pm 0.8) \cdot 10^{-3}$	1.0	1.0
		B <sub>3.5</sub>	0.20 ± 0.05	0.03 ± 0.002	0.38 ± 0.06	0.01 ± 0.0008	0.18	0.43
	B <sub>4</sub>	0.21 ± 0.05	0.04 ± 0.002	0.32 ± 0.07	$(9.0 \pm 0.6) \cdot 10^{-3}$	0.15	0.20	
	B <sub>3.5</sub>	A <sub>3</sub>	0.29 ± 0.08	0.012 ± 0.0007	0.29 ± 0.06	0.012 ± 0.0007	1.0	1.0
		A <sub>3.5</sub>	0.30 ± 0.13	0.03 ± 0.002	0.80 ± 0.24	$(1.2 \pm 0.2) \cdot 10^{-3}$	0.02	0.003
		A <sub>4</sub>	0.28 ± 0.07	0.056 ± 0.002	0.88 ± 0.17	$(3.4 \pm 0.3) \cdot 10^{-3}$	0.02	< 0.001
		B <sub>3</sub>	0.20 ± 0.05	0.01 ± 0.0007	0.13 ± 0.03	0.03 ± 0.002	4.6	2.3
		B <sub>3.5</sub>	0.36 ± 0.12	0.02 ± 0.001	0.36 ± 0.10	0.02 ± 0.001	1.0	1.0
	B <sub>4</sub>	0.36 ± 0.11	0.024 ± 0.001	0.77 ± 0.19	0.023 ± 0.002	0.45	0.46	
	B <sub>4</sub>	A <sub>3</sub>	0.18 ± 0.08	$(3.0 \pm 0.5) \cdot 10^{-3}$	0.18 ± 0.21	$(3.0 \pm 0.5) \cdot 10^{-3}$	1.0	1.0
		A <sub>3.5</sub>	0.20 ± 0.08	0.10 ± 0.01	0.09 ± 0.03	$(1.4 \pm 0.1) \cdot 10^{-3}$	0.03	0.001
		A <sub>4</sub>	0.37 ± 0.11	0.11 ± 0.004	1.18 ± 0.29	$(7.4 \pm 1.2) \cdot 10^{-4}$	0.02	< 0.001
		B <sub>3</sub>	0.22 ± 0.05	$(8.5 \pm 0.5) \cdot 10^{-3}$	0.14 ± 0.03	0.04 ± 0.003	7.4	5.1
		B <sub>3.5</sub>	0.43 ± 0.21	0.022 ± 0.002	0.20 ± 0.09	0.029 ± 0.002	2.8	2,27
		B <sub>4</sub>	0.44 ± 0.3	0.041 ± 0.02	0.43 ± 0.34	0.041 ± 0.007	1.0	1.0
N-A <sub>3.5</sub>	B <sub>3</sub>	A <sub>3</sub>	0.06 ± 0.02	$(6.8 \pm 1.1) \cdot 10^{-4}$	0.21 ± 0.11	0.02 ± 0.004	8.4	5.5
		A <sub>3.5</sub>	0.28 ± 0.09	0.036 ± 0.003	0.28 ± 0.08	0.037 ± 0.003	1.03	1.0
		A <sub>4</sub>	0.46 ± 0.17	0.11 ± 0.006	0.29 ± 0.11	$(9.5 \pm 0.5) \cdot 10^{-3}$	0.14	0.32
		B <sub>3</sub>	0.27 ± 0.09	0.017 ± 0.01	0.26 ± 0.3	0.017 ± 0.006	1.04	1.0
		B <sub>3.5</sub>	0.16 ± 0.03	0.02 ± 0.0009	0.99 ± 0.14	0.01 ± 0.002	0.08	0.008
		B <sub>4</sub>	0.25 ± 0.09	0.07 ± 0.004	0.31 ± 0.1	$(4.1 \pm 0.3) \cdot 10^{-3}$	0.05	0.001
	B <sub>3.5</sub>	A <sub>3</sub>	0.39 ± 0.24	$(2.5 \pm 0.4) \cdot 10^{-3}$	0.11 ± 0.06	0.03 ± 0.002	42.5	> 100
		A <sub>3.5</sub>	0.26 ± 0.05	0.028 ± 0.006	0.31 ± 0.11	0.03 ± 0.002	0.90	1.0
		A <sub>4</sub>	0.36 ± 0.14	0.048 ± 0.003	0.28 ± 0.09	0.01 ± 0.0006	0.30	0.14
		B <sub>3</sub>	0.36 ± 0.19	0.01 ± 0.003	0.05 ± 0.02	0.02 ± 0.0007	14.4	> 100
		B <sub>3.5</sub>	0.32 ± 0.07	0.037 ± 0.002	0.33 ± 0.06	0.04 ± 0.002	1.0	1.0
		B <sub>4</sub>	0.44 ± 0.18	0.094 ± 0.007	0.16 ± 0.06	0.01 ± 0.0005	0.35	0.16
	B <sub>4</sub>	A <sub>3</sub>	0.17 ± 0.05	$(1.4 \pm 0.1) \cdot 10^{-3}$	0.38 ± 0.12	0.09 ± 0.01	28.8	> 100
		A <sub>3.5</sub>	0.20 ± 0.11	$(6.4 \pm 1.0) \cdot 10^{-3}$	0.20 ± 0.10	$(6.4 \pm 1.0) \cdot 10^{-3}$	1.0	1.0
		A <sub>4</sub>	0.19 ± 0.042	0.02 ± 0.0009	0.50 ± 0.07	0.01 ± 0.0009	0.19	0.55
		B <sub>3</sub>	0.16 ± 0.09	$(4.2 \pm 0.2) \cdot 10^{-3}$	0.14 ± 0.03	0.07 ± 0.006	19.0	> 100
		B <sub>3.5</sub>	0.37 ± 0.06	0.011 ± 0.0005	0.91 ± 0.12	0.09 ± 0.011	3.5	6.4
		B <sub>4</sub>	0.28 ± 0.06	0.03 ± 0.001	0.28 ± 0.05	0.03 ± 0.001	1.0	1.0
N-A <sub>4</sub>	B <sub>3</sub>	A <sub>3</sub>	0.31 ± 0.18	$(1.4 \pm 0.2) \cdot 10^{-3}$	0.34 ± 0.2	$(9.2 \pm 1.3) \cdot 10^{-2}$	6.0	5.1
		A <sub>3.5</sub>	0.39 ± 0.06	$(6.7 \pm 0.4) \cdot 10^{-3}$	1.51 ± 0.3	0.21 ± 0.05	8.1	2.2
		A <sub>4</sub>	0.58 ± 0.13	0.02 ± 0.0007	0.50 ± 0.10	0.02 ± 0.0007	1.10	1.0
		B <sub>3</sub>	0.14 ± 0.03	0.04 ± 0.01	0.14 ± 0.12	0.04 ± 0.007	1.0	1.0
		B <sub>3.5</sub>	0.22 ± 0.04	0.12 ± 0.004	0.51 ± 0.09	$(5.7 \pm 0.6) \cdot 10^{-4}$	0.002	0.004
		B <sub>4</sub>	0.20 ± 0.04	0.096 ± 0.003	0.84 ± 0.13	$(1.5 \pm 0.2) \cdot 10^{-3}$	0.004	0.002
	B <sub>3.5</sub>	A <sub>3</sub>	0.29 ± 0.1	$(4.1 \pm 0.4) \cdot 10^{-3}$	0.07 ± 0.02	0.06 ± 0.003	60.6	> 100
		A <sub>3.5</sub>	0.24 ± 0.07	0.01 ± 0.0009	0.21 ± 0.05	0.03 ± 0.002	3.4	6.9
		A <sub>4</sub>	0.20 ± 0.05	0.026 ± 0.002	0.20 ± 0.04	0.025 ± 0.002	0.96	1.0
		B <sub>3</sub>	0.19 ± 0.03	$(9.9 \pm 0.9) \cdot 10^{-4}$	0.03 ± 0.007	0.11 ± 0.003	> 100	> 100
		B <sub>3.5</sub>	0.22 ± 0.05	0.03 ± 0.002	0.24 ± 0.04	0.04 ± 0.002	1.22	1.0
		B <sub>4</sub>	0.27 ± 0.08	0.09 ± 0.006	0.09 ± 0.02	0.01 ± 0.0005	0.33	0.62
	B <sub>4</sub>	A <sub>3</sub>	0.34 ± 0.13	$(8.1 \pm 0.9) \cdot 10^{-4}$	0.14 ± 0.05	0.13 ± 0.008	> 100	> 100
		A <sub>3.5</sub>	0.17 ± 0.04	0.01 ± 0.0009	0.07 ± 0.01	0.02 ± 0.001	4.9	1.7
		A <sub>4</sub>	0.11 ± 0.24	0.013 ± 0.04	0.11 ± 0.30	0.013 ± 0.04	1.0	1.0
		B <sub>3</sub>	0.25 ± 0.06	$(1.2 \pm 0.1) \cdot 10^{-3}$	0.07 ± 0.02	0.11 ± 0.005	> 100	> 100
		B <sub>3.5</sub>	0.17 ± 0.02	0.01 ± 0.0004	0.38 ± 0.03	0.07 ± 0.006	3.1	1.6
		B <sub>4</sub>	0.32 ± 0.08	0.013 ± 0.0006	0.32 ± 0.06	0.013 ± 0.0006	1.0	1.0

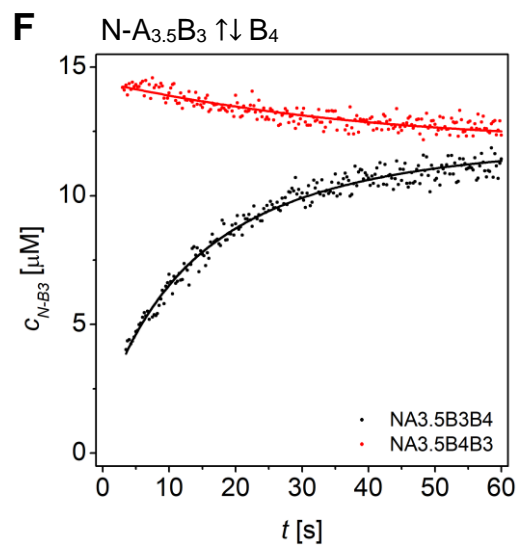
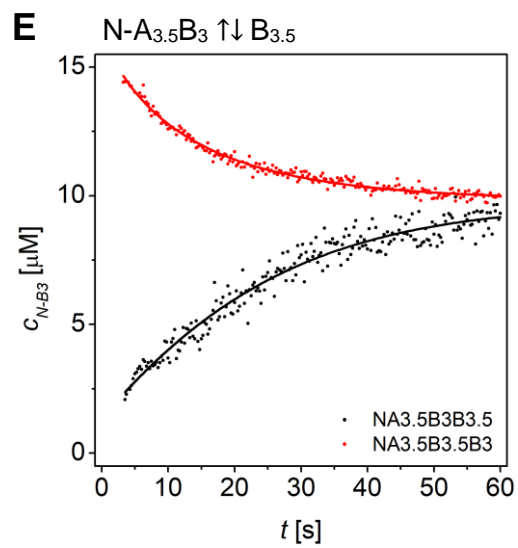
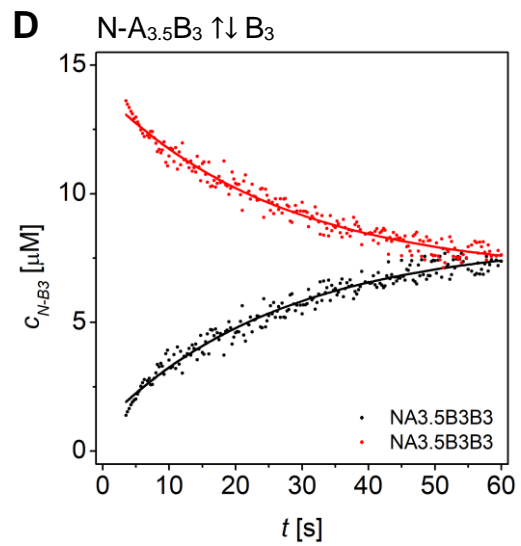
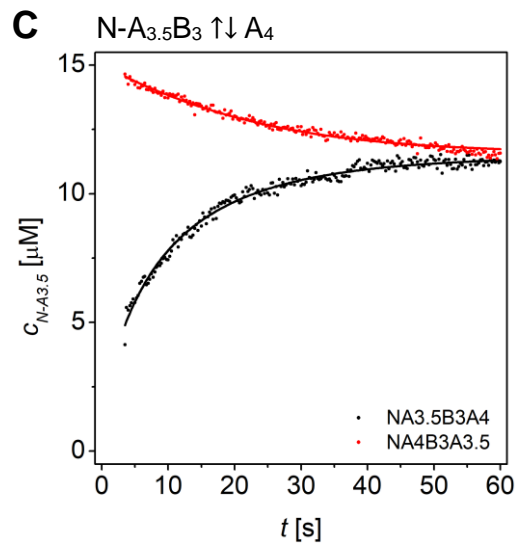
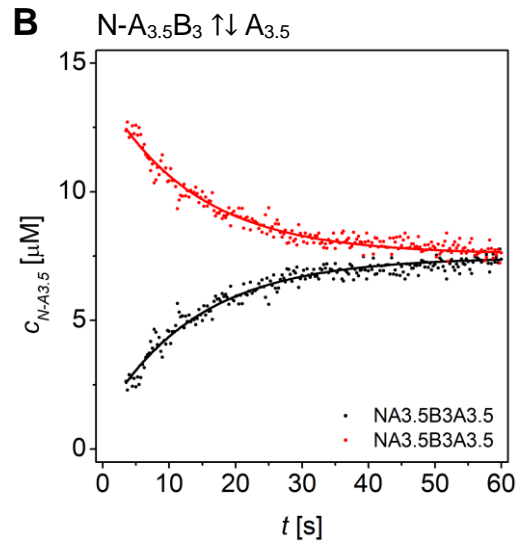
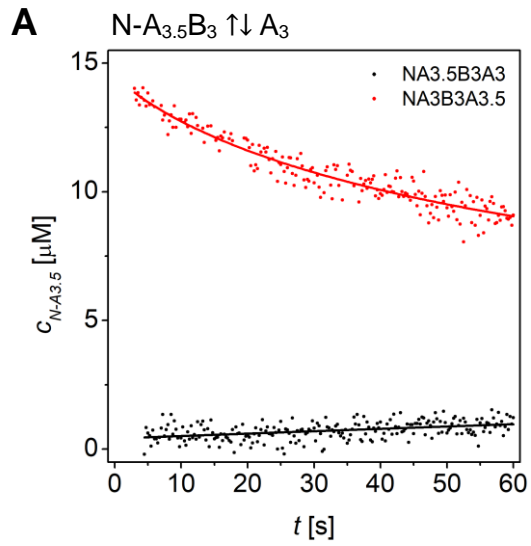


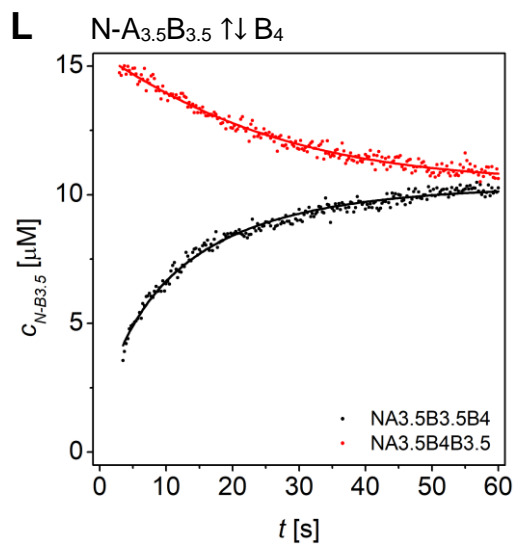
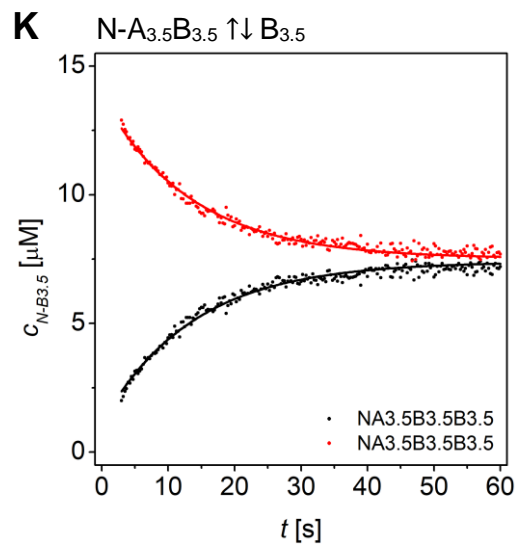
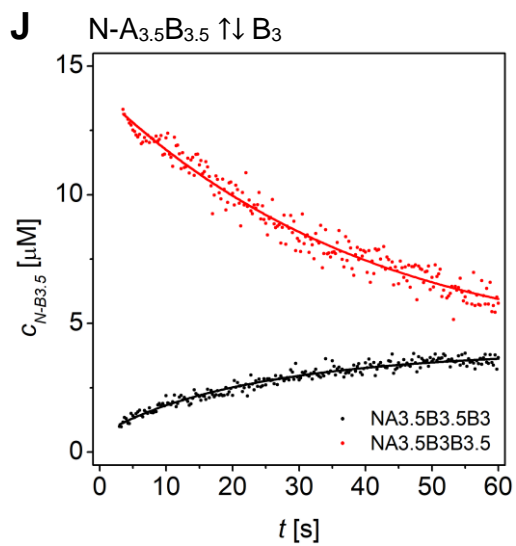
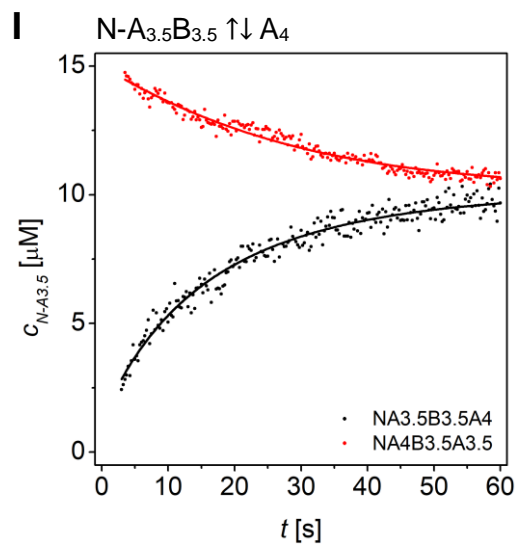
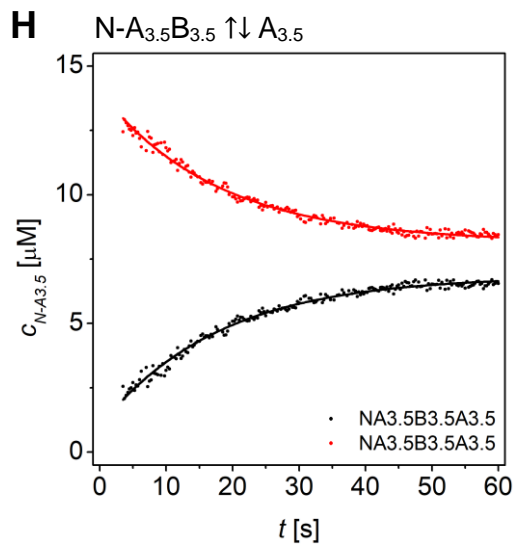
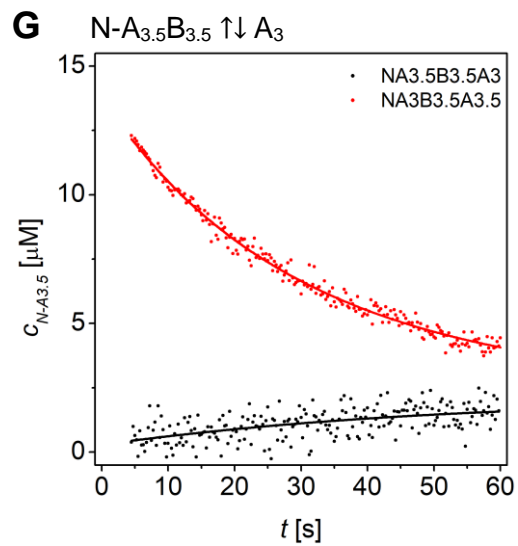


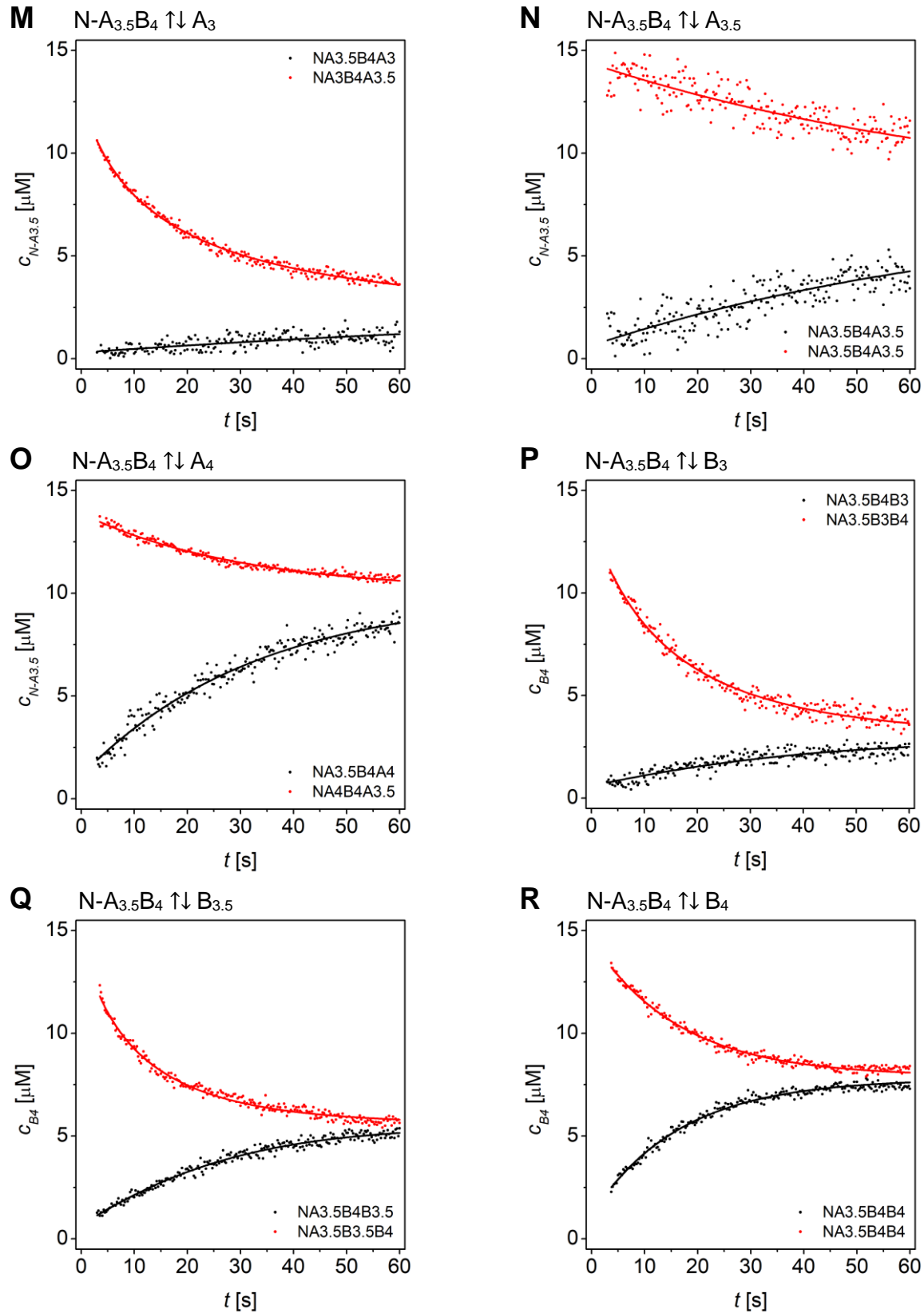




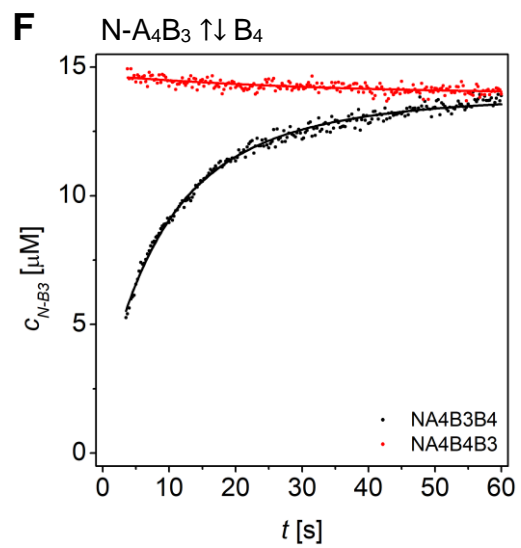
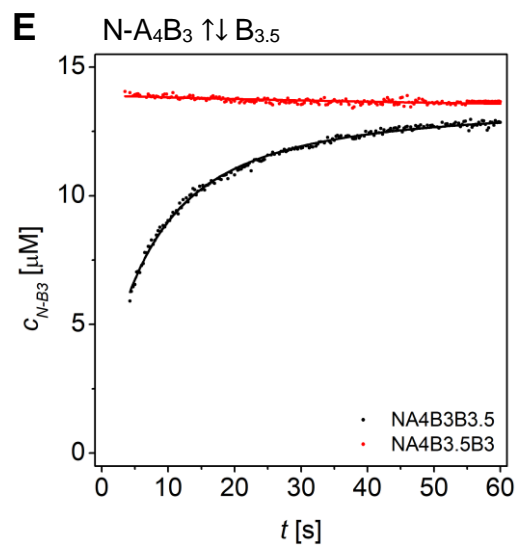
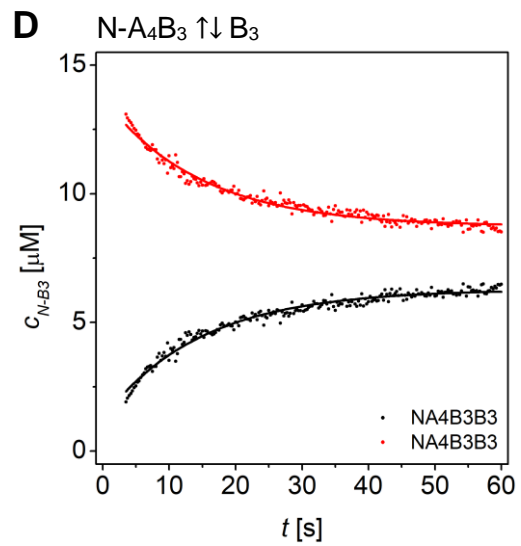
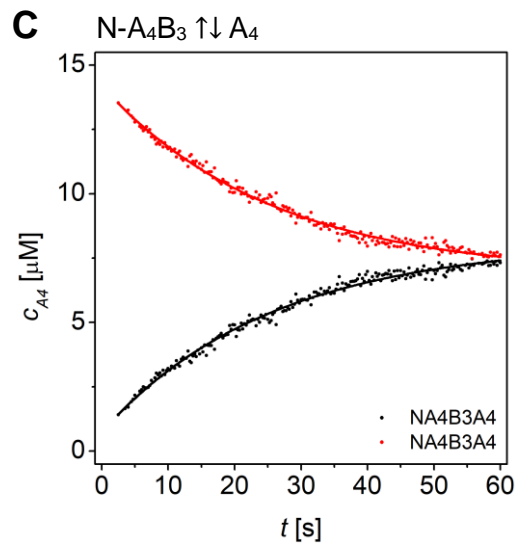
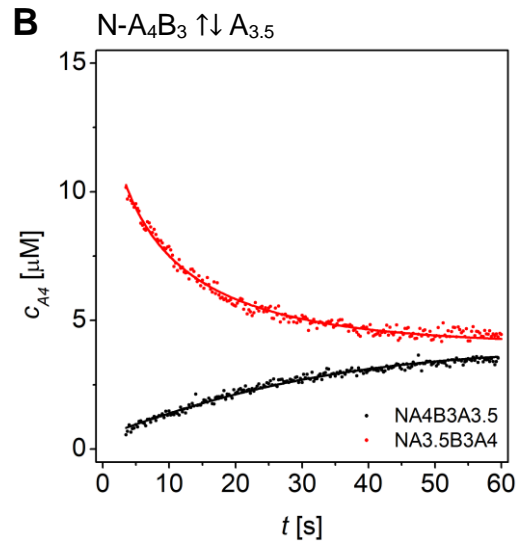
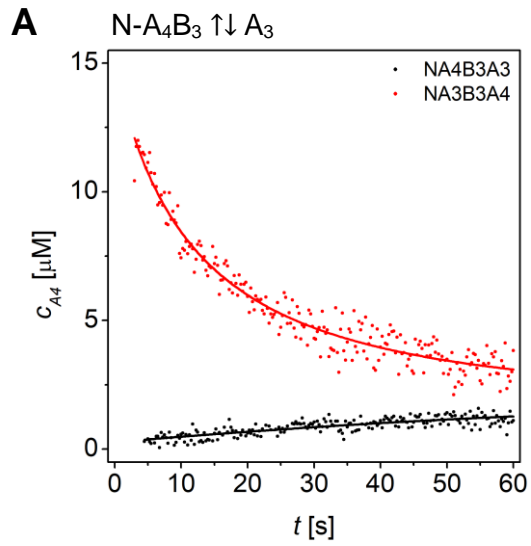
**Figure S8.** Dynafit results of least-squares fits of strand displacement in N-A<sub>3</sub>B peptides using a competitive binding model.

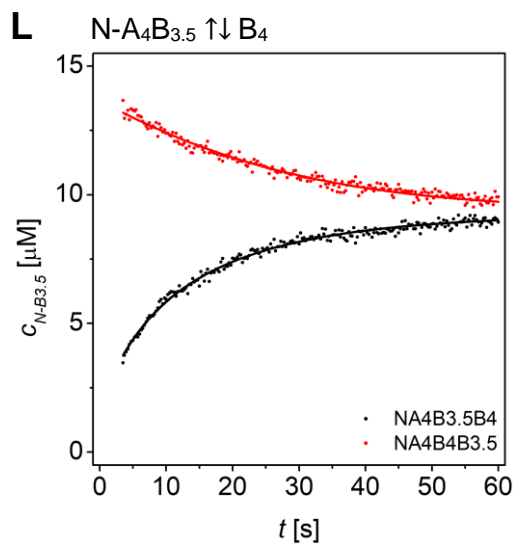
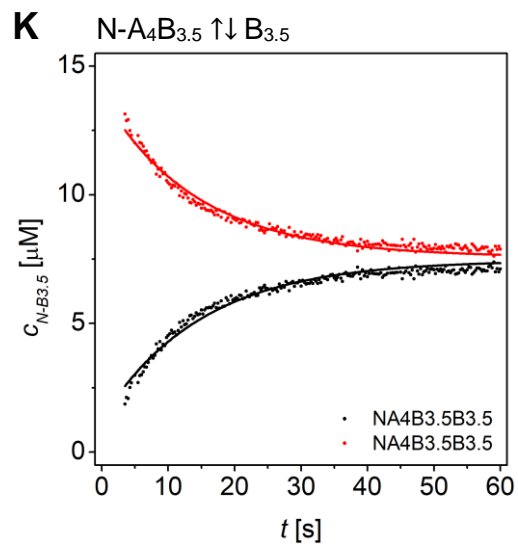
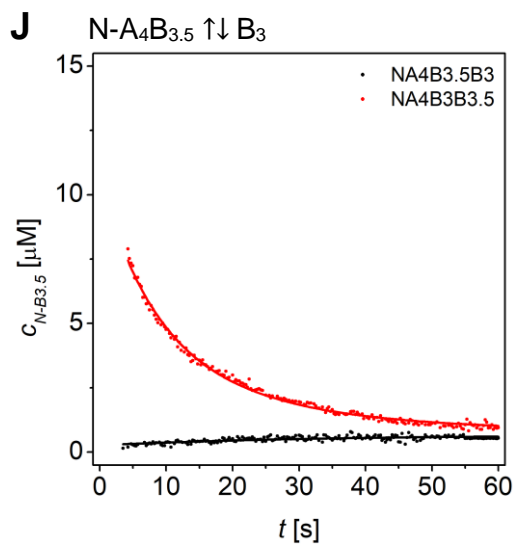
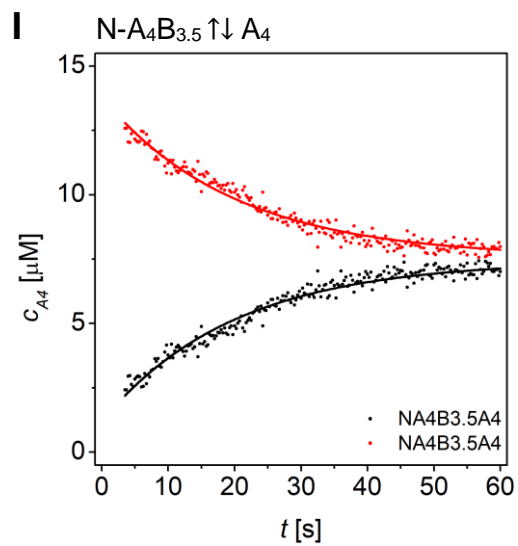
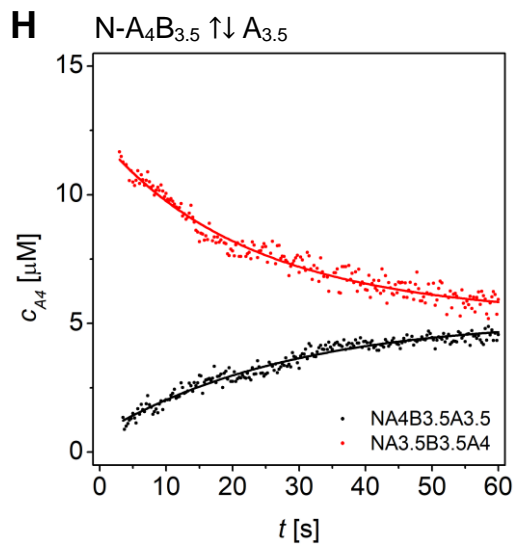
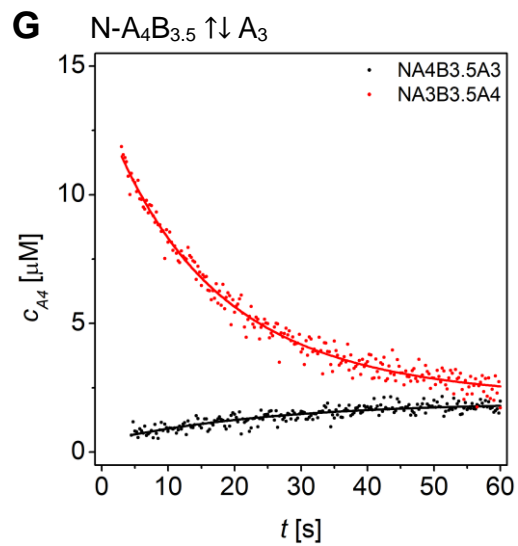




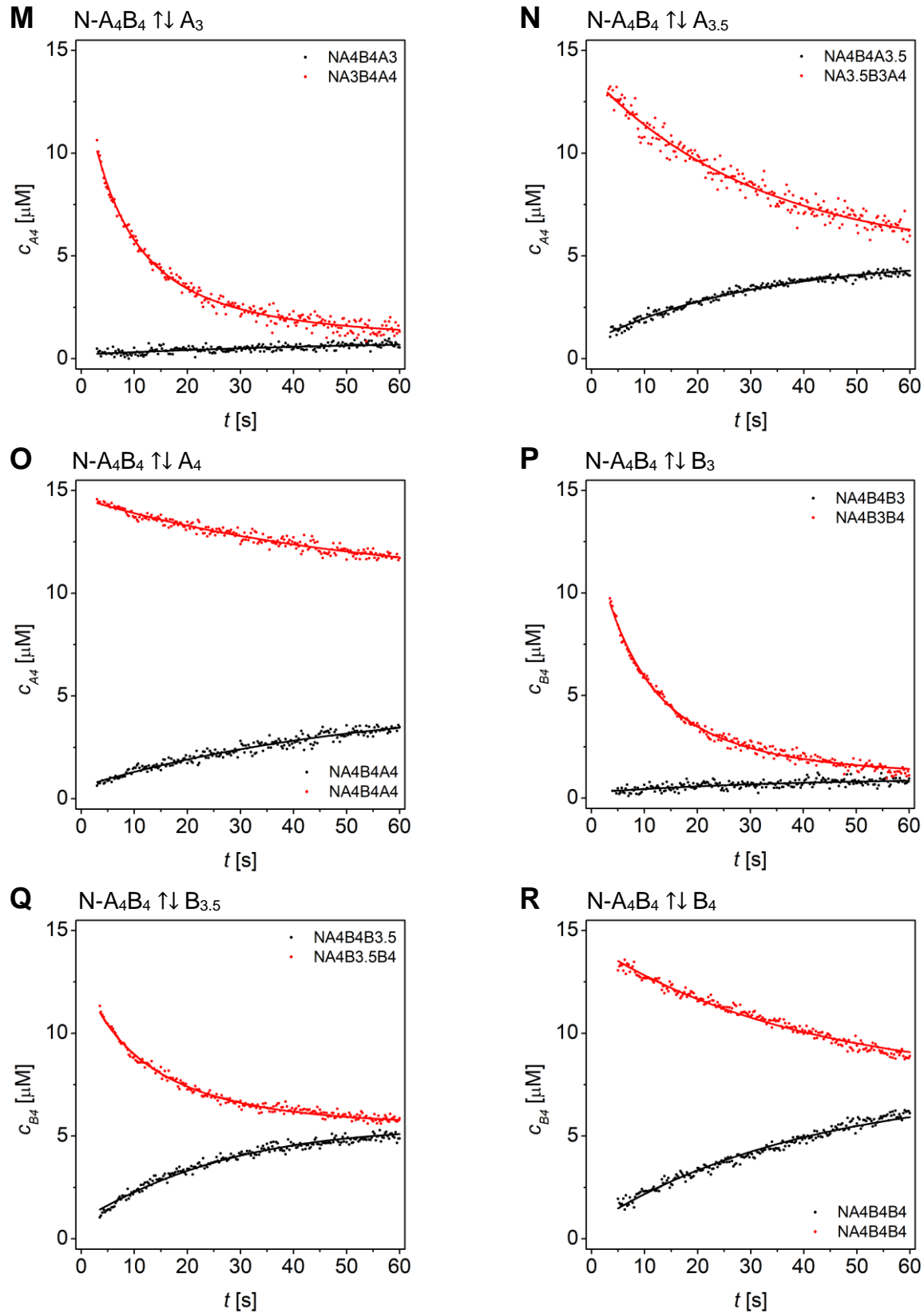


**Figure S9.** Dynafit results of least-squares fits strand displacement in N-A<sub>3.5</sub>B peptides using a competitive binding model.





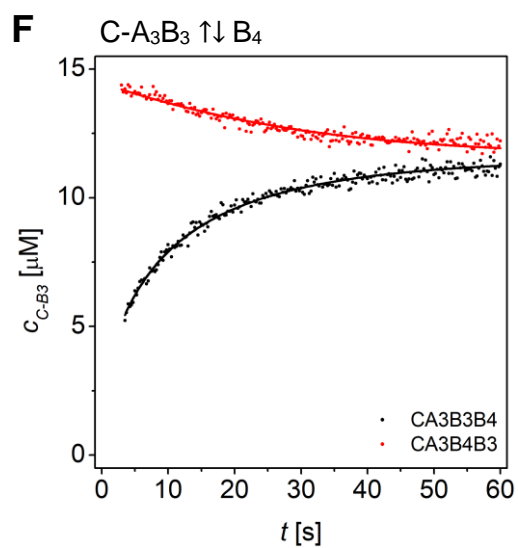
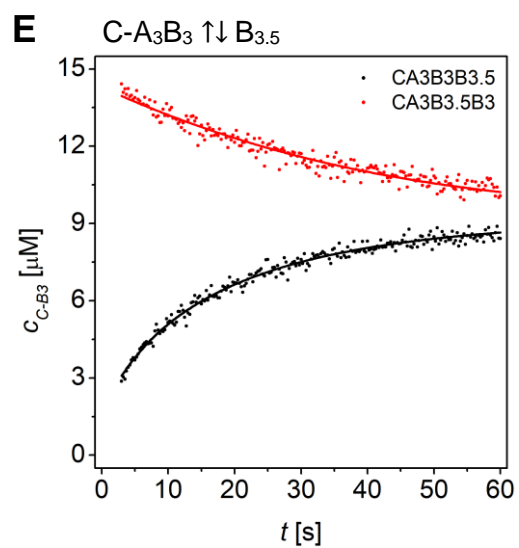
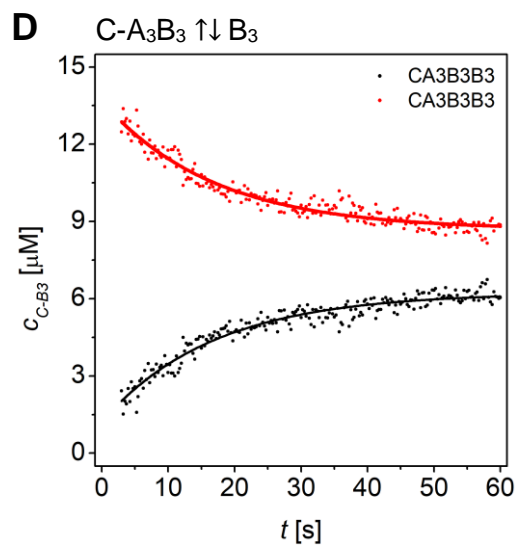
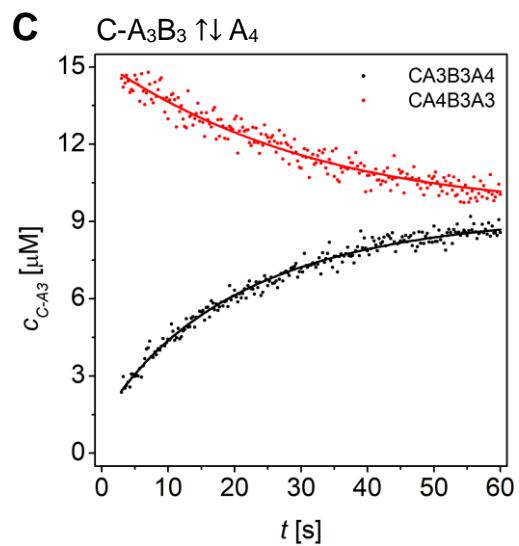
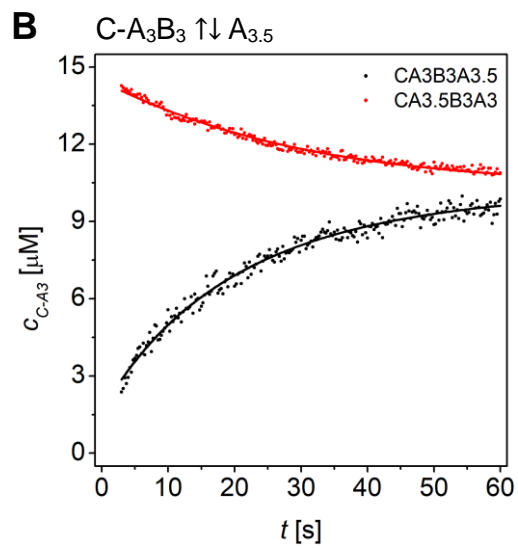
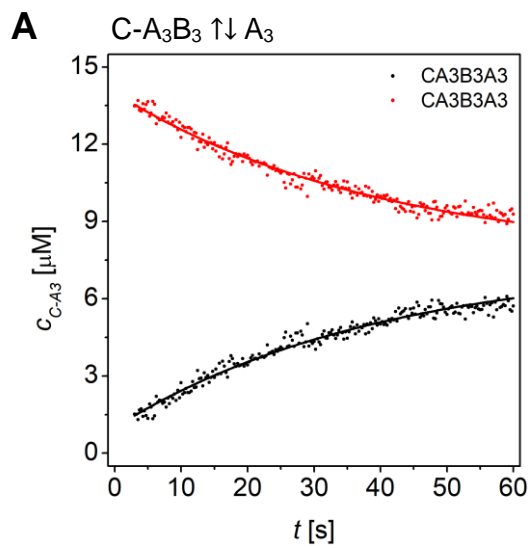


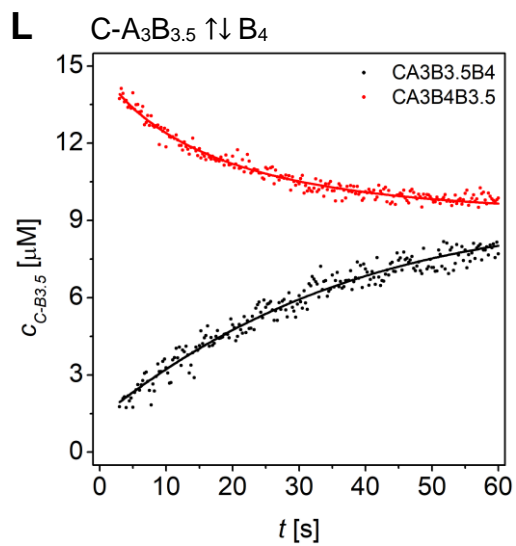
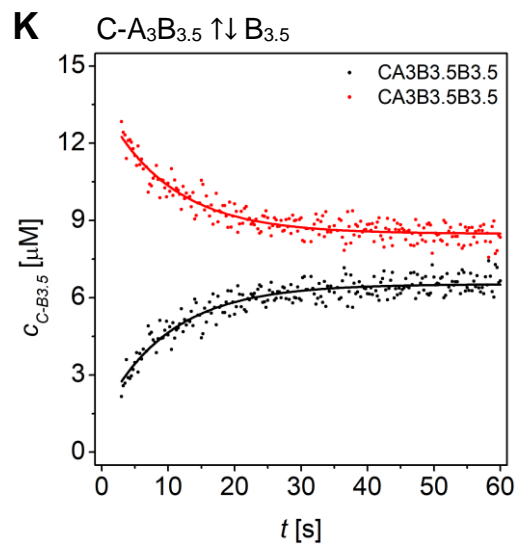
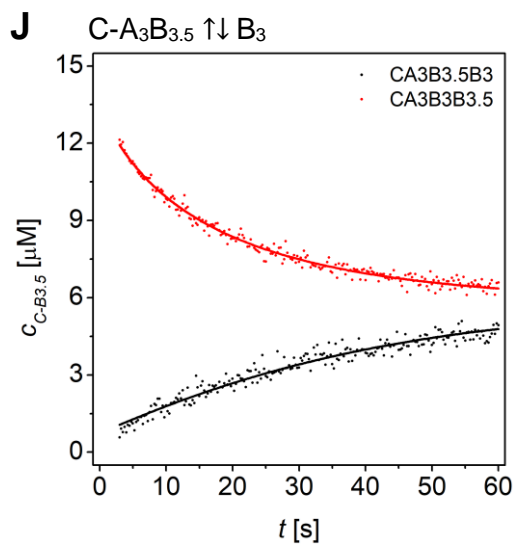
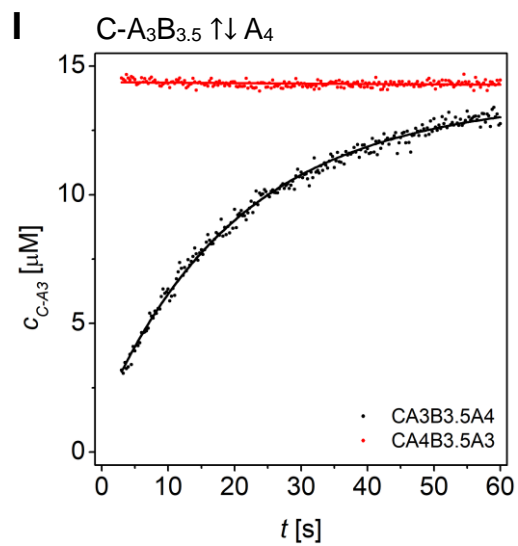
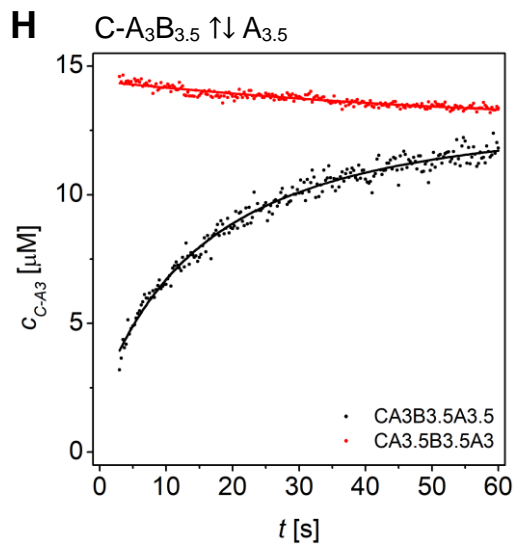
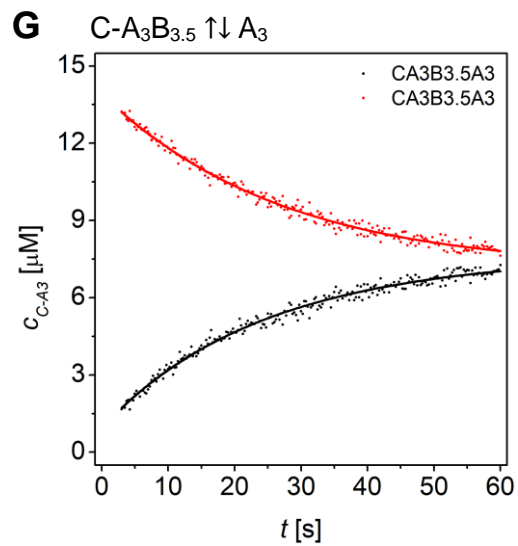


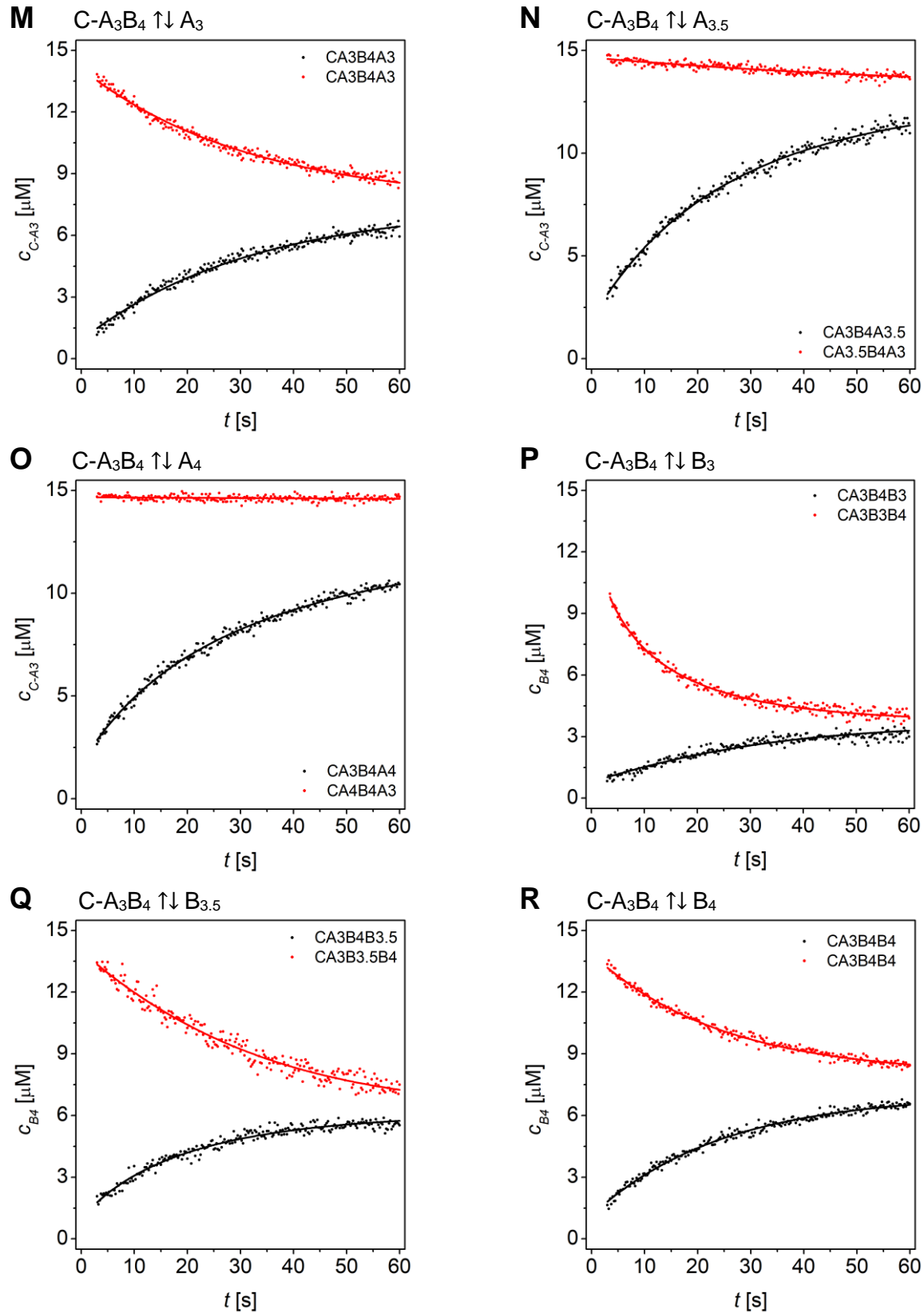
**Figure S10.** Dynafit results of least-squares fits strand displacement in N-A<sub>4</sub>B peptides using a competitive binding model.

**Table S8.** Best-fit values of rate constants of competitive strand displacement in C-A<sub>x</sub>B<sub>y</sub> peptides obtained from DynaFit analysis. Ratio of overall affinities ( $k_1k_4/k_2k_3$ ) matches well with the ration of the  $K_D$  values determined from CD-thermal denaturation curves. P<sub>comp</sub> is the general term for peptide competitor (A<sub>comp</sub> or B<sub>comp</sub>).

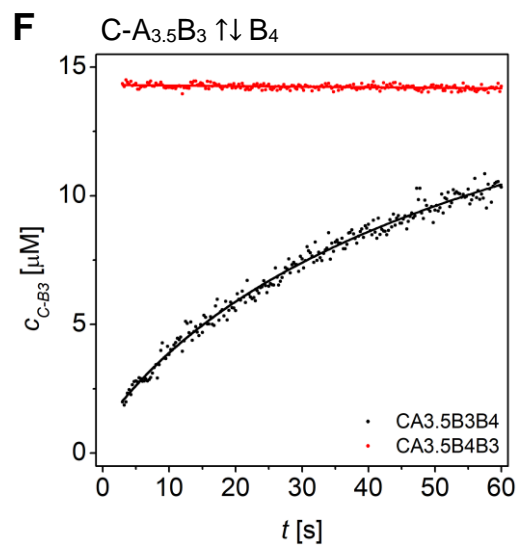
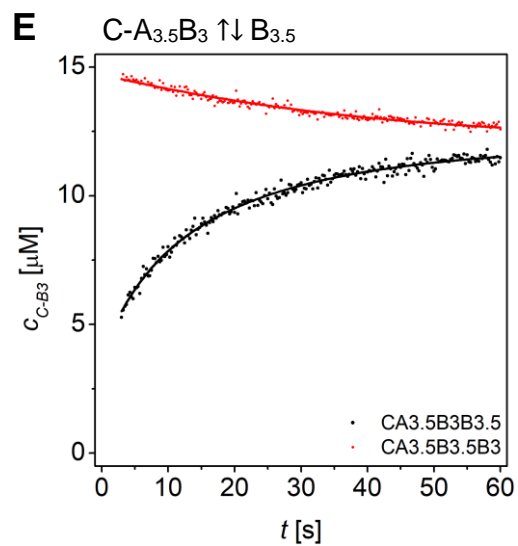
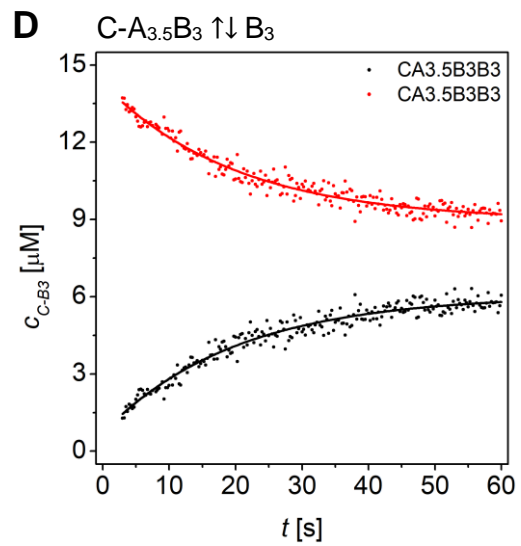
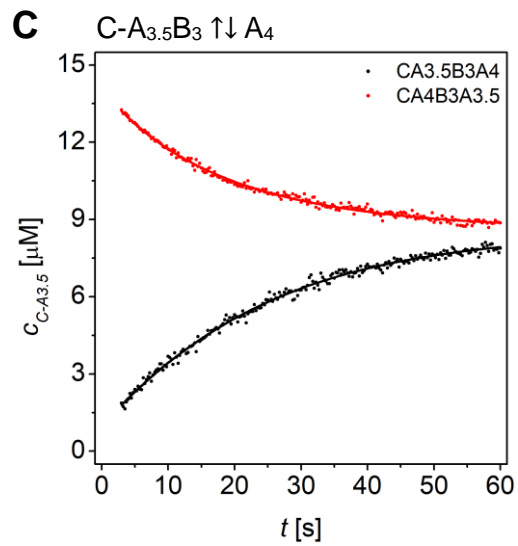
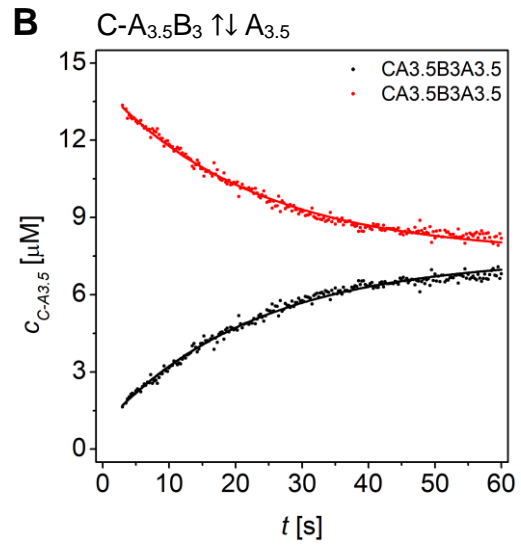
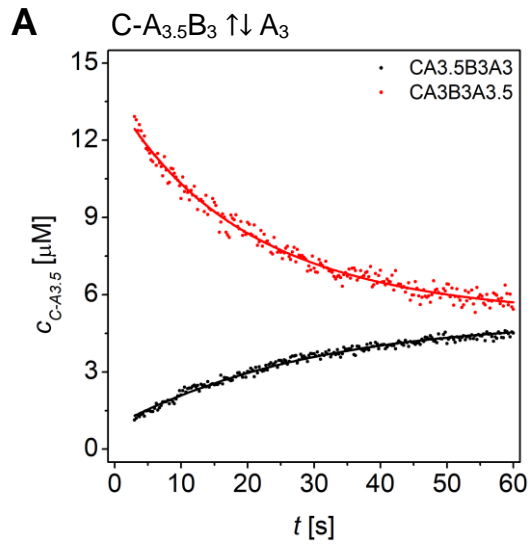
AB peptide	P <sub>comp</sub>	$k_1$ [ $\mu\text{M}^{-1}\text{s}^{-1}$ ]	$k_2$ [ $\text{s}^{-1}$ ]	$k_3$ [ $\mu\text{M}^{-1}\text{s}^{-1}$ ]	$k_4$ [ $\text{s}^{-1}$ ]	$k_1k_4/k_2k_3$	$K_D(\text{comp})/K_D$	
C-A <sub>3</sub>	B <sub>3</sub>	A <sub>3</sub>	0.15 ± 0.02	0.01 ± 0.0006	0.15 ± 0.02	0.01 ± 0.0006	1.0	1.0
		A <sub>3.5</sub>	0.15 ± 0.02	0.04 ± 0.002	0.17 ± 0.02	0.01 ± 0.0004	0.22	0.57
		A <sub>4</sub>	0.23 ± 0.07	0.03 ± 0.002	0.17 ± 0.04	0.01 ± 0.0006	0.45	0.63
		B <sub>3</sub>	0.13 ± 0.04	0.035 ± 0.02	0.13 ± 0.2	0.035 ± 0.01	1.0	1.0
		B <sub>3.5</sub>	0.21 ± 0.06	0.07 ± 0.007	0.06 ± 0.01	$(8.9 \pm 0.4) \cdot 10^{-3}$	0.45	0.31
		B <sub>4</sub>	0.21 ± 0.06	0.18 ± 0.02	0.06 ± 0.02	$(6.8 \pm 0.5) \cdot 10^{-3}$	0.13	0.18
	B <sub>3.5</sub>	A <sub>3</sub>	0.31 ± 0.06	0.021 ± 0.0009	0.25 ± 0.04	0.018 ± 0.0007	1.06	1.0
		A <sub>3.5</sub>	0.13 ± 0.03	0.06 ± 0.003	0.17 ± 0.03	$(2.1 \pm 0.2) \cdot 10^{-3}$	0.03	0.06
		A <sub>4</sub>	0.25 ± 0.03	0.047 ± 0.0007	4.9 ± 0.57	$(1.7 \pm 0.9) \cdot 10^{-4}$	< 0.001	0.04
		B <sub>3</sub>	0.20 ± 0.03	$(8.9 \pm 0.3) \cdot 10^{-3}$	0.55 ± 0.08	0.05 ± 0.006	2.0	3.3
		B <sub>3.5</sub>	0.17 ± 0.09	0.06 ± 0.04	0.17 ± 0.23	0.06 ± 0.01	1.0	1.0
		B <sub>4</sub>	0.12 ± 0.02	0.02 ± 0.0006	0.59 ± 0.08	0.04 ± 0.006	0.41	0.57
	B <sub>4</sub>	A <sub>3</sub>	0.24 ± 0.04	0.02 ± 0.0006	0.24 ± 0.03	0.02 ± 0.0006	1.0	1.0
		A <sub>3.5</sub>	0.11 ± 0.01	0.04 ± 0.001	0.29 ± 0.02	$(1.6 \pm 0.1) \cdot 10^{-3}$	0.02	0.008
		A <sub>4</sub>	0.12 ± 0.02	0.04 ± 0.001	0.15 ± 0.01	$(9.4 \pm 5.1) \cdot 10^{-5}$	0.002	< 0.001
		B <sub>3</sub>	0.12 ± 0.01	$(6.6 \pm 0.3) \cdot 10^{-3}$	0.30 ± 0.05	0.14 ± 0.03	8.5	5.7
		B <sub>3.5</sub>	0.28 ± 0.11	0.03 ± 0.003	0.07 ± 0.02	0.02 ± 0.0007	2.7	1.7
		B <sub>4</sub>	0.15 ± 0.02	0.02 ± 0.007	0.15 ± 0.12	0.02 ± 0.005	1.0	1.0
C-A <sub>3.5</sub>	B <sub>3</sub>	A <sub>3</sub>	0.15 ± 0.02	0.01 ± 0.0004	0.12 ± 0.01	0.04 ± 0.002	5.0	1.8
		A <sub>3.5</sub>	0.33 ± 0.05	0.02 ± 0.0007	0.33 ± 0.04	0.02 ± 0.0007	1.0	1.0
		A <sub>4</sub>	0.29 ± 0.03	0.02 ± 0.0004	0.66 ± 0.05	0.03 ± 0.001	0.66	1.1
		B <sub>3</sub>	0.35 ± 0.14	0.03 ± 0.018	0.35 ± 0.52	0.03 ± 0.01	1.0	1.0
		B <sub>3.5</sub>	0.13 ± 0.03	0.19 ± 0.03	0.03 ± 0.003	$(5.2 \pm 0.2) \cdot 10^{-3}$	0.11	0.03
		B <sub>4</sub>	0.45 ± 0.25	0.02 ± 0.002	0.19 ± 0.06	$(9.9 \pm 4.2) \cdot 10^{-5}$	0.01	0.003
	B <sub>3.5</sub>	A <sub>3</sub>	0.21 ± 0.06	$(1.7 \pm 0.1) \cdot 10^{-3}$	0.24 ± 0.06	0.07 ± 0.005	36	18
		A <sub>3.5</sub>	0.21 ± 0.04	0.02 ± 0.006	0.21 ± 0.17	0.02 ± 0.004	1.0	1.0
		A <sub>4</sub>	0.24 ± 0.03	0.03 ± 0.0007	0.40 ± 0.03	0.02 ± 0.0007	0.4	0.58
		B <sub>3</sub>	0.26 ± 0.04	$(5.2 \pm 0.2) \cdot 10^{-3}$	0.36 ± 0.05	0.07 ± 0.005	9.7	31
		B <sub>3.5</sub>	0.21 ± 0.06	0.05 ± 0.02	0.21 ± 0.13	0.05 ± 0.005	1.0	1.0
		B <sub>4</sub>	0.16 ± 0.04	0.18 ± 0.02	0.05 ± 0.008	$(1.8 \pm 0.1) \cdot 10^{-3}$	0.03	0.10
	B <sub>4</sub>	A <sub>3</sub>	0.14 ± 0.03	$(1.4 \pm 0.09) \cdot 10^{-3}$	0.08 ± 0.02	0.04 ± 0.002	50	>100
		A <sub>3.5</sub>	0.20 ± 0.03	0.01 ± 0.0004	0.20 ± 0.02	0.01 ± 0.0004	1.0	1.0
		A <sub>4</sub>	0.18 ± 0.02	0.01 ± 0.002	0.92 ± 0.23	0.002 ± 0.0005	0.04	0.08
		B <sub>3</sub>	0.15 ± 0.05	$(5.5 \pm 0.7) \cdot 10^{-4}$	0.05 ± 0.02	0.02 ± 0.0007	>100	>100
		B <sub>3.5</sub>	0.14 ± 0.03	$(1.8 \pm 0.1) \cdot 10^{-3}$	0.27 ± 0.06	0.16 ± 0.03	46	12
		B <sub>4</sub>	0.19 ± 0.03	0.03 ± 0.001	0.19 ± 0.02	0.03 ± 0.001	1.0	1.0
C-A <sub>4</sub>	B <sub>3</sub>	A <sub>3</sub>	0.21 ± 0.04	0.01 ± 0.0006	0.25 ± 0.04	0.03 ± 0.002	2.5	1.6
		A <sub>3.5</sub>	0.31 ± 0.05	0.03 ± 0.001	0.13 ± 0.02	0.02 ± 0.0004	1.59	0.9
		A <sub>4</sub>	0.24 ± 0.02	0.016 ± 0.0004	0.21 ± 0.02	0.014 ± 0.0004	1.0	1.0
		B <sub>3</sub>	0.16 ± 0.39	0.02 ± 0.07	0.17 ± 4.2	0.02 ± 0.08	1.0	1.0
		B <sub>3.5</sub>	0.11 ± 0.07	0.46 ± 0.26	0.012 ± 0.0009	$(5.1 \pm 0.3) \cdot 10^{-3}$	0.10	0.02
		B <sub>4</sub>	0.20 ± 0.09	0.63 ± 0.21	0.03 ± 0.004	$(1.3 \pm 0.1) \cdot 10^{-3}$	0.01	< 0.001
	B <sub>3.5</sub>	A <sub>3</sub>	0.24 ± 0.06	$(7.1 \pm 0.7) \cdot 10^{-4}$	$(1.6 \pm 0.5) \cdot 10^{-3}$	0.05 ± 0.0006	>100	27
		A <sub>3.5</sub>	0.23 ± 0.03	0.01 ± 0.0004	0.17 ± 0.02	0.03 ± 0.0009	4.1	1.6
		A <sub>4</sub>	0.29 ± 0.03	0.02 ± 0.0006	0.29 ± 0.03	0.02 ± 0.0006	1.0	1.0
		B <sub>3</sub>	0.25 ± 0.05	$(3.3 \pm 0.1) \cdot 10^{-3}$	0.27 ± 0.05	0.06 ± 0.003	17	56
		B <sub>3.5</sub>	0.25 ± 0.05	0.031 ± 0.002	0.20 ± 0.03	0.025 ± 0.001	1.0	1.0
		B <sub>4</sub>	0.22 ± 0.07	0.45 ± 0.08	0.05 ± 0.009	$(9.1 \pm 0.9) \cdot 10^{-4}$	0.009	0.01
	B <sub>4</sub>	A <sub>3</sub>	0.16 ± 0.04	$(9.9 \pm 0.7) \cdot 10^{-4}$	0.13 ± 0.03	0.03 ± 0.001	37	>100
		A <sub>3.5</sub>	0.15 ± 0.04	$(1.9 \pm 0.5) \cdot 10^{-3}$	0.01 ± 0.001	0.01 ± 0.0008	79	13
		A <sub>4</sub>	0.11 ± 0.24	0.013 ± 0.04	0.11 ± 0.30	0.013 ± 0.04	1.0	1.0
		B <sub>3</sub>	0.05 ± 0.009	$(1.1 \pm 0.06) \cdot 10^{-3}$	0.14 ± 0.03	0.21 ± 0.05	68	>100
		B <sub>3.5</sub>	0.20 ± 0.06	$(9.2 \pm 0.8) \cdot 10^{-4}$	0.20 ± 0.06	0.13 ± 0.01	>100	97
		B <sub>4</sub>	0.32 ± 0.08	0.013 ± 0.0006	0.32 ± 0.06	0.013 ± 0.0006	1.0	1.0

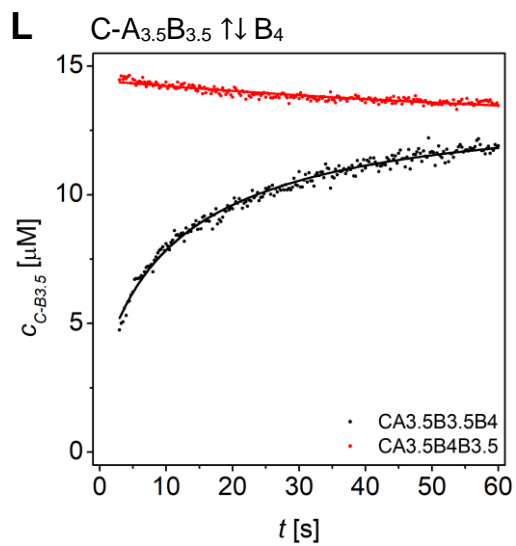
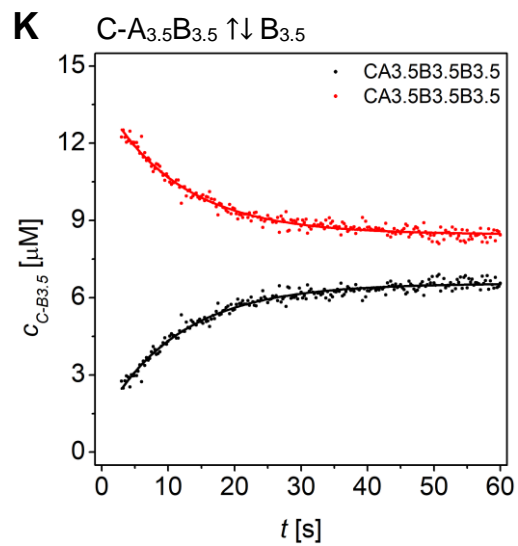
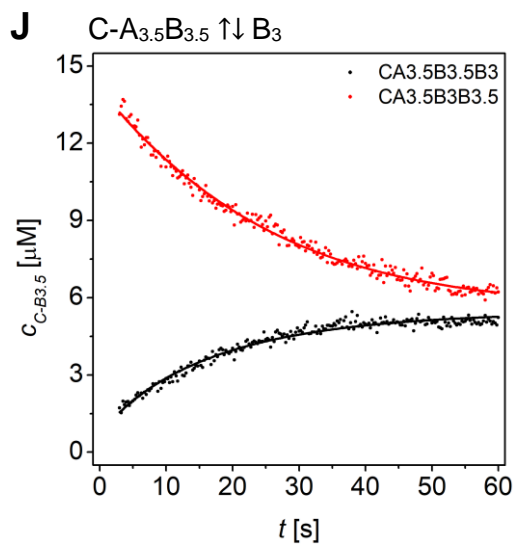
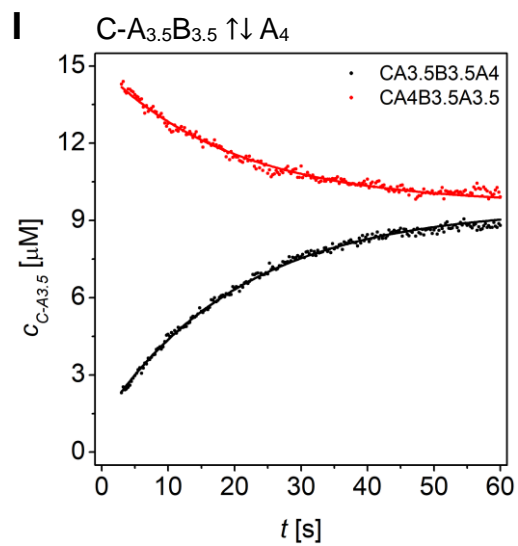
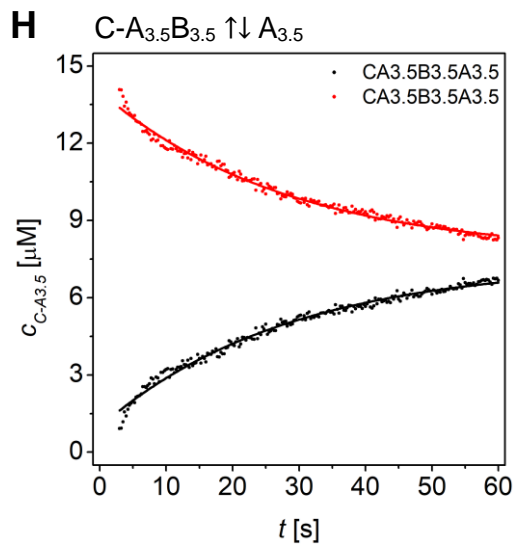
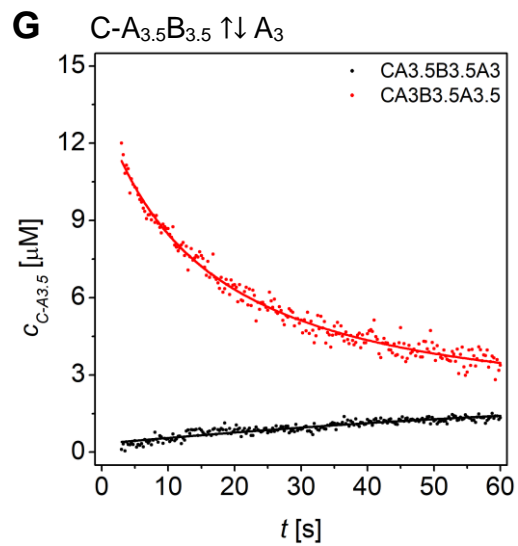


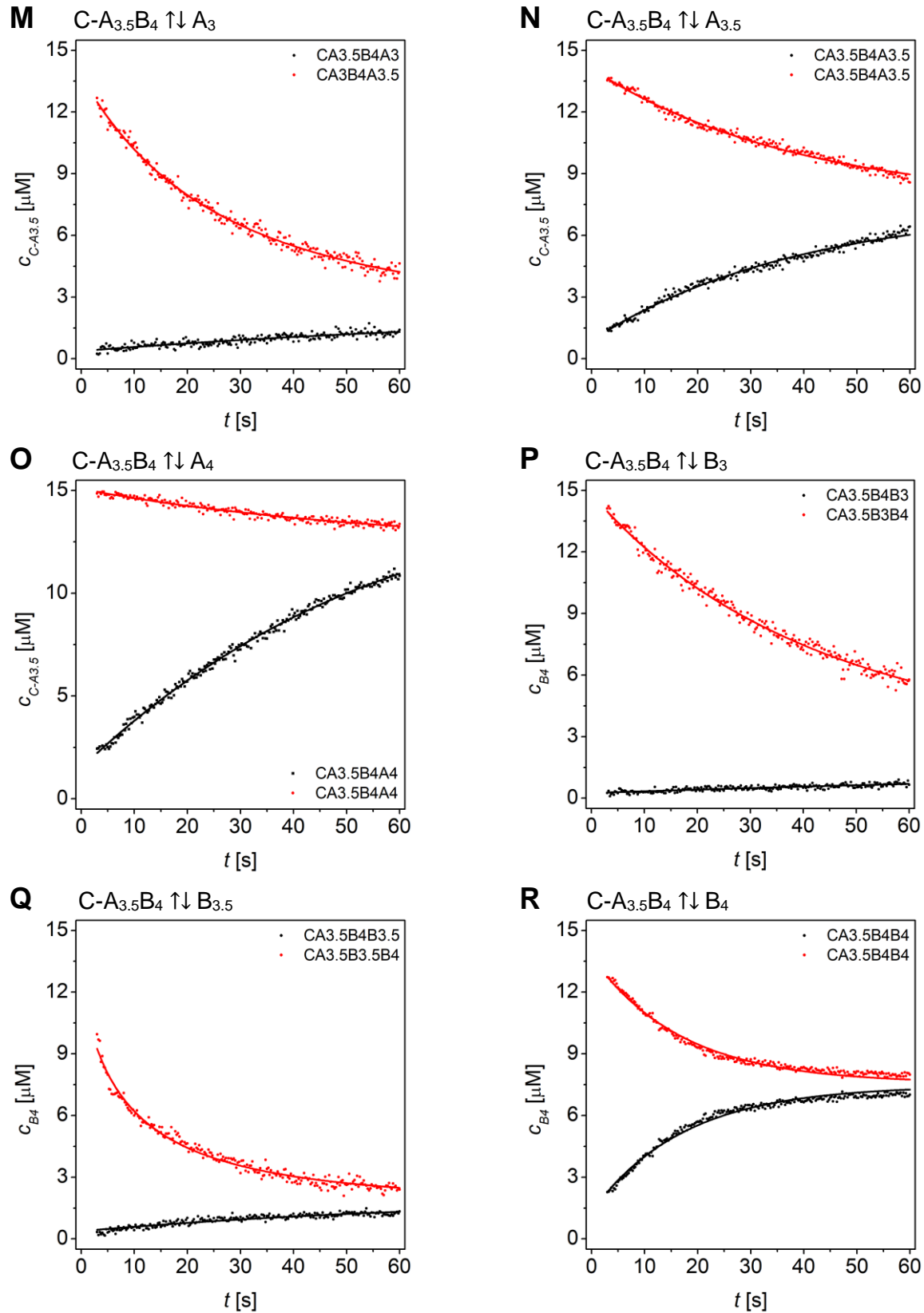




**Figure S11.** Dynafit results of least-squares fits strand displacement in C-A<sub>3</sub>B peptides using a competitive binding model.

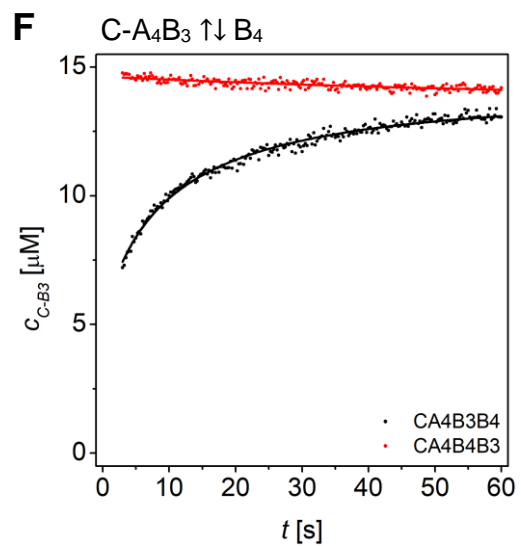
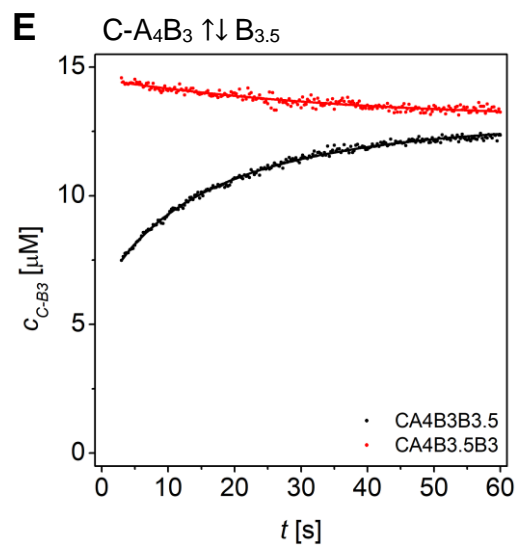
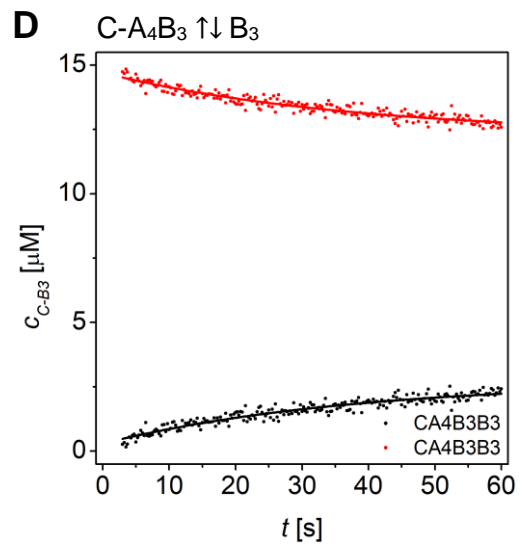
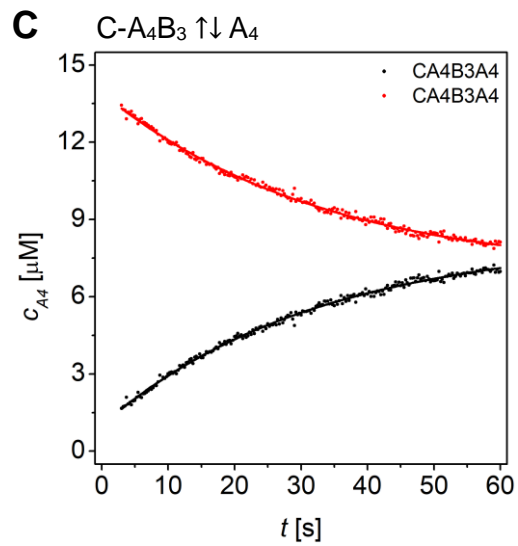
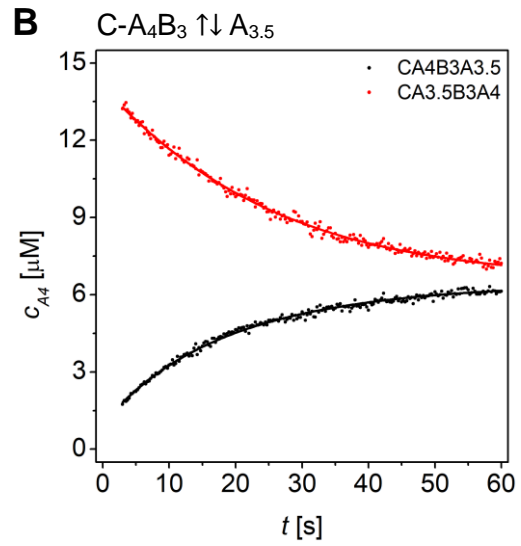
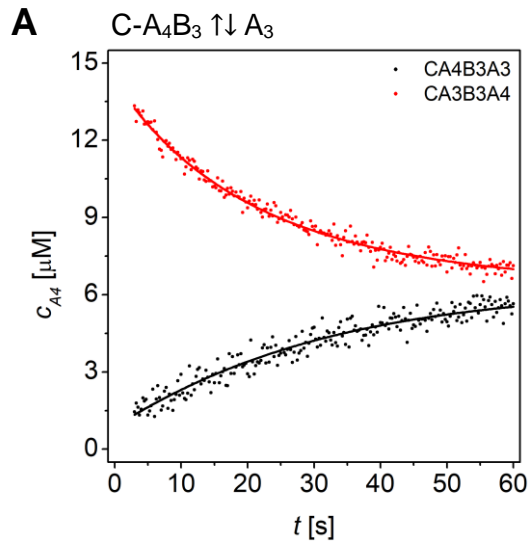


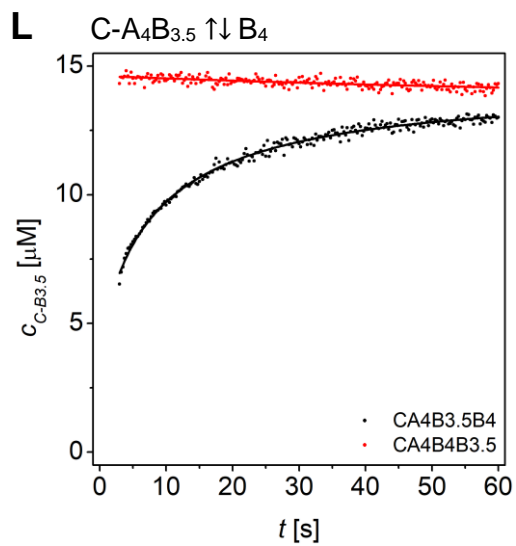
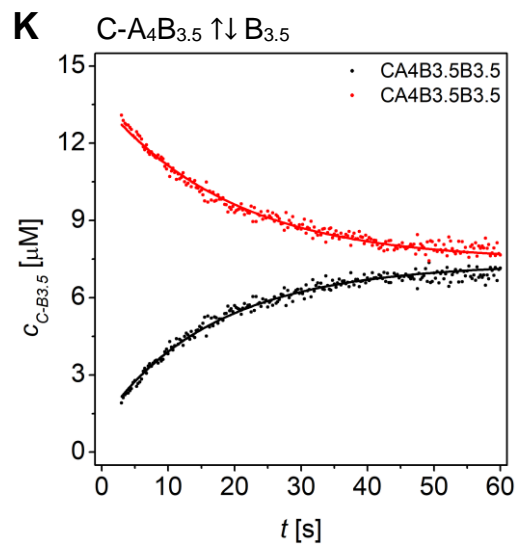
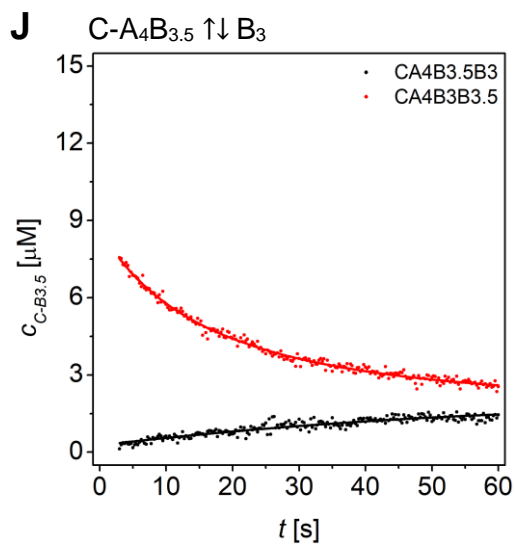
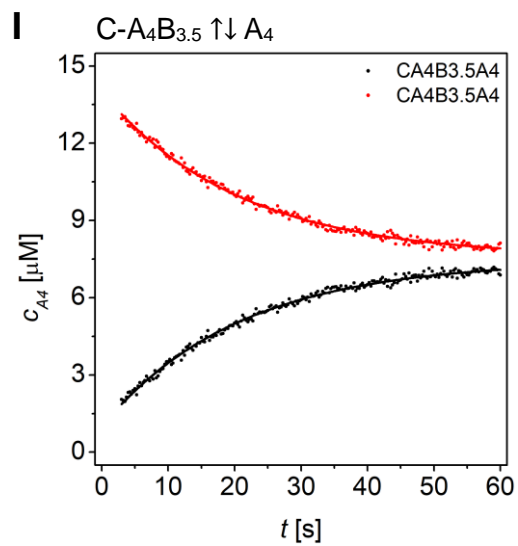
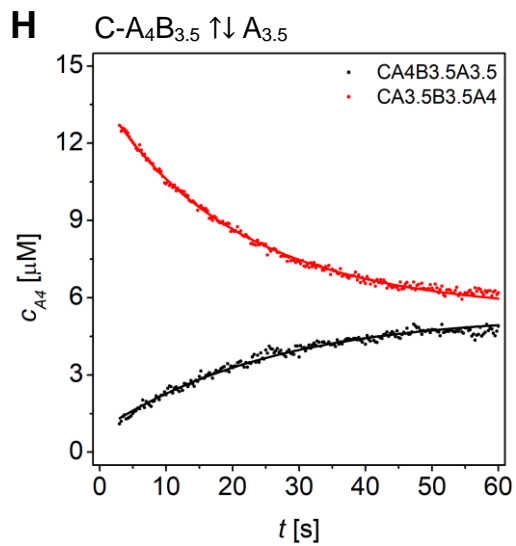
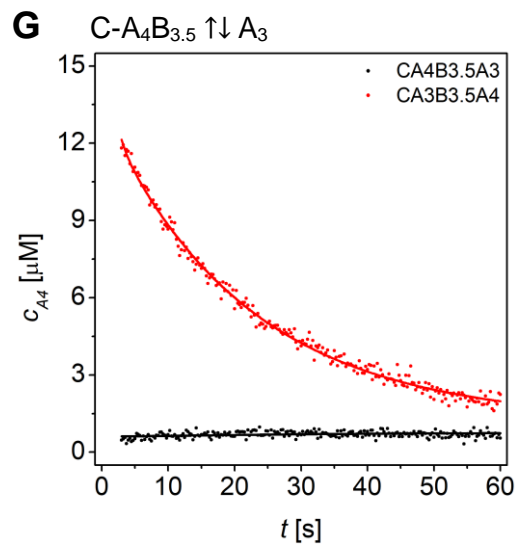


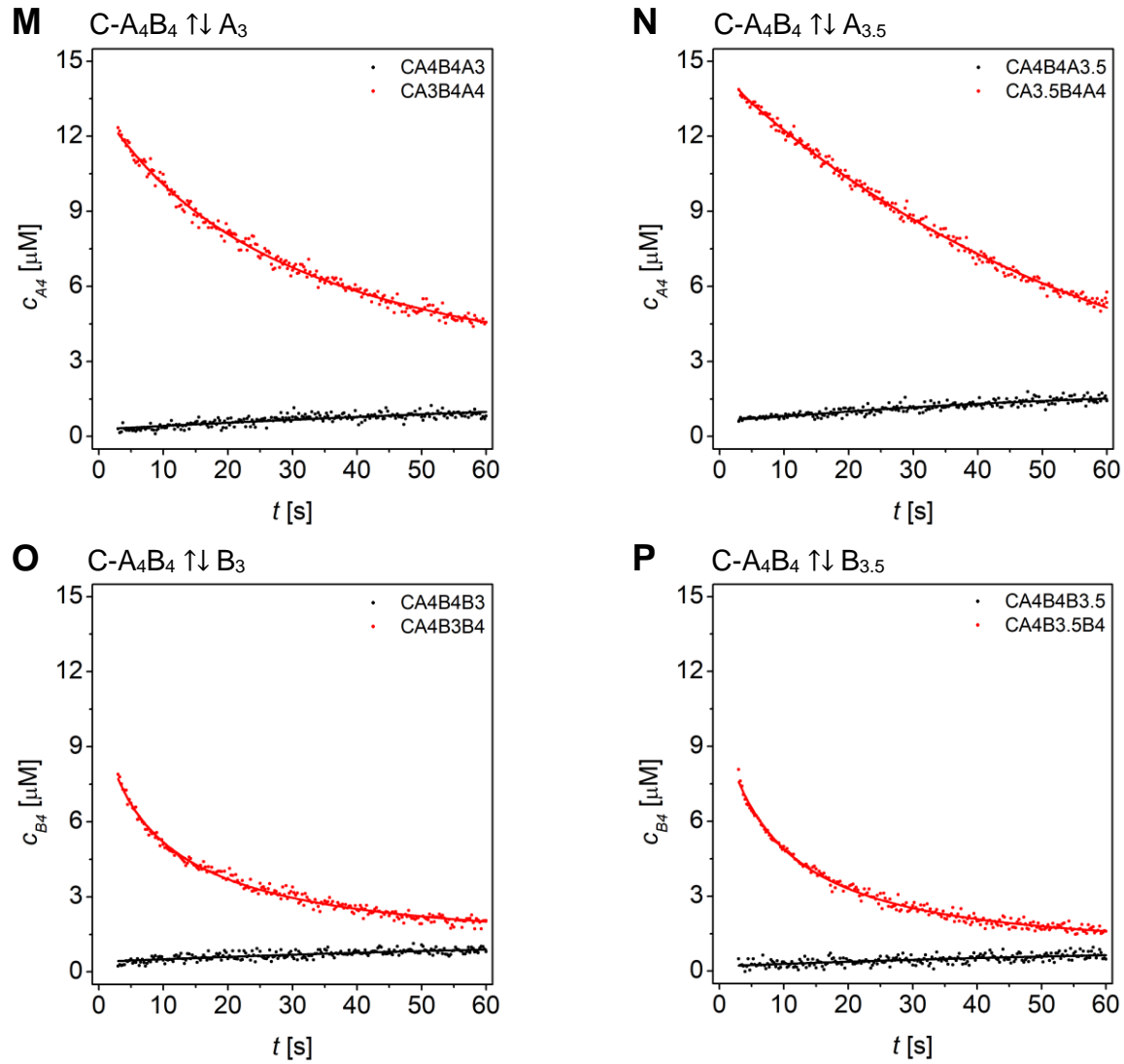


**Figure S12.** Dynafit results of least-squares fits strand displacement in C-A<sub>3.5</sub>B peptides using a competitive binding model.



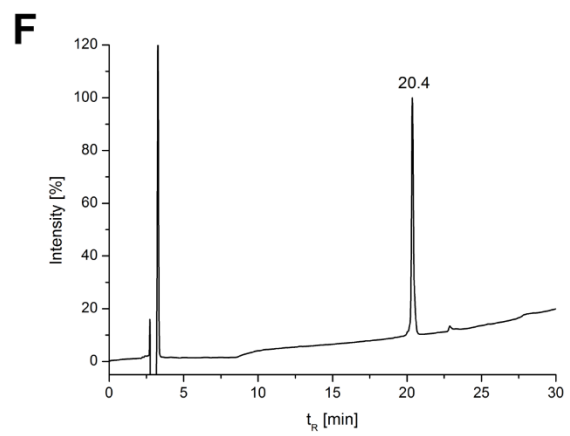
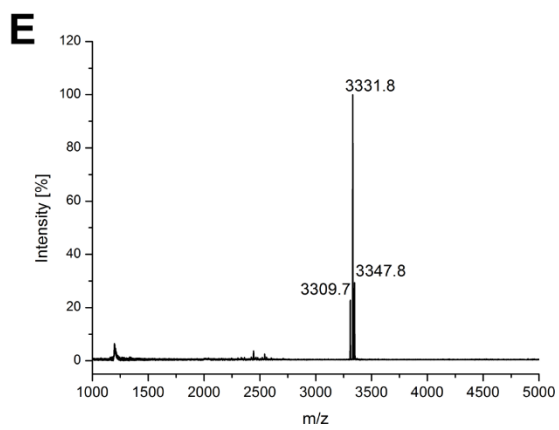
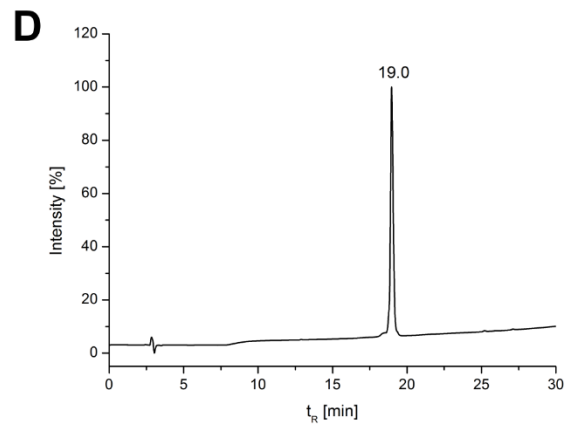
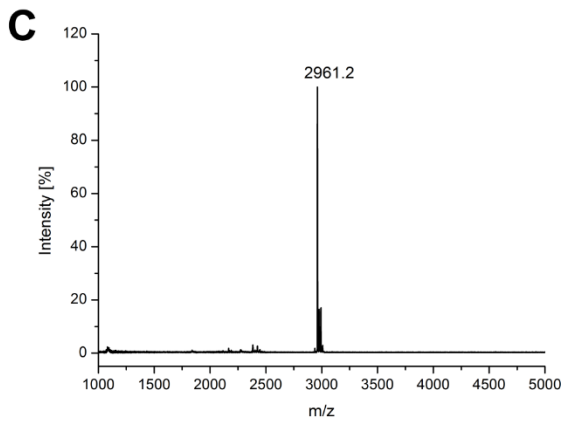
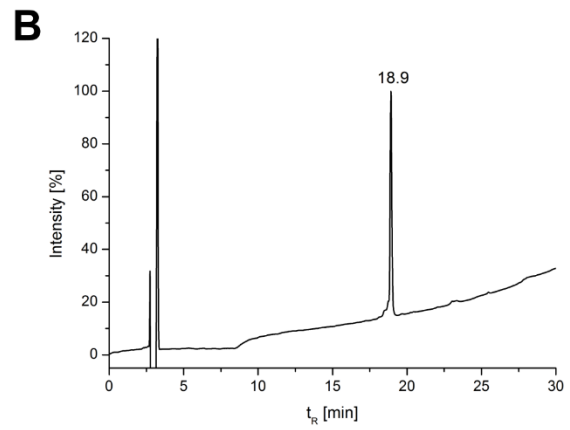
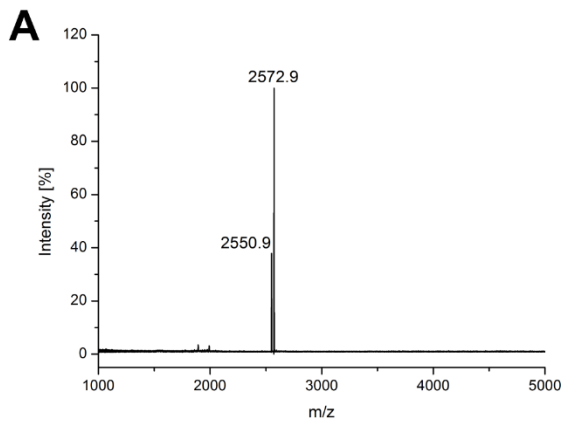


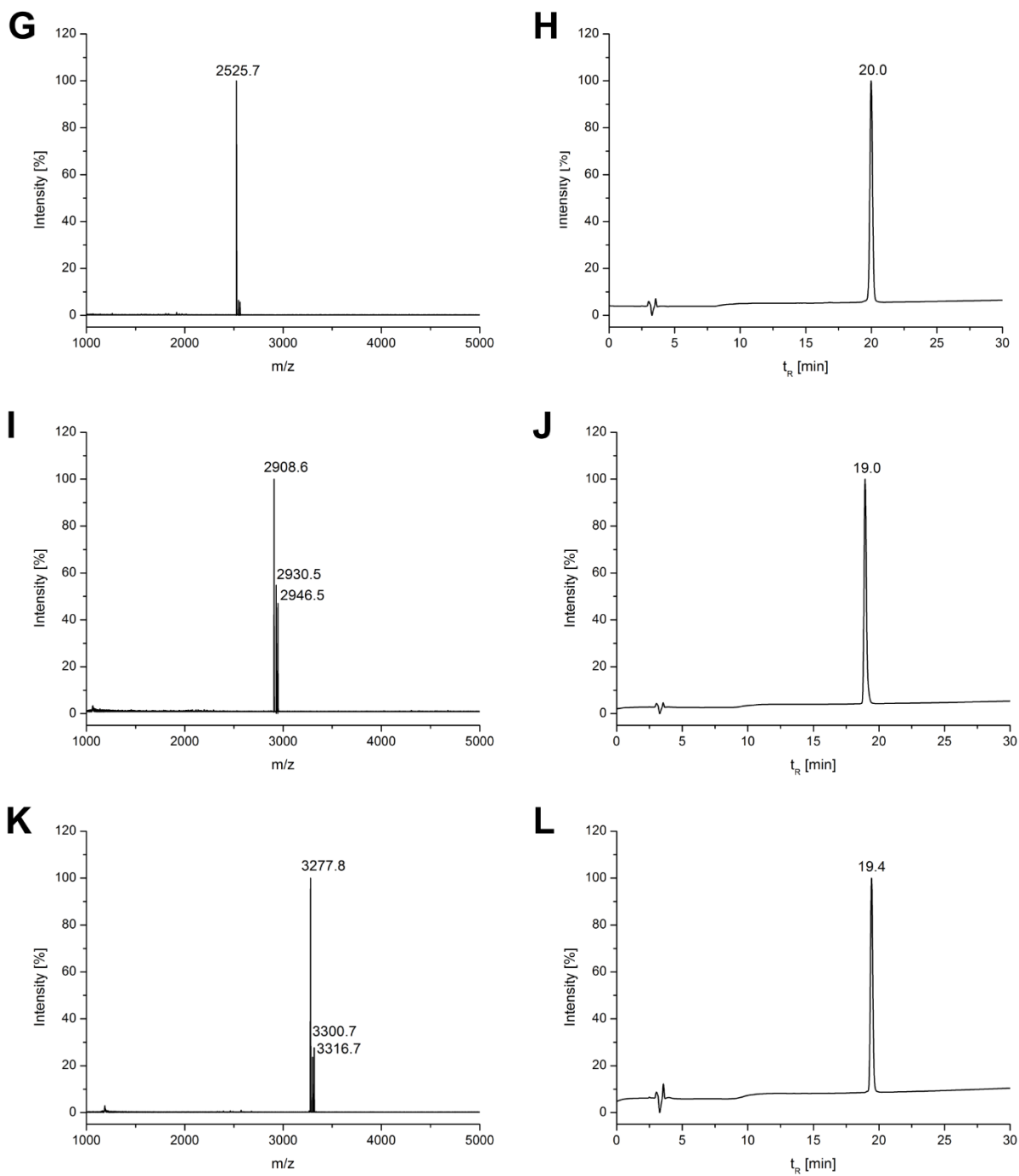




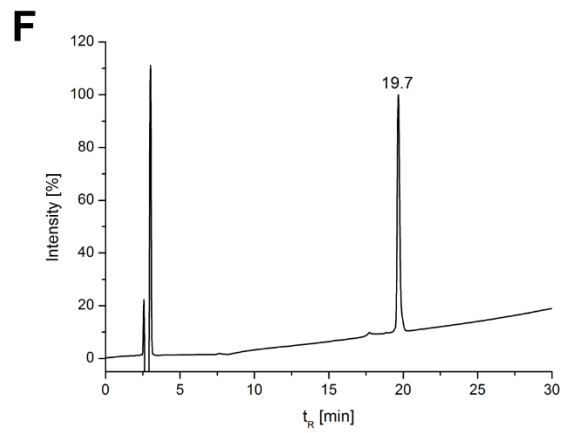
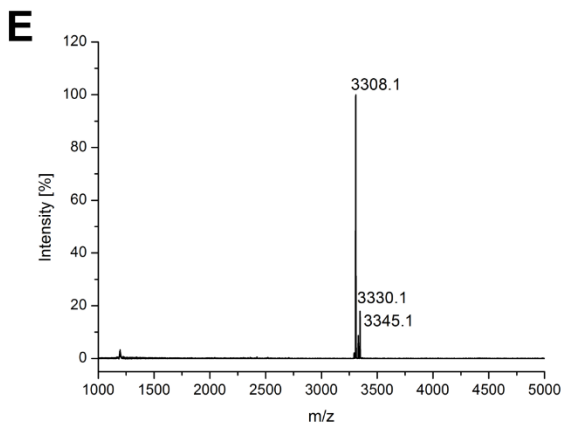
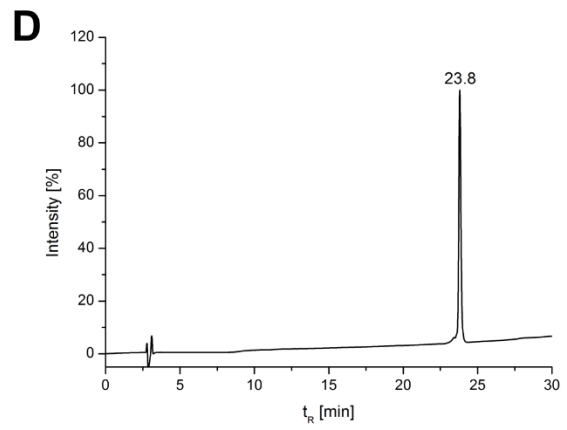
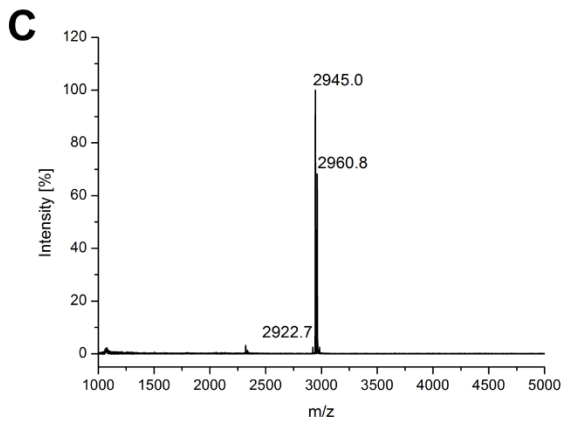
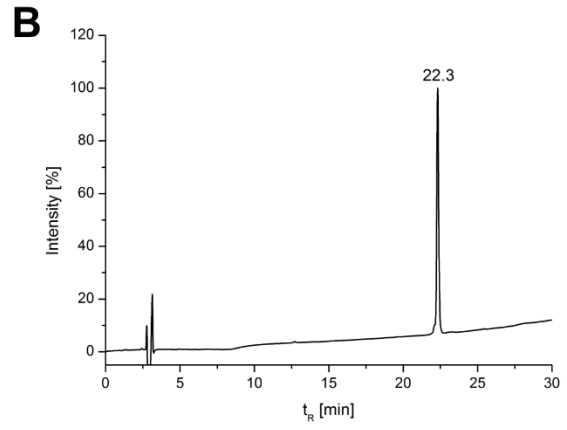
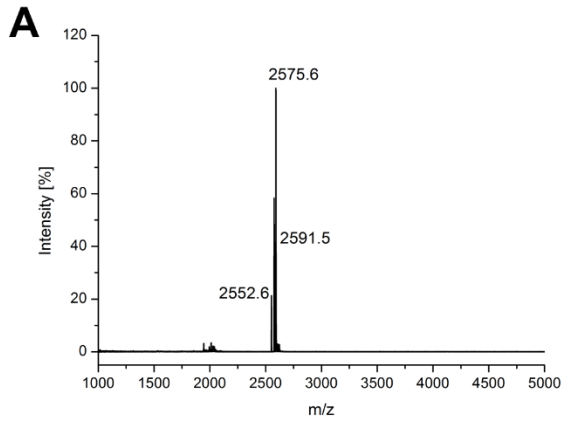
**Figure S13** Dynafit results of least-squares fits strand displacement in C-A<sub>4</sub>B peptides using a competitive binding model.

## 5. MALDI-TOF mass spectrometry and HPLC





**Figure S14** MALDI/TOF mass spectra and HPLC traces of coiled-coil single strands of the C-truncated set of heterodimeric coiled coils (A-B: C-A<sub>3</sub> calc. [M+H<sup>+</sup>]: 2552.2, C-D: C-A<sub>3.5</sub> calc. [M+Na<sup>+</sup>]: 2961.2, E-F: A<sub>4</sub> calc. [M+H<sup>+</sup>]: 3309.6, G-H: C-B<sub>3</sub> calc. [M+H<sup>+</sup>]: 2525.1, I-J: C-B<sub>3.5</sub> calc. [M+H<sup>+</sup>]: 2909.6, K-L: B<sub>4</sub> calc. [M+H<sup>+</sup>]: 3279.0).



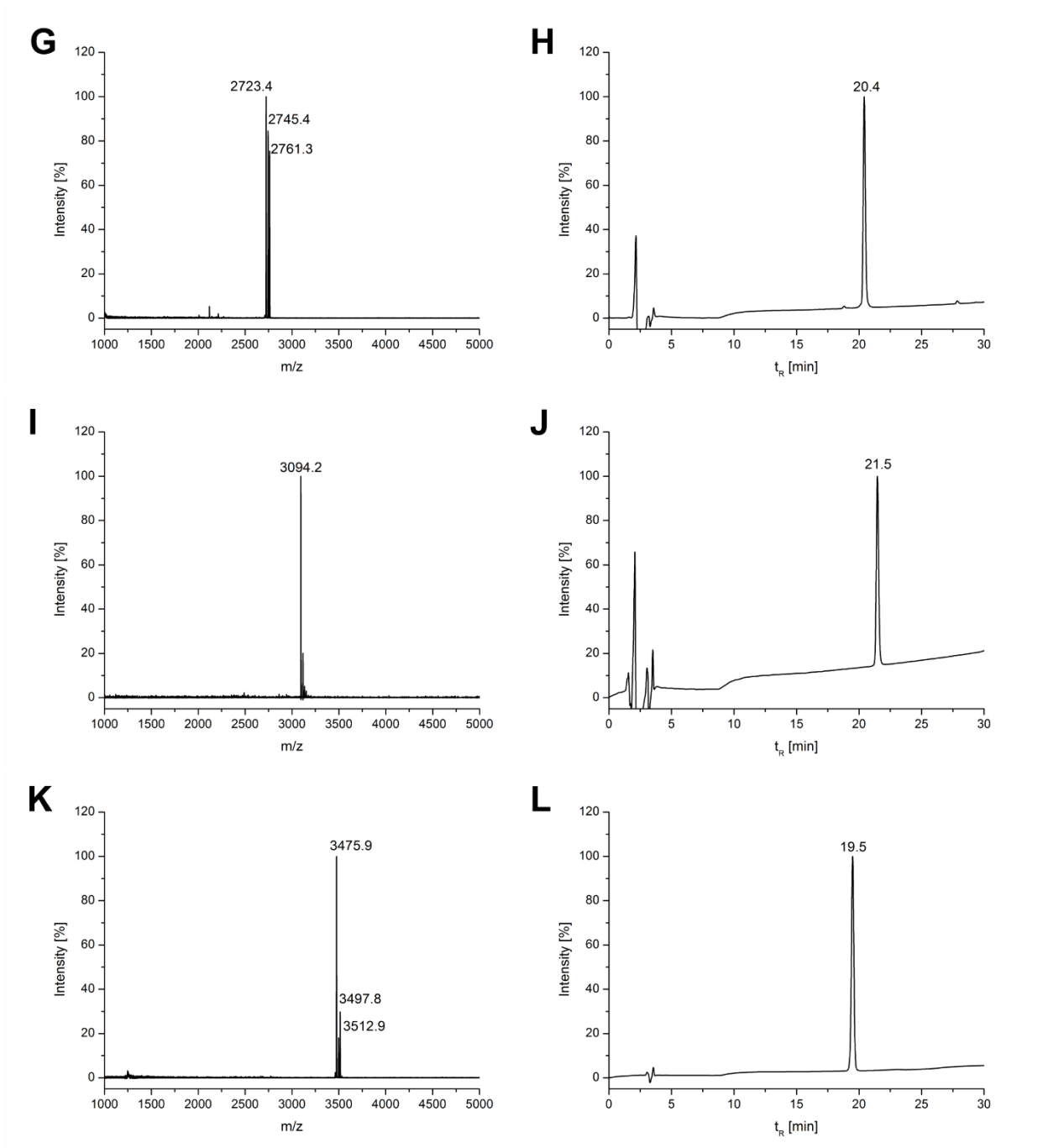


**Figure S15.** MALDI/TOF mass spectra and HPLC traces of coiled-coil single strands of the N-truncated set of heterodimeric coiled coils (A-B: N-A<sub>3</sub><sup>+</sup> calc. [M+H]<sup>+</sup>: 2553.3, C-D: N-A<sub>3.5</sub><sup>+</sup> calc. [M+Na]<sup>+</sup>: 2945.5, E-F: A<sub>4</sub><sup>+</sup> calc. [M+H]<sup>+</sup>: 3309.6, G-H: N-B<sub>3</sub><sup>+</sup> calc. [M+H]<sup>+</sup>: 2723.3, I-J: N-B<sub>3.5</sub><sup>+</sup> calc. [M+H]<sup>+</sup>: 3093.8, K-L: B<sub>4</sub><sup>+</sup> calc. [M+H]<sup>+</sup>: 3476.3).

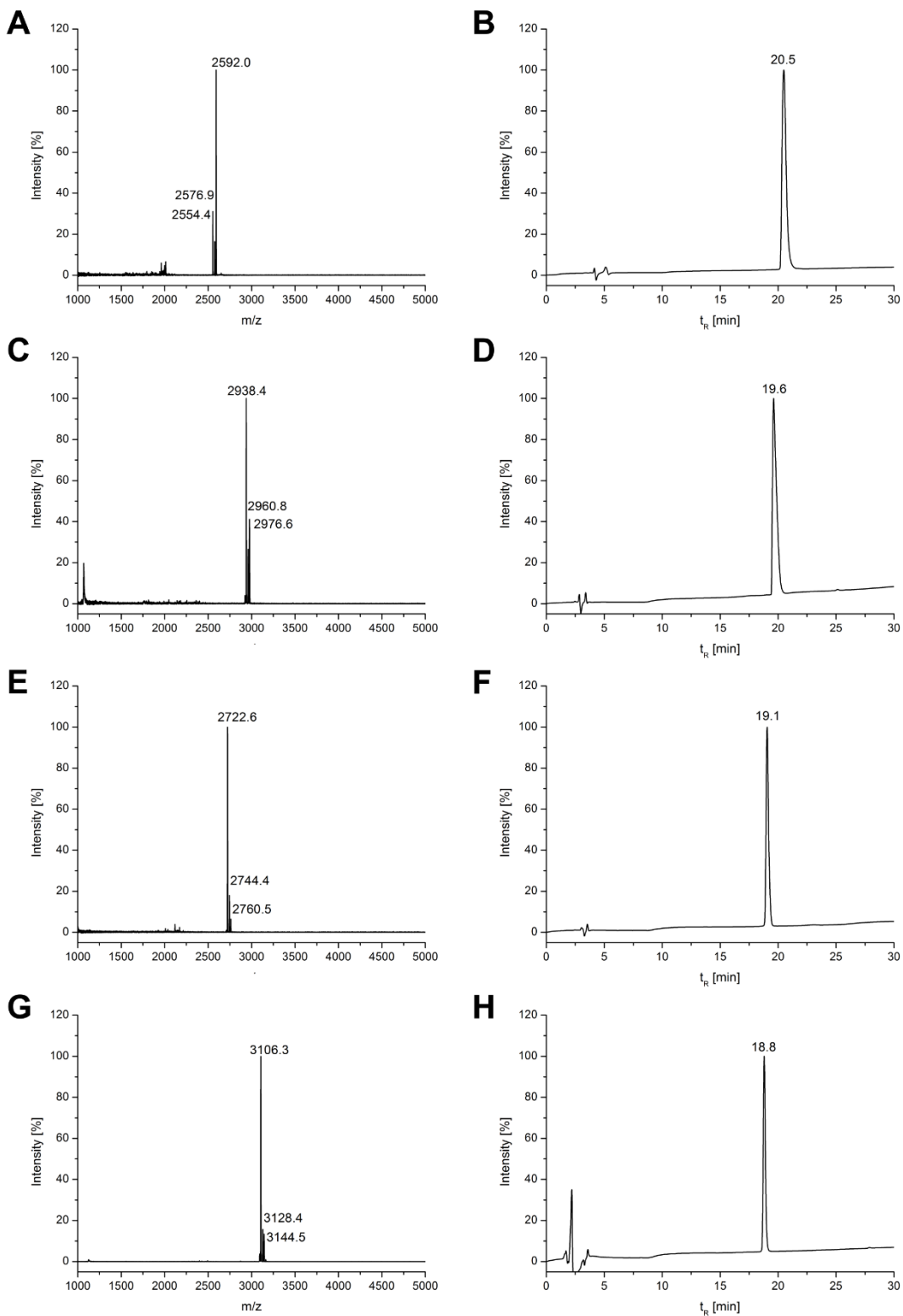


**Figure S16.** MALDI/TOF mass spectra and HPLC traces of coiled-coil single strands of the C-truncated set of heterodimeric coiled coils (A-B: C-A<sub>3</sub>\* calc. [M+H]<sup>+</sup>: 2553.2, C-D: C-A<sub>3.5</sub>\* calc. [M+H]<sup>+</sup>: 3937.4, E-F: C-B<sub>3</sub>\* calc. [M+H]<sup>+</sup>: 2723.3, G-H: C-B<sub>3.5</sub>\* calc. [M+H]<sup>+</sup>: 3106.9).



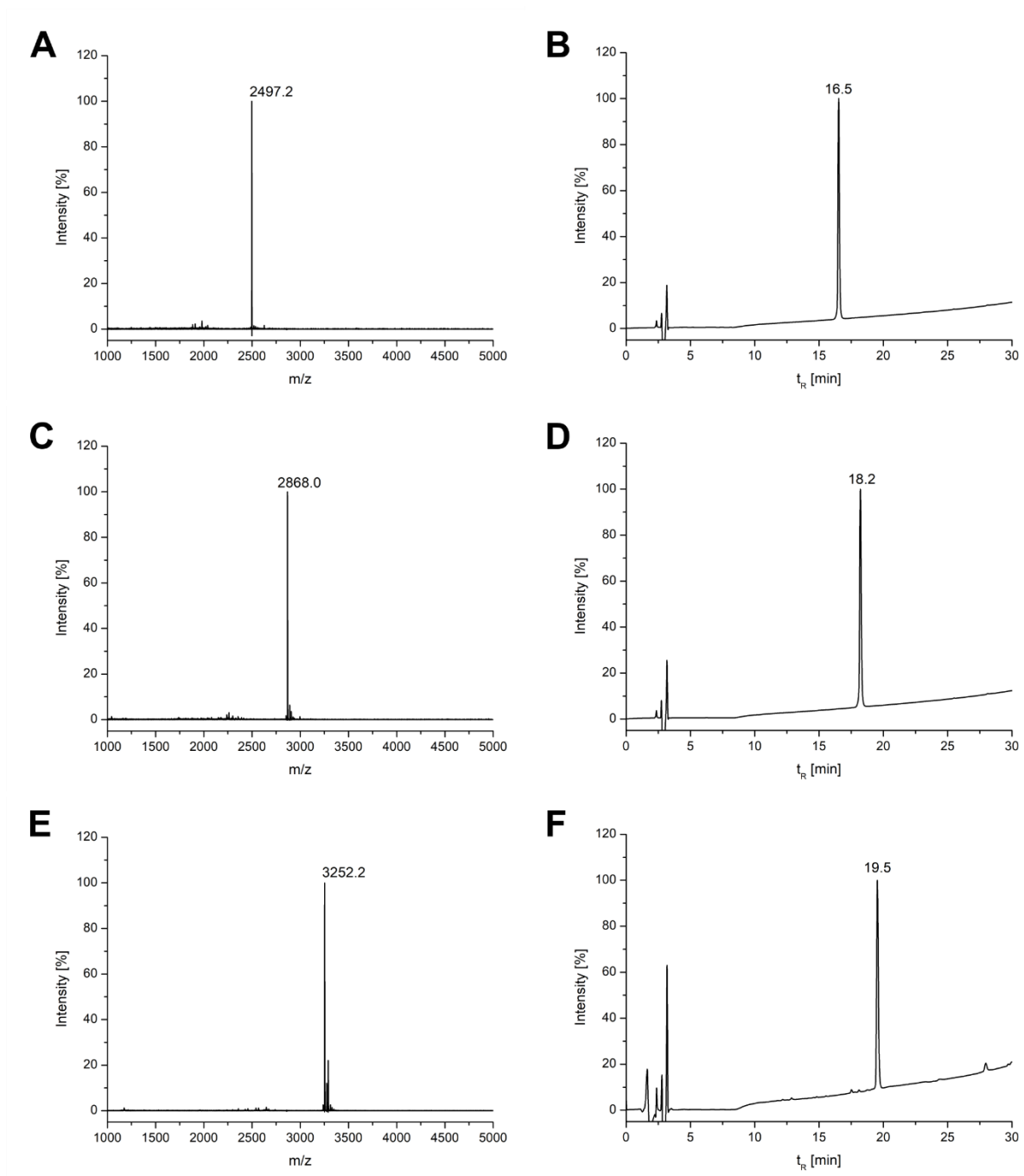


**Figure S17.** MALDI/TOF mass spectra and HPLC traces of non-labelled A-peptides of the *N*-truncated set of heterodimeric coiled coils (A-B: N-A3\_W15K calc.  $[M+H]^+$ : 2496.7, C-D: N-A3.5\_W18K calc.  $[M+H]^+$ : 2867.1, E-F: A4\_W22K calc.  $[M+H]^+$ : 3251.6).

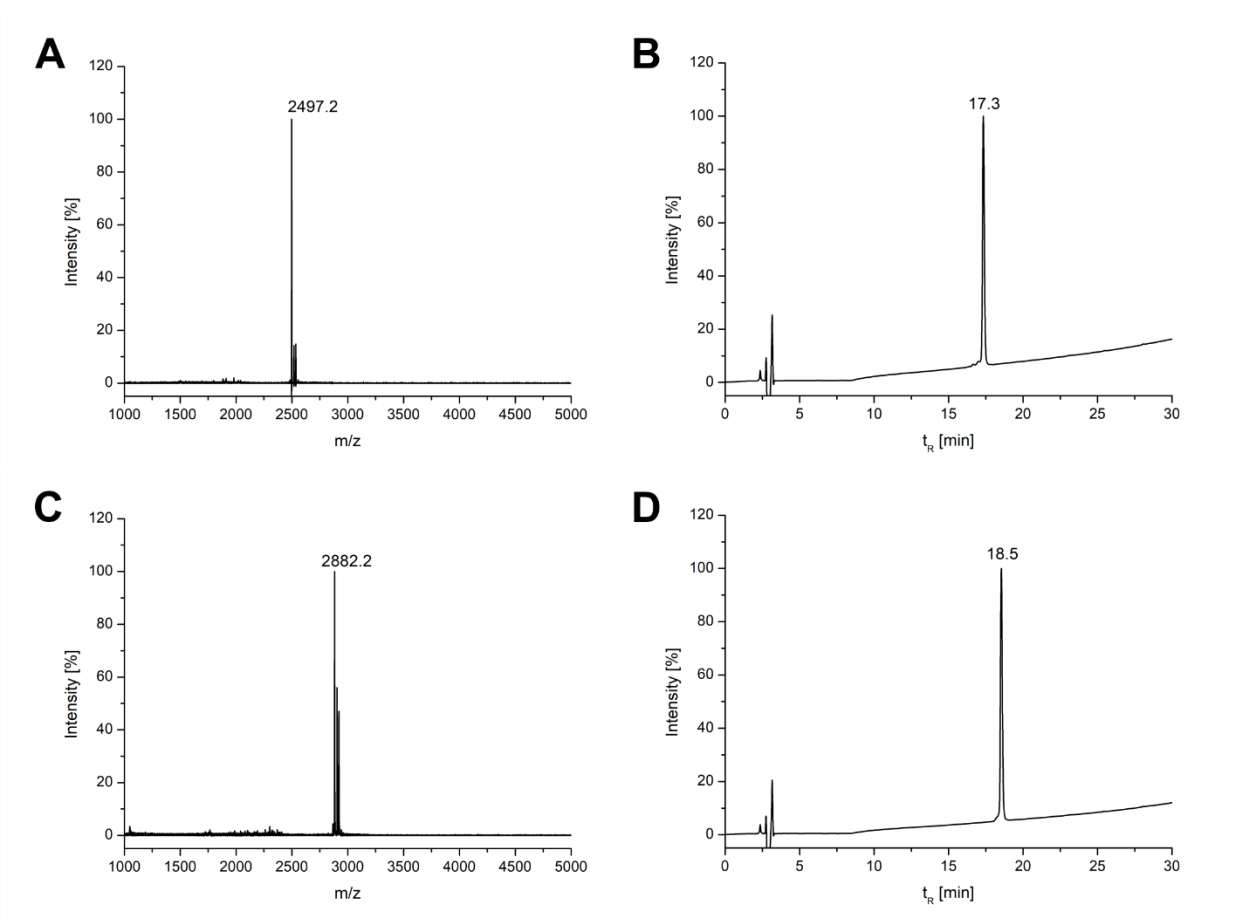
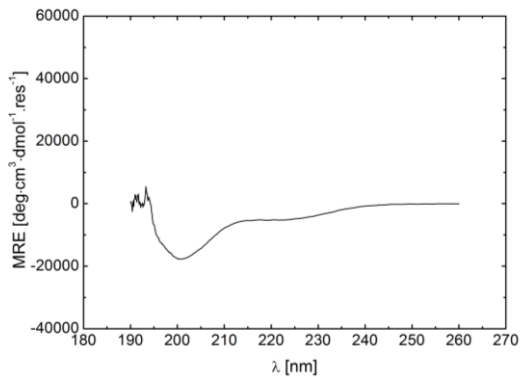


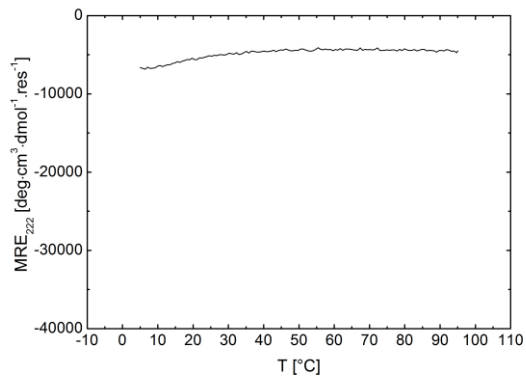
**Figure S18.** MALDI/TOF mass spectra and HPLC traces of coiled-coil single strands of the C-truncated set of heterodimeric coiled coils (A-B: C-A<sub>3</sub>\_W22K calc. [M+H<sup>+</sup>]: 2496.7, C-D: C-A<sub>3.5</sub>\_W22K calc. [M+H<sup>+</sup>]: 2881.2).

## 6. CD spectroscopy and thermal denaturation of C-truncated heterodimeric coiled coils

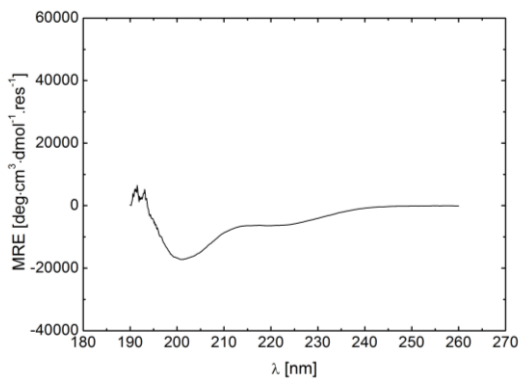
**A** C-A<sub>3</sub>



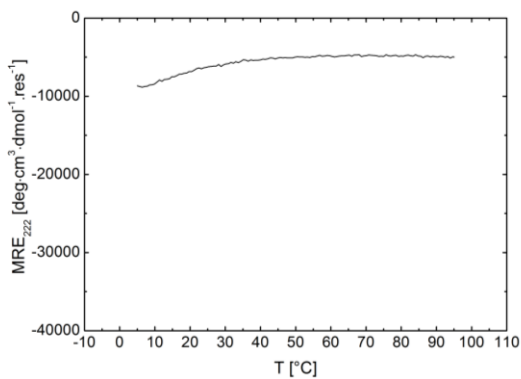
**B** C-A<sub>3</sub> CD melt



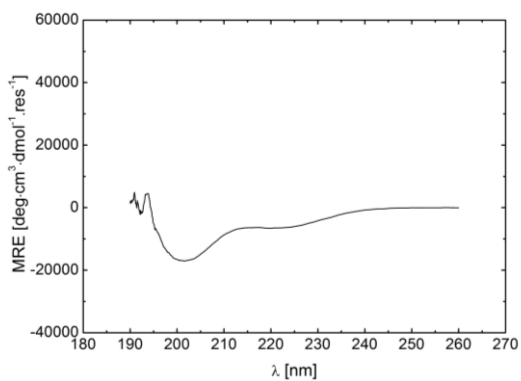
**C** C-A<sub>3.5</sub>



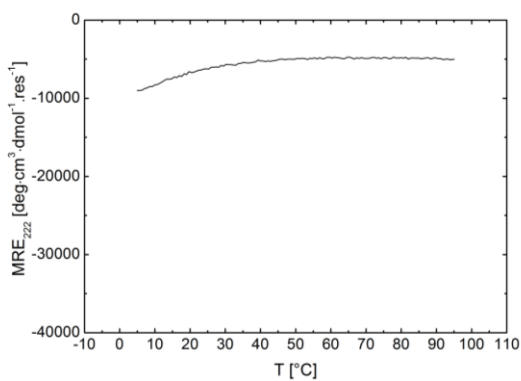
**D** C-A<sub>3.5</sub> CD melt

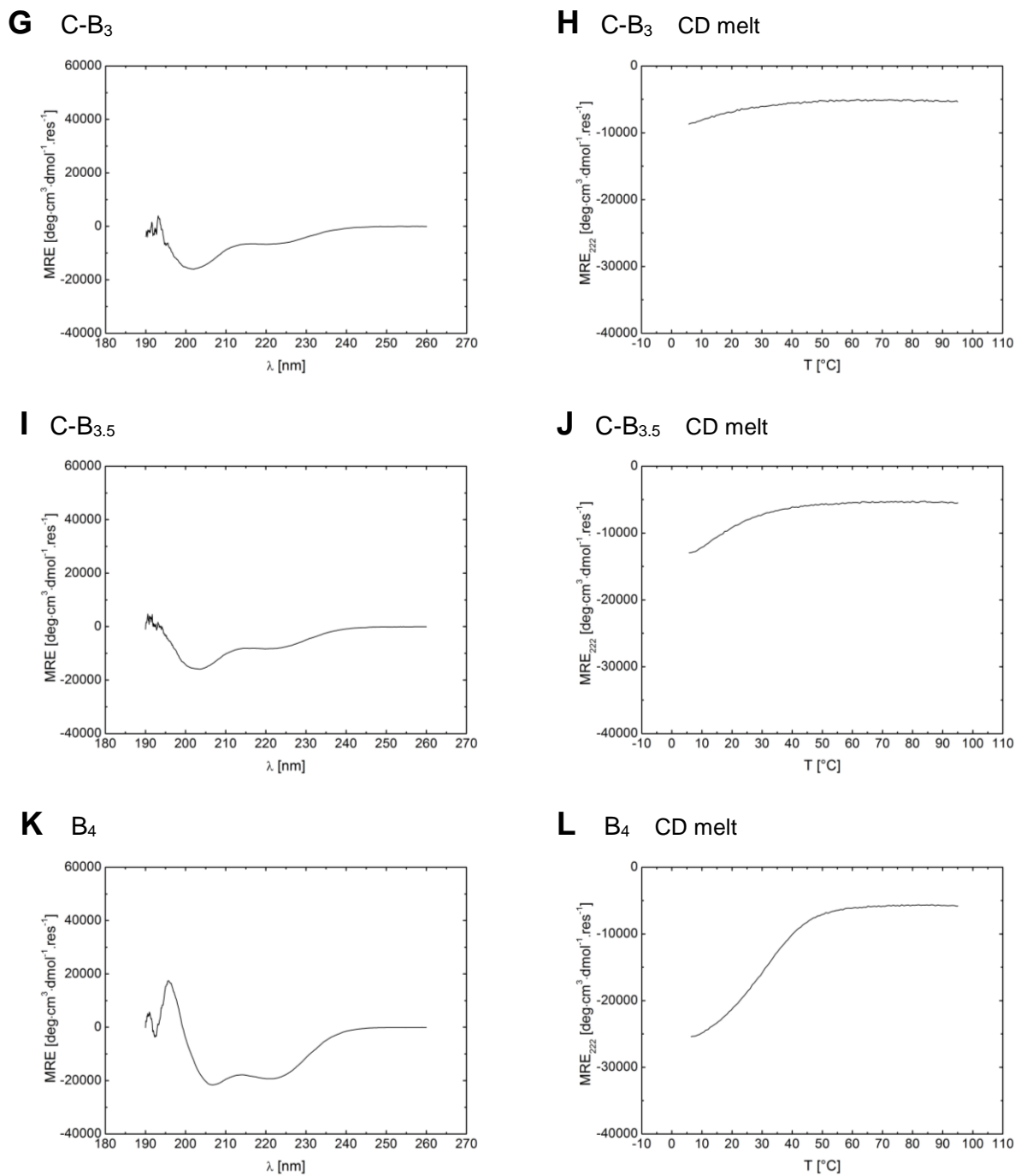


**E** A<sub>4</sub>

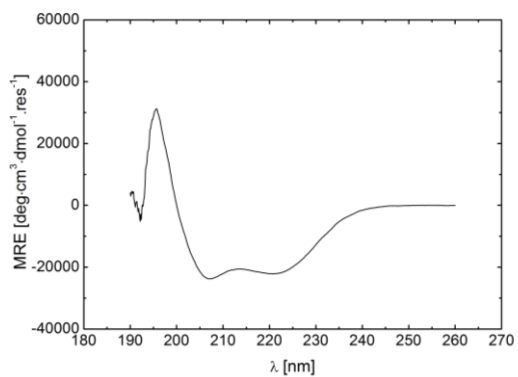
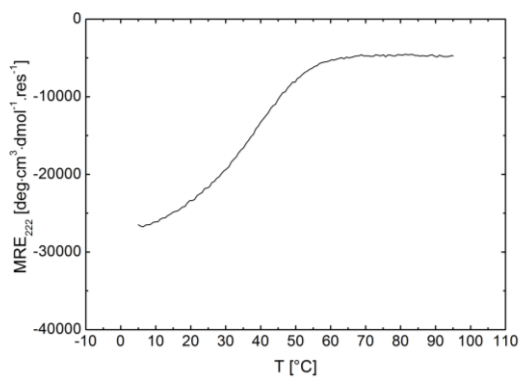
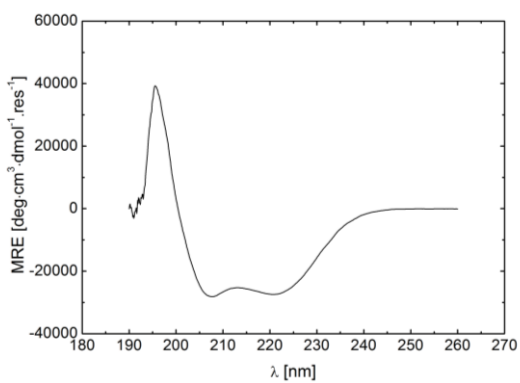
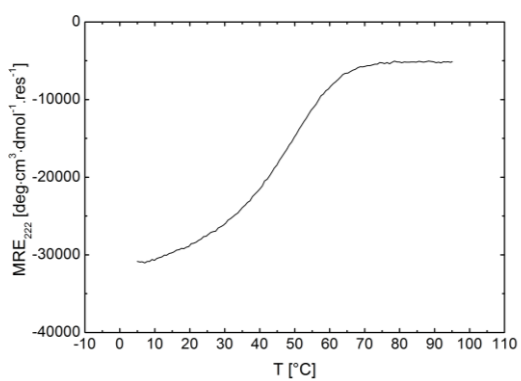
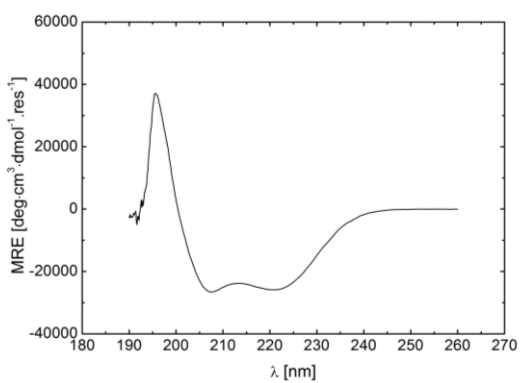
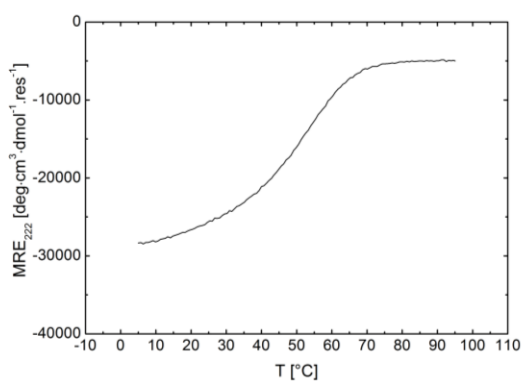


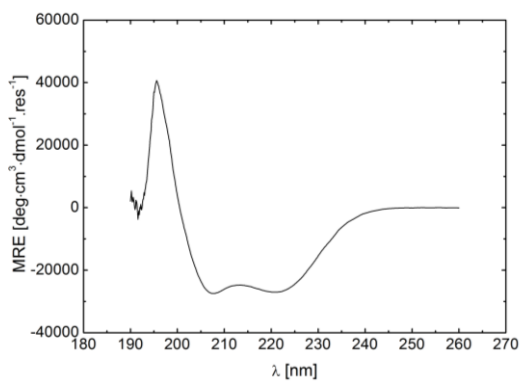
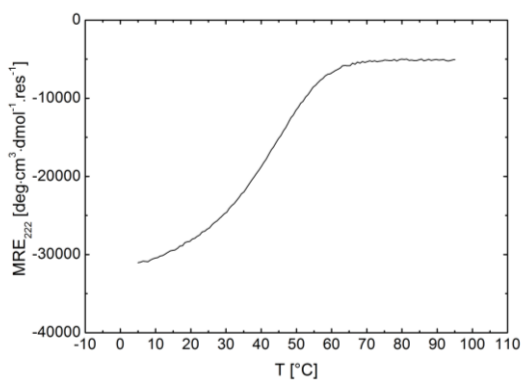
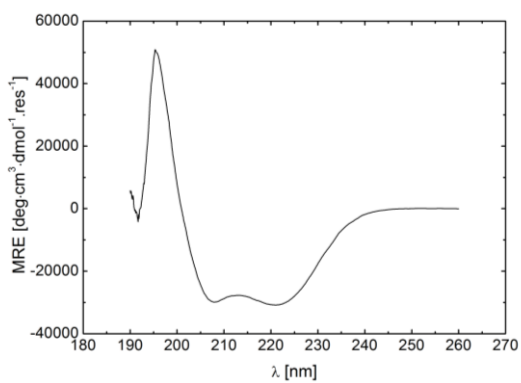
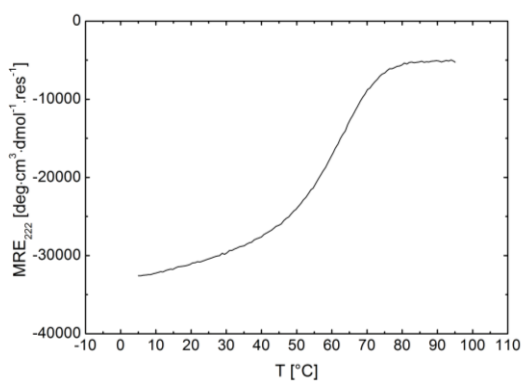
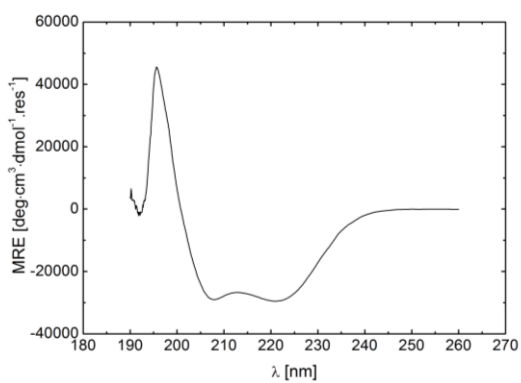
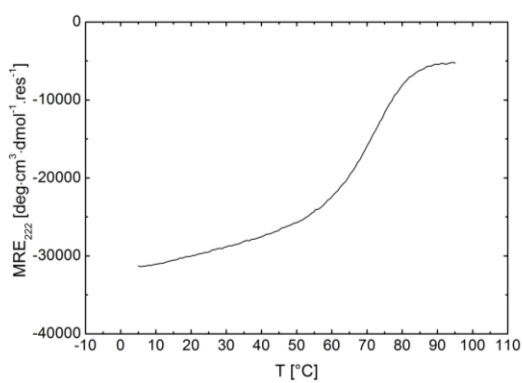
**F** A<sub>4</sub> CD melt



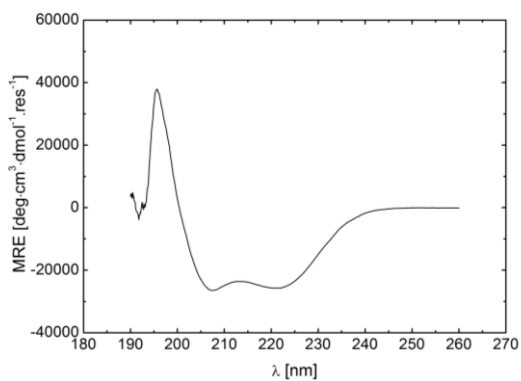


**Figure S19.** CD spectra (left) and thermal denaturation curves (right) of the coiled-coil single strands of the C-terminal truncated set of parallel heterodimeric coiled coils.

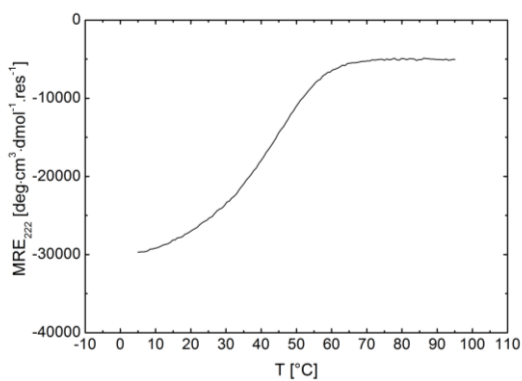
**A** C-A<sub>3</sub>B<sub>3</sub>**B** C-A<sub>3</sub>B<sub>3</sub> CD melt**C** C-A<sub>3</sub>B<sub>3.5</sub>**D** C-A<sub>3</sub>B<sub>3.5</sub> CD melt**E** C-A<sub>3</sub>B<sub>4</sub>**F** C-A<sub>3</sub>B<sub>4</sub> CD melt

**E** C-A<sub>3.5</sub>B<sub>3</sub>**F** C-A<sub>3.5</sub>B<sub>3</sub> CD melt**G** C-A<sub>3.5</sub>B<sub>3.5</sub>**H** C-A<sub>3.5</sub>B<sub>3.5</sub> CD melt**I** C-A<sub>3.5</sub>B<sub>4</sub>**J** C-A<sub>3.5</sub>B<sub>4</sub> CD melt

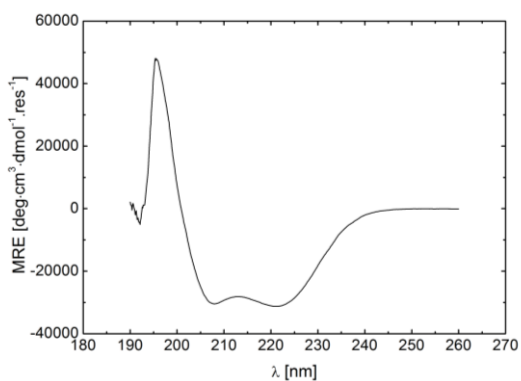
**K** C-A<sub>4</sub>B<sub>3</sub>



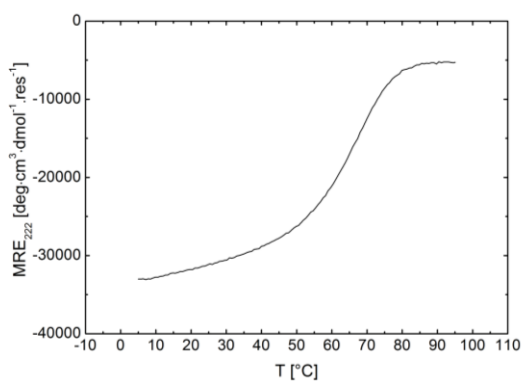
**L** C-A<sub>4</sub>B<sub>3</sub> CD melt



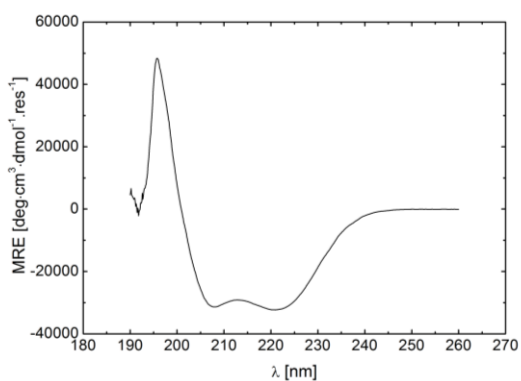
**M** C-A<sub>4</sub>B<sub>3.5</sub>



**N** C-A<sub>4</sub>B<sub>3.5</sub> CD melt



**O** A<sub>4</sub>B<sub>4</sub>



**P** A<sub>4</sub>B<sub>4</sub> CD melt

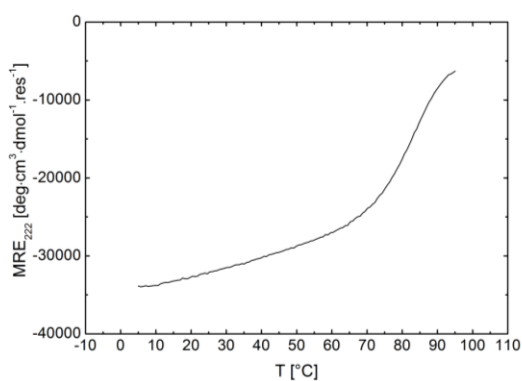


**Figure S20.** CD spectra (left) and thermal denaturation curves (right) of all possible combinations of C-terminal truncated set of parallel heterodimeric coiled coils.

## 7. References

- 1 M. Rabe, A. Boyle, H. R. Zope, F. Versluis and A. Kros, *Biopolymers*, 2015, **104**, 65–72.
- 2 P. Kuzmic, *Anal. Biochem.*, 1996, **237**, 260–273.
- 3 P. Kuzmic, *Anal. Biochem.*, 1999, **267**, 17–23.